PART I: MEASUREMENT OF gf-VALUES FOR SINGLY IONIZED CHROMIUM USING THE REFLECTED WAVE REGION OF A SHOCK TUBE

PART II: EXPERIMENTAL INVESTIGATION OF THE APPROACH TO EQUILIBRIUM IONIZATION AND ELECTRONIC EXCITATION IN SHOCK-HEATED MIXTURES OF CHROMIUM AND ARGON

PART III: APPROXIMATE SPECTRAL ABSORPTION COEFFICIENT CALCULATIONS FOR ELECTRONIC BAND SYSTEMS BELONGING TO DIATOMIC MOLECULES

Thesis by

William L. Shackleford

In Partial Fulfillment of the Requirements

For the Degree of

Doctor of Philosophy

California Institute of Technology

Pasadena, California

1964

(Submitted May 25, 1964)

ACKNOWLEDGMENTS

The author wishes to express his appreciation to Professor S. S. Penner for the invaluable advice, supervision and encouragement which he provided while on the faculty of the California Institute and afterwards until the completion of the research presented here.

The experimental program was greatly facilitated by the use of the shock tube, optical accessories and much of the gas-handling equipment previously assembled with great care by Dr. Ronald Watson, and by helpful discussions the author has had with him. The assistance of Dr. Gerhard Adomeit with much of the experimental work is greatly appreciated. Stimulating discussions with Professor H. W. Liepmann were instrumental in the decision to carry out a large part of the experimental program described in Part II of this manuscript. The author is grateful to the first-named author of Part III, Richard W. Patch, for fruitful discussions and for assistance with the maintenance of the experimental equipment, and wishes to thank the Diamond Alkali Company for contributing samples of chromium carbonyl.

The author also wishes to express particular appreciation to his wife, Christa Shackleford, who provided indispensable encouragement and cheerfully assisted with the experiments.

Grateful appreciation is extended to the National Science Foundation for Regular and Cooperative Fellowships during the years 1959-1963. The United States Air Force contributed financial support to the research under Contract AF 49(638)-758 until November 15, 1962, and thereafter under Grant No. AFOSR-7163 with the California Institute of Technology.

ABSTRACT FOR PART I

Absolute gf-values for 21 lines of singly ionized chromium (Cr II) in the spectral region 3118-4559 Å are presented. Mixtures of $Cr(CO)_6$ and argon, heated by reflected shock waves to temperatures in the range 7920°K to 8730°K, were used to measure the emission intensity of ionized chromium lines. A three inch diameter shock tube was employed, with the light being observed along the shock tube axis in order to observe directly the curve of growth of each spectral line. The emitted intensities observed were converted to gf-values by means of a comparison with a calibrated tungsten strip lamp. Results are compared with values obtained from arc spectra by Corliss and Bozman[1] at the National Bureau of Standards. In general, our results are a factor of 9 below the latter measurements. Possible reasons for this discrepancy are discussed.

ABSTRACT FOR PART II

An experimental investigation of the approach to equilibrium ionization and electronic excitation for chromium behind shock waves in $Cr(CO)_6$ - argon mixtures is described. Mixtures composed of from 0.0043% to 0.036% $Cr(CO)_6$ were heated by reflected shock waves to temperatures between 6170°K and 8600°K, and the emission from excited states of Cr I and Cr II was simultaneously measured by photoelectric means with a time resolution of about 3 microseconds. Relaxation toward equilibrium ionization and excited state population was observed to occur within from 12 to 60 microseconds, depending upon

the temperature and chromium concentration behind the reflected shock.

In measurements in which equilibrium ionization is 95% or more, the populations of excited states of Cr I show a pronounced "overshoot" as these states become populated before ionization has depleted the supply of neutral chromium. From a study of the relaxation of Cr I and Cr II upper state populations, it is concluded that ionization proceeds by a multistep autocatalytic process dominated by collisions between chromium atoms and electrons released in prior ionization of chromium. The dependence of the relaxation rates upon the temperature behind the reflected shock wave and upon the concentration of chromium was determined. If it is assumed that the electron and atom temperatures did not differ appreciably during the relaxation period, the variation in the relaxation rate with temperature indicates a 3.1 ± 0.3 ev activation energy for chromium ionization, which is significantly less than the ionization potential (6.74 ev).

A simplified reaction mechanism is proposed which qualitatively explains the observed relaxation behavior of Cr I and Cr II.

ABSTRACT FOR PART III

The spectral absorption coefficients in electronic band systems of diatomic emitters have been computed in the past by models that may be described as "the just overlapping line model" and a model "utilizing a smeared out rotational structure". Although the basic relations are obtained by utilizing somewhat different physical arguments, the resulting equations are, in fact, identical.

Spectral absorption coefficients have been calculated for the NO γ-bands at 2000°K by using the approximate theoretical relations. The calculated results are in good agreement with estimates derived by numerical calculations in which, however, the absorption coefficient data were averaged over intervals of 2000 cm^{-1}.

TABLE OF CONTENTS

PART I - MEASUREMENTS OF gf-VALUES FOR SINGLY IONIZED CHROMIUM USING THE REFLECTED WAVE REGION OF A SHOCK TUBE

I. INTRODUCTION

A. Introduction

The determination of absolute gf-values for neutral and ionized atoms has received considerable attention in recent years. The gf-value is a dimensionless number which is related to the probability of spontaneous or induced transition between electronic levels of the atom, and hence to the observed strength of emission or absorption lines. These data find application, for example, in the determination of abundances of elements in stars and nebulae, and in the calculation of radiative heat transfer in gases heated by re-entry bodies or electrical discharges.

In principle, the gf-value of a transition is calculable from the wave functions of the initial and final states involved. However, with the important exception of one- and two-electron atoms and atoms with one or two valence electrons far removed from filled inner shells, the accurate calculation of wave functions by solving the Schrödinger equation numerically is an almost prohibitively complicated and tedious problem. Our present knowledge of gf-values relies most heavily on experimental measurements performed by a variety of methods, with the results of different workers differing in some cases by a few per-cent and in other cases by several orders of magnitude. The various theoretical and experimental techniques which have been applied to the

determination of gf-values are summarized in the next section.

In our experiments, a conventional shock tube was used to heat mixtures of argon and chromium carbonyl, $Cr(CO)_6$, to temperatures of up to about 9000°K behind the reflected shock wave. By measuring the emission from ionized chromium lines, and performing the required absolute calibrations, gf-values of 21 lines in the spectral region 3118-4559° Å were obtained.

Chromium carbonyl is a solid with an accurately known vapor pressure of about 0.25 mm Hg at room temperature. The usefulness of chromium carbonyl as a means of introducing controllable concentrations of metal atoms into the test section of a shock tube has been noted previously by several authors.[2-5] In particular, Wilkerson[2] and Charatis[3] have used the reflected wave region of a shock tube to measure gf-values of 60 lines of neutral and singly ionized chromium, using a different recording and calibration technique from the one described in this dissertation.

At the time our experimental program began, gf-values for lines of neutral chromium (Cr I) had been independently measured or theoretically estimated by nine investigators with wide disagreement in results -- as much as a factor of 500 in the extreme cases. The only gf-values of singly ionized chromium (Cr II) then available were those determined by Wilkerson for eight transitions. Because of the large discrepancies which exist between gf-values (or analogous electronic f-numbers for molecular bands) determined by shock tube emission and other techniques, and between shock tube determinations

reported by different workers, it was felt that further careful chromium gf-value measurements, for as many transitions as could be accurately measured, would help to clarify the situation.

The difficulty in obtaining accurate gf-values with shock tubes is due to three principal problems: 1. The first of these is the inherent difficulty in any absolute calibration of light intensity. Although great progress has been made in the development of tungsten lamps and carbon arcs as radiation standards, an error of 10% or more can usually be expected. 2. Since the emitted intensity is proportional to the number of radiating atoms along the line of sight (assuming self-absorption is negligible) accurate knowledge of the concentration of the radiating species is essential. This concentration must usually be of the order 10^{12} cm^{-3} in the test section before firing the shock tube, to meet the requirement of negligible self-absorption. Such low concentrations are difficult to measure and can be significantly altered by preferential adsorption on the walls of the shock tube and manifold. This effect has been observed by Watson for water vapor.[6] 3. The third major source of uncertainty in shock-tube emission experiments is the requirement that the temperature must be known to within a few percent at temperatures in the range 5000-10,000°K, in order to compute accurately the ionization and upper state populations. Small deviations from ideal shock tube behavior can thus have a large effect on the calculated gf-values.

Some or all of the three major difficulties mentioned above, in addition to other problems, plague other experimental techniques as

well; however, in the opinion of the writer, it now appears that the atomic beam technique (described in the next section) is superior for gf-value measurements on low-excitation lines of neutral atoms, while the shock tube is presently the most reliable tool for gf-value measurements of ions and highly excited lines of neutral atoms. The shock tube is, however, restricted to the study of those elements which may be introduced in gaseous form and in measurable concentrations.

The shock tube gf-value measurements described here involve photoelectric recording of the emission from isolated Cr II lines or close multiplets by means of two monochromators. Radiation from the gas behind the reflected wave was observed along the axis of the shock tube, causing the optical depth of the heated gas to increase linearly with time after reflection of the shock from the end wall. The absolute emission with changing optical depth was then compared with the emission from a tungsten lamp calibrated by the National Bureau of Standards. A continuous flushing technique was used in filling the tube with the $Cr(CO)_6$-Ar mixtures in order to permit adsorption equilibrium to become established. Temperatures behind the reflected shock were computed from the incident shock velocity using ideal shock theory. Although numerous lines of neutral chromium were also observed, gf-values could not be obtained because light from a non-equilibrium "overshoot" region dominated the Cr I emission when observed along the shock tube axis. At lower temperatures where this phenomenon was not present, electronic relaxation times were longer than the available testing time and might have led to erroneous results

(compare Part II).

B. Outline of Part I

The various experimental and theoretical techniques which have been used to obtain gf-values for polyelectronic atoms and ions are outlined in the next section.

In Section III the well-known theory of the ideal shock tube is summarized, and the accuracy of the ideal theory is examined in view of available experimental evidence. This discussion is followed by a presentation of the theory of radiation, as it applies to the shock tube experiment.

The apparatus and experimental procedure are described in Sections IV and V, respectively. Results are presented and compared with other available measurements in Section VI.

In Section VII the experimental program is summarized and suggestions concerning future experiments are presented.

II. SUMMARY OF TECHNIQUES FOR DETERMINING gf-VALUES OF POLYELECTRONIC ATOMS AND IONS

A. Relationships Between gf-Values, Transition Rates, and Atomic Structure

According to non-relativistic quantum theory, all observable properties of an atom are obtainable from the complex state vector, $\Psi(t)$. In the Schrodinger representation Ψ has an infinite number of components, corresponding to the two possible spin projections and indenumerably infinite possible spatial positions of each electron with respect to the nucleus. In this case Ψ is identified with the wave function

$$\psi(\vec{r}_1, \sigma_1, \vec{r}_2, \sigma_2, \ldots \vec{r}_N, \sigma_N, t),$$

where $\vec{r}_i$ is the position vector of the i^{th} electron, σ_i is its spin projection ($+\frac{1}{2}$ or $-\frac{1}{2}$) on a given axis, and N is the number of electrons in the atom. By the choice of an appropriate normalization factor for ψ, the product of $\psi(\vec{r}, \sigma_1, \ldots, \vec{r}_N, \sigma_N, t)$ with its complex conjugate is equal to the probability, at time t, of simultaneously observing the first electron within a unit volume at $\vec{r}_1$ and with spin projection σ_1, the second electron at $\vec{r}_2$ with spin σ_2, etc. The time variation of Ψ (or ψ) is expressed by

$$H\Psi = -\frac{h}{2\pi i}\frac{\partial \Psi}{\partial t} \qquad (1)$$

where H is the Hamiltonian operator, derivable from the classical Hamiltonian function by means of quantization postulates, and h is Planck's constant.

For a more detailed discussion of the theory of the interaction of the atom with a radiation field, the reader is referred to the numerous books on atomic structure and quantum mechanics, e. g., the works of Condon and Shortley,[7] Dirac,[8] Messiah,[9] and Heitler.[10] In order to make the formulae more manageable, it has become customary to use the abstract notation of Dirac, in which the state vector Ψ is represented equivalently by a vector in "ket" space $|\Psi\rangle$ or a dual vector in a separate "bra" space $\langle\Psi|$. The scalar product of two state vectors Ψ_a and Ψ_b is represented by $\langle\Psi_a|\Psi_b\rangle$ or, more simply, by $\langle a|b\rangle$. The Schrödinger wave function, ψ, may be used to evaluate this scalar product; in this case one finds

$$\langle a|b\rangle = \langle b|a\rangle^*$$

$$= \sum_{\sigma_i} \int \cdots \int \psi_a^*(\vec{r}_1, \sigma_1 \cdots \vec{r}_N, \sigma_N)\, \psi_b(\vec{r}_1, \sigma_1 \cdots \vec{r}_N, \sigma_N) d\vec{r} \cdots d\vec{r}_N \quad (2)$$

where the integration is performed over all spatial configurations of the electrons for each of the possible 2^N combinations of electron spin coordinates σ_i, and these integrals are summed. When an operator A acts upon the state vector Ψ_a, the resulting vector, $A\Psi_a$, is $A|a\rangle$ in the Dirac notation. The scalar product of Ψ_b with $A\Psi_a$ is written $\langle b|A|a\rangle$. In the following discussion we shall use the wave function, state vector and Dirac notations interchangeably.

If we denote by H^o the Hamiltonian operator for the atom in the absence of explicitly time-dependent perturbations due to interaction with a radiation field or other external influences, the possible solutions

of the eigenvalue equation

$$H^{o}\,\Psi_{n}^{o} = E_{n}^{o}\,\Psi_{n}^{o} \tag{3}$$

yield the allowed energy values E_n^{o} and the corresponding eigenvectors Ψ_n^{o}. If H^{o} were the actual Hamiltonian, the atom could exist indefinitely in any of these energy eigenstates, with Ψ undergoing only changes in its complex phase. When the influence of radiation is considered, however, the actual Hamiltonian operator becomes the sum of H^{o} and a time dependent perturbation H'. If an atom, initially in a state Ψ_i^{o}, has its state vector at subsequent times expressed in terms of the complete set of eigenvectors of Equation (3),

$$\Psi(t) = \sum_{n} c_n(t)\,\Psi_n^{o}(t) \qquad \Psi(t=0) = \Psi_i^{o} \tag{4}$$

one finds from Equation (1) that

$$\frac{dc_n}{dt} = \frac{2\pi}{ih} \sum_{m} c_m \langle n|H'|m\rangle \quad . \tag{5}$$

As a result of the interaction of the atom with an external electromagnetic field, the energy of the atom alone is no longer conserved, but is exchanged with the field by the emission or absorption of a quantum of radiation. The probability of transition of the atom from initial state Ψ_i^{o}, with energy, E_i^{o}, to a final state Ψ_f^{o} with energy E_f^{o}, is

$$\frac{d}{dt}\,(c_f^{*} c_f)$$

where dc_f/dt is given by Equation (5). A consideration of the quantization of the radiation field would reveal that energy in a certain mode

of the electromagnetic field changes by an amount $E_i^o - E_f^o$. The frequency, ν, of this mode is given very nearly by

$$h\nu = \left| E_i^o - E_f^o \right| . \qquad (6)$$

Actually there is a small but important dispersion in the frequency of the emitted or absorbed radiation due to Doppler shifts and to the fact that Ψ_i^o and Ψ_f^o are not quite eigenvectors of the complete Hamiltonian operator. This matter is discussed further in Section III. B.

For most transitions, and all of those which we shall consider, by far the major contribution to the matrix element $\langle n|H'|m\rangle$ in Equation (5) is due to the Coulomb interaction of the electric field vector of the radiation field with the dipole moment of the atom. There are higher order terms in the expressions for the transition rate due to higher order electrical multipole interactions and interaction of the electron orbital and spin magnetic moments with the perturbing magnetic field. These terms are typically 10^{-6} as large as the electrical dipole contribution and are negligible for all cases where the dipole matrix element does not vanish.

The probability of absorption or emission of radiation along a given direction is the pertinent quantity in problems of radiative transfer. To describe this, we define the steradiancy, I_ν, to be the rate of energy transfer into a unit solid angle per unit frequency interval, and through a unit area perpendicular to the direction of propagation. The steradiancy has units erg $(\text{steradian})^{-1}$ cm^{-2}, and in general is a function of spatial location and direction of propagation.

The frequency of atomic transitions can be related to the local

value of I_ν by means of a technique deduced from thermodynamic considerations by Einstein. Einstein proposed that atomic transitions are of three types: 1. Spontaneous transitions from higher to lower energy levels, proportional to the density of atoms n_u in the upper level, and accompanied by emission of radiation of frequency given by Equation (6). 2. Induced absorption of radiation accompanied by atomic transitions from lower to higher energy levels, proportional to the density of atoms in the lower level, n_ℓ, and the local energy density of radiation. 3. Induced emission, proportional to n_u and the radiation density.

As a result of spontaneous emission due to a particular atomic transition, the steradiancy in a given direction is increased in a distance ds by an amount*

$$dI_\nu^{(1)} = n_u \frac{A_{u\ell}}{4\pi} ds\ P(\nu)\ .\ h\nu\ , \tag{7}$$

where $A_{u\ell}$ is the Einstein coefficient for spontaneous emission, and $P(\nu)$ is a "line shape parameter" which takes into account spectral line broadening and satisfies the relation

$$\int_0^\infty P(\nu)d\nu = 1\ . \tag{8}$$

---

* The appearance of $1/4\pi$ and $1/c$ in Eqs. (7), (9) and (10) results from using Einstein's original definition of the A and B coefficients. In Einstein's derivation, transition rates were expressed in terms of the radiation energy density. Recently astrophysicists have defined these coefficients by relating transition rates to steradiancies or absorption coefficients to steradiancies, and as a result various definitions are in use.

There is also a diminution of the steradiancy in distance ds by the amount

$$-dI_\nu^{(2)} = \frac{I_\nu}{c}(n_\ell B_{\ell u} - n_u B_{u\ell})ds\, P(\nu)h\nu \ , \tag{9}$$

where $B_{\ell u}$ and $B_{u\ell}$ are the Einstein coefficients of induced absorption and emission, respectively. The resultant equation of radiative transfer is therefore

$$\frac{dI_\nu}{ds} = \frac{dI_\nu^{(1)}}{ds} + \frac{dI_\nu^{(2)}}{ds} = \left[n_u \frac{A_{u\ell}}{4\pi} - \frac{I_\nu}{c}(n_\ell B_{\ell u} - n_u B_{u\ell}) \right] P(\nu)h\nu \ . \tag{10}$$

The Einstein coefficients are related to the electric dipole matrix elements, $\langle u|\vec{P}|\ell\rangle$, as follows:

$$g_\ell B_{\ell u} = g_u B_{u\ell} = \frac{8\pi^3}{3h^2} \sum_{g_u,\, g_\ell} \left|\langle u|\vec{P}|\ell\rangle\right|^2 \ , \tag{11}$$

$$g_u A_{u\ell} = \frac{64\pi^4 \nu^3}{3hc^3} \sum_{g_u,\, g_\ell} \left|\langle u|\vec{P}|\ell\rangle\right|^2 \ , \tag{12}$$

where g_u and g_ℓ are the degeneracies of the upper and lower states involved in the transition, respectively (the degeneracy of a particular energy level equals the number of independent atomic eigenstates which have that particular eigenvalue for the energy). The summation $\sum_{g_u,\, g_\ell}$ extends over all matrix elements linking degenerate states of the upper level with those of the lower level.

The f-value, or "oscillator strength" is a dimensionless number which relates the total absorption of a given spectral line to the

absorption of radiation by a classical electron harmonic oscillator of frequency ν. It is related to the Einstein coefficient for induced absorption by

$$f_{\ell u} = \frac{h\nu m}{\pi e^2} B_{\ell u} . \tag{13}$$

The product $g_\ell f_{\ell u}$, more frequently written simply gf, is therefore

$$gf = \frac{h\nu m}{\pi e^2} g_\ell B_{\ell u} \tag{14}$$

$$= \frac{mc^3}{8\pi^2 e^2 \nu^2} g_u A_{u\ell} \tag{15}$$

$$= \frac{8\pi^2 m\nu}{3h} \sum_{g_u,\, g_\ell} \left| \langle u | \vec{P} | \ell \rangle \right|^2 . \tag{16}$$

Because of its symmetry between upper and lower states and the fact that it is more directly obtained from emission and absorption measurements than the f-value, the gf-value is the quantity most frequently tabulated.

B. Theoretical Methods for Calculating Absolute gf-Values

According to Equation (16), the gf-value for an atomic transition is calculable from the wave functions of the upper and lower states involved. The wave functions are exactly known only for the case of one-electron atoms and ions; for systems with more than one electron the wave equation is greatly complicated by the quadratic increase in the number of electron-electron interaction terms in the Hamiltonian, the requirement of antisymmetry of the wave function with respect to

electron interchange, and spin-orbit interactions.

For the calculation of gf-values highly accurate wave functions are required, since the dipole matrix element $\langle u|\vec{P}|\ell\rangle$ is quite sensitive to the relative phases and nodal positions of ψ_u and ψ_ℓ. An accurate prediction of the energy levels is not always a guarantee that the wave functions used will be sufficiently accurate for the calculation of gf-values, since the expression for the expectation value of the energy for an approximate eigenfunction ψ_n,

$$E_n = \langle n|H|n\rangle \quad , \tag{17}$$

is much less sensitive to small variations in the wave function than is the dipole matrix element. Hence another inherent disadvantage of theoretical techniques of computing gf-values, aside from the difficulties involved, is the fact that the various approximation procedures usually rely upon experimentally measured gf-values, rather than energy values, for an estimate of their accuracy.

One theoretical device which has been used to estimate absolute f-values of atoms for which extensive experimental data on relative f-values are available is the Thomas-Reiche-Kuhn sum rule, which states that the sum of the f-values for electric-dipole transitions from a given level equals the number of electrons in the atom,

$$\sum_{n'} f_{nn'} = N \quad , \tag{18}$$

where the value $f_{nn'}$ for transitions to lower states is considered negative, and the sum includes an integral of the f-values for transitions to the continuum. For polyelectronic atoms the sum rule

is of little usefulness in this form, as it requires knowledge of relative f-values for transitions involving all electrons, the frequencies of which extend into the X-ray region. In practice, the sum rule is usually applied in an approximate way for transitions involving only valence electrons, which are assumed to move in the potential field of the nucleus and inner electrons. In this form

$$\sum_{n'} f_{nn'} \cong N_v \tag{19}$$

where N_v is the number of valence electrons. The summation must often include f-values for transitions to lower levels which are already filled by inner electrons, and therefore prohibited by the Pauli exclusion principle. Although such transitions do not take place, a formal value of what the f-values would be if they were allowed must be included in the sum. This is a consequence of the assumption that the only effect of the inner electrons upon the valence electrons is their contribution to the potential field in which the valence electrons move.

Use of the f-sum rule appears to be justified for atoms for which extensive experimental relative f-values, but no accurate absolute values, are available. Allen,[11] using relative f-values for eight neutral atoms Sc, Ti, V, Cr, Mn, Fe, Co and Ni, has employed the f-sum rule to establish an absolute scale for these elements. A comparison with later experimental measurements of absolute gf-values by Corliss and Bozmann[1] suggests that the f-sum technique resulted in absolute f-values about 40 percent low. Allen and Corliss[12] have suggested that the discrepancy may be due in part to the neglect of

hypothetical transitions forbidden by the exclusion principle, and in part due to the approximate way in which relative f-values for transitions to highly excited states and the continuum are estimated.

Several approximate techniques have been employed for the solution of the wave equation for polyelectronic atoms. At present, gf-values in good agreement with experiment have been obtained from theoretically calculated wave functions for atoms and ions with two electrons, or with one or two s or p electrons outside closed shells. In view of the increase in the number of workers concerned with the calculation of wave functions and the potentialities of high-speed electronic computers, it is possible that fairly reliable gf-values for more complicated systems will be successfully computed in the near future. Theoretical methods have the advantage that they are applied with equal facility to ions as well as atoms, while experimental measurements of gf-values for ions are subject to larger systematic errors at the high temperatures and electron pressures required to produce ions in abundance. At present, however, the most reliable gf-values for most transitions of astrophysical interest are those obtained experimentally.

The most striking success in the theoretical calculation of gf-values has been achieved by the simplest method, that of Bates and Damgaard,[4] when applied to alkali metals or alkali-type ions. In this method, only the single valence electron is considered, and it is assumed to move in the Coulomb field of a charge (Z-N+1)e,

where Z is the atomic number and N is the number of electrons. The wave function at $r \rightarrow \infty$, where this approximation to the field is correct, is matched with the correct wave function by the use of experimental energy values, E_n, in the radial hydrogenic wave equation

$$\frac{1}{r^2}\frac{d}{dr}\left[r^2\left(\frac{dR_{n\ell}}{dr}\right)\right] + \frac{2m}{\hbar^2}\left[E_n + \frac{(Z-N+1)e^2}{r} - \frac{\hbar^2\ell(\ell+1)}{2mr^2}\right] R_{n\ell} = 0, \tag{20}$$

where n and ℓ are the principal and orbital angular momentum quantum numbers for the valence electron and m is the electron reduced mass. The quantity $R_{n\ell}$ is related to the wave function $\psi_{n\ell m}$ by

$$\psi_{n\ell m} = A_{n\ell}\, R_{n\ell}\, Y_{\ell m}, \tag{21}$$

where the $Y_{\ell m}$ are spherical harmonics and $A_{n\ell}$ represents a normalization factor. The fact that the wave function is a poor approximation inside the core of inner electrons is of little consequence to the calculation of gf-values in this case, since the valence electron spends most of its time outside the core and the dipole matrix elements, $< u|\vec{P}|\ell >$, weight contributions for large r most heavily.

For neutral sodium, the Bates-Damgaard procedure yields gf-values in agreement with experiment to within 5 percent or better, being best for transitions involving high radial quantum numbers. Although the technique has also been applied to other than alkali atoms and alkali-type ions, it has not met with much success in these cases.

For transitions for which the Bates-Damgaard method is inadequate -- and these make up the vast majority -- numerous other, more complicated, techniques have been employed. These

will be only briefly discussed here; the reader is referred to Helliwell's dissertation,[13] or chapter 18 of Slater's book,[14] for a more detailed description of the various techniques in use, the results obtained, and extensive references (to 1962).

The method of the self-consistent field, proposed by Hartree[15] and later modified by Fock to satisfy the requirement that the wave functions be antisymmetric with respect to electron interchange,[16] involves solving the wave equation for a single electron moving in the potential field of the nucleus and a spherically symmetrized charge distribution of the other electrons. The Hartree-Fock procedure requires an iteration technique, since the field of the other electrons requires prior knowledge of their eigenfunctions. As a result of spin-orbit coupling, the assumption that the field in which an electron moves is spherically symmetric, and the assumption that each energy level is associated with a certain set of one-electron eigenfunctions or "configuration", exact solutions of the Hartree-Fock equations still do not satisfy the Schrodinger wave equation exactly. Once a set of orthonormal Hartree-Fock wave functions has been calculated, the effects of spin-orbit coupling, polarization of the core by valence electrons, and mixing of configurations can be included approximately by perturbation and matrix diagonalization procedures. In many cases these techniques are too slowly convergent to yield wave functions of sufficient accuracy for gf-value calculations.

Various modifications of the Hartree-Fock procedure have been found to predict gf-values, usually to within better than a factor of

two, for He I, Li II, and atoms and ions with two valence s or p electrons outside closed inner shells. Helliwell[13] has calculated gf-values for thirteen atoms and ions by this technique using a simplified "nodal boundary condition" application of the Hartree-Fock technique which considers only the wave function of the valence electrons. In an earlier publication[17] Helliwell has presented f-value computations for four transitions of PbI, for which he used a somewhat different two-electron technique, which are in quite good agreement with experimental measurements by Bell and King.[18] In this treatment the valence electrons were assumed to move independently in a Thomas-Fermi potential, while spin-orbit and electrostatic interactions were taken into account by diagonalization of the energy matrix.

Most of the wave functions so far obtained are finite sums of products of one-electron wave functions. The Hamiltonian is approximated by a sum of terms involving the coordinates of single electrons moving in a central field, with remaining terms treated as a perturbation. The wave equation with the unperturbed Hamiltonian can then be separated into wave equations for individual electrons. In the method of Hartree, this results in a system of N coupled ordinary non-linear integro-differential equations which must be solved numerically. The analytic variational technique of Boys and collaborators[19] involves the use of wave functions which are products of one-electron wave functions of an assumed analytic form with adjustable parameters. These parameters are chosen to minimize off-diagonal

terms in the energy matrix, and the resulting eigenfunctions are used as an orthonormal basis in a diagonalization procedure. While the initial set of wave functions is not as accurate as Hartree-Fock wave functions, the diagonalization is more easily performed because of the ease with which the analytic functions can be manipulated. In this manner energy levels for neutral B, Be and C have been calculated with an accuracy of about 0.2%, but the technique has not as yet been extensively applied to the calculation of gf-values.

A method which does not involve the use of one-electron product wave functions is that of Hylleraas.[20] These calculations employ wave functions which depend explicitly upon the inter-electron separation r_{ij}. The most accurate computations of the ground state energy of HeI have been obtained by this technique; however, because of the quadratic increase in the number of variables with N, it is probably too difficult to apply to systems with more than three or four electrons.

As was noted earlier in this discussion, the prospects for theoretical calculations of more accurate gf-values for polyelectronic atoms and ions appear quite promising. This statement is particularly true for transitions between states where the inner electron shells are filled and only one or two valence electrons are involved. The problem is exceedingly complicated and tedious, however; investigators with the ability and facilities at their disposal usually prefer to devote themselves to the study of more glamorous fields. Also, most of the transitions of astrophysical interest are those which are most difficult

to treat analytically. For these transitions experimental gf-value measurements, usually accurate to within a factor of two to five for neutral atoms and less accurate for ions, are still the most reliable estimates available.

C. Experimental Measurements of gf-Values

The experimental techniques which have been used to obtain oscillator strengths are of five basic types: emission, absorption, anomalous dispersion, magneto-rotation of polarized light, and excited state lifetime measurements. The first three of these are somewhat alike, in that the effects observed depend directly upon the number density of atoms in the initial state of the transition being investigated. Besides differing in the technique of measurement, experiments vary in the manner whereby atoms are excited to the initial state of the transition under investigation. Electric ovens, shock tubes, atomic beams, and electric arcs have been used extensively for this purpose. No single experimental technique is best suited to the analysis of all elements, or all lines of a given element.

The number of references on experimental measurements of transition probabilities runs into the hundreds, with results of different investigators often disagreeing by large factors. In the remainder of this section the physical theory involved in each measurement technique is outlined, and a few of the more important or most recent contributions are noted. A summary of experimental and theoretical data for neutral lines of 42 elements is presented in the paper of Goldberg,

Müller, and Aller[21] (1960), and an extensive bibliography on absolute and relative gf-values for atoms and ions has been published by Glennon and Wiese[22] (1962).

1. Emission Measurements

Emission experiments, of which the shock tube measurements presented here are an example, require higher temperatures than the other techniques in order to adequately populate the initial state of the transition, which is usually several electron volts above the ground state. In addition, there must be local thermodynamic equilibrium and the temperature must be known, so that the population of atoms in this state can be accurately computed. Besides the shock tube,[2, 3] electrical arcs[1, 23, 24] and flames[25] have been used as sources of excited atoms and ions. Flames have proven to be the least reliable, presumably because of thermal gradients and departures from local thermodynamic equilibrium. When arcs are used, the temperature must be experimentally determined, and the effects of temperature and concentration gradients taken into account. The shock tube, when of sufficient diameter and length, is capable of providing gaseous samples with a fairly uniform temperature of up to about 15,000°K for periods of a few hundred microseconds. The temperatures can be computed directly from the shock speed using ideal shock theory and have been shown to be in acceptable agreement with measured temperatures (cf. Section III. A.).

According to Equation (11), the emission from a column of gas of length ℓ, integrated over a spectral line, is

$$I = \int_0^{\ell} \int_{\text{line}} \frac{dI_\nu}{ds}\, d\nu\, ds$$

$$= h\nu \frac{A_{u\ell}}{4\pi} n_u \ell + \frac{h}{c} \int_0^{\ell} \int_{\text{line}} I_\nu (n_\ell B_{\ell u} - n_u B_{u\ell})\, P(\nu)\, \nu\, d\nu\, ds, \qquad (22)$$

where the integrations are performed over the spectral line width and along the optical path. If no light is incident at s=0, and if I_ν is, at all positions, much less than the steradiancy of a black body at the temperature of the gas, the second term may be neglected and one obtains the "low optical depth" relation,

$$I = \frac{h\nu A_{u\ell} n_u \ell}{4\pi}$$

$$= \frac{2\pi e^2 n_u h\ell}{m\lambda^3 g_u}\, gf \quad . \qquad (23)$$

By making use of the thermodynamic equilibrium relationship $n_u = g_u (n/Q) \exp(-E_u/kT)$, where Q(T) is the partition function and n is the total number density for the species considered, the above equation may be written

$$I = gf \frac{2\pi hc^2}{m\lambda^3} \frac{n\ell}{Q} e^{-E_u/kT} \quad . \qquad (24)$$

From the preceding relation it is apparent that measurements of gf-values by the emission method require an absolute calibration of the integrated steradiancy, I, and accurate knowledge of n and T. If n is not accurately known, relative gf-values may be obtained by comparing

the relative intensities of suitably chosen lines. Relative intensities are much easier to measure than absolute intensities.

The most extensive measurements of gf-values are those carried out by Corliss and Bozman and associates,[1] using emission from a copper arc to which trace amounts of the element of interest were added. Their publication lists 25,000 lines of 70 neutral and 42 singly ionized atoms. Although they essentially performed relative gf-value measurements, their values have been placed on an absolute scale by comparison with the most accurate experimental and theoretical gf-values available at that time.

2. Absorption Measurements

When a cool or moderately heated gas or vapor is irradiated by a strong continuum light source, energy is removed from the light beam at frequencies corresponding to transitions for which a significant number of gas atoms are in the lower state.

Typical absorption measurements are performed at temperatures in the range 1000-3000°K. At these temperatures spontaneous and induced emission is negligible and Equation (10) may be integrated along the optical path to yield the expression

$$I_\nu(\ell) = I_\nu^o \exp\left[\frac{-n_\ell B_{\ell u} P(\nu) h\nu\ell}{c}\right], \qquad (25)$$

where I_ν^o is the steradiancy of the incident light, which may be assumed constant over the width of the line. Most accurate measurements are made at low optical depths, for which $n_\ell B_{\ell u} P(\nu) h\nu\ell / c \ll 1$.

In this case we may write

$$I_\nu \cong I_\nu^o \left[1 - \frac{n_\ell B_{\ell u} P(\nu) h\nu_{\ell}}{c}\right], \tag{26}$$

and, making use of Equations (10) and (13),

$$\int_{\text{line}} \frac{I_\nu^o - I_\nu}{I_\nu^o} d\nu = \frac{n_\ell B_{\ell u} h\nu_{\ell}}{c} \tag{27}$$

$$= \frac{\pi e^2}{mc} f n_\ell \ell \tag{28}$$

$$= g f \frac{\pi e^2}{mc} \frac{n\ell}{Q} e^{-E_\ell / kT}. \tag{29}$$

As can be seen from the last relation, measurement of gf-values by absorption requires an accurate knowledge of the temperature and the density of absorbing species; unlike emission measurements, however, only relative intensity measurements I_ν / I_ν^o are involved.

Early measurements were performed on metal vapors in electrically heated ovens by King and others.[26] These were presented either as relative f-values or as absolute values which relied upon somewhat uncertain vapor pressure estimates. The absorption technique has been made more accurate by the use of atomic beams, first used by Kopfermann and Wessel,[27] and since applied extensively to gf-value measurements for low-lying transitions of neutral metals by King and associates at the California Institute of Technology.[28] In these experiments the number density of absorbers is obtained experimentally by collecting and weighing the

atoms in the beam. It is generally believed that the most accurate experimental gf-values have been obtained by this method. Unfortunately, it is applicable only to low-excitation lines of a limited number of metals.

3. Anomalous Dispersion

The technique of anomalous dispersion makes use of the peculiar behavior of the refractive index in the vicinity of absorption lines. The relationship between the refractive index, n, and the f-value of the line is given by

$$n-1 = \frac{e^2 n_\ell f}{4\pi m c^2} \frac{\lambda_o^3}{\lambda - \lambda_o} , \qquad (30)$$

where m is the electron mass and λ_o is the wavelength at the line center.

A very accurate device for measuring f-values by means of this effect is the "hooks-method" of Rozhdestvenski, which has been used extensively in the Soviet Union. A detailed discussion of this method may be found in the article of Korff and Breit.[29] Translations of the Russian literature in this field (to 1960) have recently become available.[30] A summary of experimental f-value measurements in the Soviet Union (to 1964) may be found in an article by Penkin.[31]

The "hooks" technique makes use of a Jamin interferometer and a spectrograph. Light from a continuum source is split by the interferometer into two beams, one of which passes through a heated absorption tube filled with vapor of the element under investigation.

The two light beams are recombined and the resulting interference pattern is focused on the spectrograph slit. The fringes appear as horizontal lines in the focal plane of the spectrograph; when a compensating plate is interposed along one of the light paths the fringes in the focal plane become oblique, with "hooks" symmetrically located on each side of absorption lines. The separation of these hooks is proportional to the f-value and the number density of the absorbing species. The use of vapor pressure data in the determination of the latter quantity is the main cause of uncertainty in absolute f-values obtained by this method.

4. Magneto-Rotation of Polarized Light

The frequency dependence of the refractive index in the vicinity of absorption lines is combined with the Zeeman effect to provide the physical founcation for another technique for measuring f-values. Plane-polarized light from a continuum source is passed through an absorbing medium in the presence of a magnetic field, oriented parallel to the beam of light. The absorption lines are split into Zeeman components, each of which absorb light circularly polarized in a certain sense. The right- and left-handed circularly polarized components of the incident light are thus absorbed at slightly different frequencies and, according to Equation (30), travel through the gas at different speeds. The emerging light beam is found to be plane polarized, but the plane of polarization is rotated with respect to that of the incident beam by an angle which depends upon the magnetic

field strength, the f-value, the density of absorbers, and the frequency. A measurement of the angle of rotation can thus be used to determine the f-value.

As with the anomalous dispersion method, the accuracy of the experiment as described above depends upon the use of vapor pressure data for the determination of the absorber density; of the two techniques, anomalous dispersion is capable of better accuracy.

In 1931 Weingeroff[32] described how the magneto-rotation technique could be modified to eliminate the requirement that the density of the absorbing species be known. Instead of involving measurement of the rotation of the plane of polarization near an absorption line, the Weingeroff method is based upon a determination of the particular rotation of the analyzing Nicol for which the absorption line merges into the continuous background. This technique received little attention until 1951, when Stephenson[33] used it to obtain f-values for resonance lines of four elements. His results agree with other experimental measurements and Bates-Damgaard estimates to within about ten percent for Na, K, and Rb.

5. Lifetime Measurements

If a certain energy level, E_u, is excited by means of a beam of electrons or light of a resonant frequency, and if this source of excitation is abruptly cut off, the population in the upper state will decay exponentially with time as spontaneous transitions to lower states occur. If we let n_u equal the number density of atoms in state E_u, the rate of decay is given by

$$\frac{dn_u}{dt} = -n_u \sum_{\ell} A_{u\ell} \quad , \tag{31}$$

where the sum extends over all lower states and the following important assumptions have been made: 1. The pressure is low enough to ensure that de-excitation by collisions is negligible in comparison with de-excitation by spontaneous radiative transitions. 2. The optical depth is sufficiently low to permit photons released by spontaneous emission to escape the gas without being reabsorbed. 3. The population of level E_u is negligibly affected by spontaneous transitions leading to it from more highly excited states.

If we let n_u^o be the value of n_u at t=0, when the source of excitation is shut off, we obtain

$$n_u = n_u^o \, e^{-t/\tau} \quad , \tag{32}$$

where

$$1/\tau = \sum_{\ell} A_{u\ell} \quad . \tag{33}$$

The time constant for raciative decay, τ , is of the order 10^{-8} seconds and can be measured experimentally. If measurements or reliable estimates of relative gf-values (and therefore of relative $A_{u\ell}$-values) are available for all downward transitions from level E_u, a measurement of τ can be used to establish an absolute scale for the relative gf-values. This technique has been applied to FeI by Ziock[34] with a result that is probably within a factor of two of the correct value; Bennett and Dalby[35] have used a similar procedure to obtain electronic f-values for molecular band systems. A clear advantage

of this method is that neither absolute intensity measurements nor knowledge of the density of the radiating species is required.

III. PHYSICAL FOUNDATIONS OF THE SHOCK TUBE EXPERIMENT

A. Hydrodynamic Theory

The conventional shock tube consists of two chambers filled with gases at different pressures separated by a frangible diaphragm. When the diaphragm is caused to burst, a shock wave propagates into the lower pressure chamber and a rarefaction wave into the high pressure chamber; these waves subsequently interact with the walls of the container and with each other in a rather complicated manner until the pressure becomes uniform throughout.

For the shock tube to be useful as a tool for quantitative spectroscopy it is necessary that the flow be, to a good approximation, one-dimensional and nonviscous. This condition can be satisfied by proper tube design and choice of operating conditions, -- the articles by Mirels and White, referred to later in this section, are particularly helpful in this regard. The theory of one-dimensional non-viscous shock tube flow (hereinafter called "ideal shock tube theory") is straightforward, and several thorough discussions are available. Among the earliest publications are those of Laporte and associates,[36] and of Resler, Lin, and Kantrowitz.[37] A useful general reference is provided by a book written by Wright.[38] The dissertations of Wilkerson[2] and Charatis[3] are of particular interest in connection with the present studies, since they are concerned specifically with mixtures of chromium carbonyl and an inert diluent, and include experimental investigations of the validity of the ideal

theory under conditions very similar to those under which our experiments were performed.

For the benefit of readers familiar with spectroscopy but not with the operation of shock tubes, the behavior of an ideal tube and the customary terminology employed are represented in Fig. 1.

After the diaphragm is ruptured, a shock wave propagates into the gas to be analyzed (region (1)) at a constant speed which is determined by the initial pressure ratio p_4/p_1 and the sound speeds and specific heat ratios for the gases in the high and low pressure sections. The shock wave is followed at a slower speed by a "contact surface" discontinuity which divides the gases initially in the two sections of the tube. Across this surface the temperature and composition are discontinuous but, unlike the situation at the shock wave, the pressure and flow velocities are continuous. Between the incident shock wave and the contact surface is a slug of gas at a uniform temperature and pressure, which has been heated and compressed by the incident shock; this gas is designated as being in "region (2)".

When the incident shock wave reaches a stationary end wall, the boundary conditions require that the gas in region (2), which travels at the velocity of the contact surface, be brought to rest by means of a reflected shock wave. This results in a further heating and compression of the gas. This twice-shocked gas (region (5)) occupies the space between the shock tube end wall and the reflected shock wave, which is traveling back up the tube at constant speed.

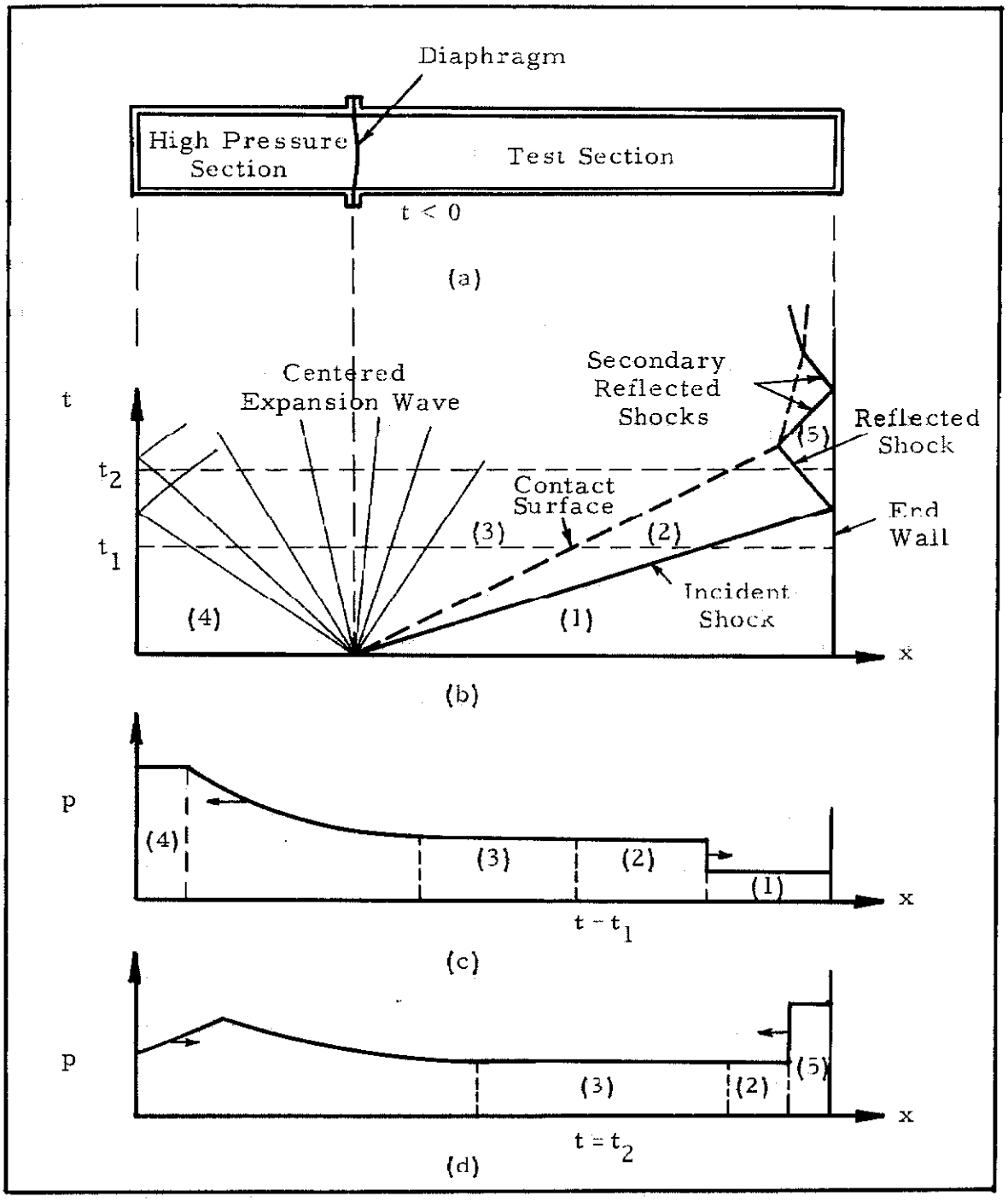

Fig. 1. Theoretical wave diagram and typical pressure distributions for an ideal shock tube. (a) Schematic of shock tube before rupture of diaphragm. (b) x - t diagram, showing shock waves, contact surface, and rarefaction waves. (c) Pressure distribution at $t = t_1$. (d) Pressure distribution at $t = t_2$, after reflection of incident shock.

It is this region that was used as a spectroscopic source in our experiments.

The reflected shock continues upstream into region (2) until it encounters the contact surface and is either transmitted into region (3) or reflected back toward the end wall (as shown in Fig. 1) depending upon the shock strength and the gases involved. These secondary reflections deviate appreciably from the ideal theory in practice, because the "contact surface" is actually not well defined, being the result of a complicated three-dimensional turbulent mixing process which occurs as the diaphragm breaks.

In spite of the highly non-ideal nature of the diaphragm rupture process, a one-dimensional incident shock wave will eventually form if the shock tube is sufficiently long. This is due to the natural tendency of compression waves in gases to steepen into shock waves. The effects of diaphragm opening time have been investigated theoretically and experimentally by White.[39] His results indicate that the incident shock wave accelerates as compression waves coalesce to increase its strength, reaches a maximum velocity when the shock is "fully formed", and then slowly decelerates. He was able to successfully relate the maximum shock speed to the initial pressure ratio, and the "shock formation distance" to the observed diaphragm opening time by means of a simple theory involving compression waves and mixing of gases at the contact surface.

If a shock tube is of sufficient length, the incident shock wave attains a nearly constant speed and ideal shock tube theory continues to be a good approximation for the flow ahead of the contact surface,

in regions (2) and (5). Deviations from ideal theory in these regions are due mainly to boundary layer effects at the tube wall. These effects have been the subject of thorough investigation in the past decade and are now quite well understood.

One effect of the wall boundary layer is to cause the distance between the contact surface and the incident shock to approach a constant value, rather than to increase linearly with time as predicted by the ideal theory. This effect was first noted by Duff[40] and correctly attributed to the transfer of gas from region (2) into region (3) through a boundary layer at the tube wall. The time variation of the separation of incident shock and contact surface was analyzed by Roshko[41] and Hooker,[42] who considered the effect of a laminar boundary layer and treated the free stream gas in region (2) as being uniform. In more refined calculations, Mirels[43] has considered the effects of both laminar and turbulent boundary layers, as well as non-uniformity of the free stream conditions. This non-uniformity is a further consequence of the presence of a boundary layer, and must be made negligible if the shock tube is to be a useful spectroscopic source. The lack of flow uniformity is most severe for shock tubes of small diameter, at high shock speeds, and at low initial test section pressures.

When the incident shock wave is reflected into region (2), more severe deviations from ideal shock tube theory are encountered. These result from the fact that the conditions in region (2) are not uniform, but rather vary with time, distance from the tube wall, and distance along the tube. Large discrepancies between observed and predicted

reflected shock speed have been a cause of concern to investigators who have wanted to use region (5) for spectroscopic or reaction rate measurements. Toennies and Greene,[44] using a two-inch diameter shock tube, noted reflected shock velocities from 10 to 40 percent lower than those predicted by ideal theory at incident shock Mach numbers in the range 4 to 10. Mark[45] observed the interaction between the reflected shock wave and the boundary layer in region (2), and was able to explain the observed interaction pattern at the foot of the reflected shock wave theoretically. He did not succeed, however, in correctly predicting the speed of the reflected shock or the conditions behind it in region (5). Strehlow and Cohen[46] confirmed Mark's theory of the reflect shock-boundary layer interaction and observed reflect shock speeds from 4 to 15 percent slower than ideal theory predictions. They employed a 2-1/2 inch diameter shock tube and incident shock Mach numbers between 1.5 and 4.6. On the basis of their observed shock speeds and an assumption that the gas is brought to rest by the reflected shock, they predicted a temperature from 300° to 500°K below ideal values of 1500° to 3000°K in region (5). Since such large deviations from ideal theory would cast serious doubt on the validity of spectroscopic and rate process measurements behind reflected shock waves, several investigators have made direct measurements of the pressure, temperature and particle velocity in this region in recent years.

Pressure measurements upstream and downstream of reflected shocks performed by Skinner,[47] and later by Brabbs, Zlatarich and Belles,[48] indicate that the gas in region (5) is not brought to rest by

the shock, but instead continues to move toward the end wall where its velocity approaches zero. From their observed pressures and use of normal shock theory without the condition that the gas in region (5) should have zero velocity, they calculated temperatures only 50^{o} below ideal theory values under conditions similar to those of Strehlow and Cohen's measurements. Wilkerson,[2] in conjunction with his work on chromium gf-values, performed pressure, wave velocity and particle velocity measurements at higher shock strengths, for which the temperature behind the reflected shock wave was about $10,000^{o}K$. He also concluded that, although the gas behind the reflected shock wave is not at rest, its temperature is given within about two percent by ideal shock theory calculations based upon the measured incident shock speed. His experiments were performed with a shock tube of 1.63 by 2.63 inch cross section, at initial test section pressures of about one cm Hg. Subsequent spectroscopic temperature measurements in region (5) by Charatis[3] (for $T_s \approx 7000^{o}K$), using the tube previously used by Wilkerson, and Watson[40] (for $T_s \approx 4000^{o}$), using the same three inch diameter shock tube used in our experiments, demonstrate that ideal shock theory predictions of the temperature were correct to within two percent, and that the temperature remained fairly uniform throughout region (5).

Although this fortunate agreement of theory with experiment is not expected to be as good for smaller shock tubes or much lower test section pressures than those used by the workers just mentioned, it is believed that the conditions of our experiment are sufficiently close

to those of Wilkerson and Charatis to justify the use of incident shock speed measurements and one-dimensional non-viscous shock theory in the determination of the temperature and pressure in region (5). The procedure involved is fully described for the case of $Cr(CO)_6$-Ar mixtures in Wilkerson's thesis, and only the physical features of the computation will be presented here.

The rates of flow of mass, momentum and energy into a shock wave are equated to the corresponding rates of flow out of the shock wave. The momentum and energy fluxes due to radiation are negligible compared to other terms under our experimental conditions and are consequently not included. The conditions of the gas entering the incident shock wave are known, and the flow velocity of this gas (in shock-fixed coordinates) equals the measured shock speed. The unknown quantities in the three conservation equations for the incident shock are the enthalpy, pressure, density and velocity in region (2). An equation of state, relating the enthalpy to the pressure and density of the gas, completes the set of equations required for a solution of the problem. Once the conditions of region (2) have been determined, a similar set of equations are applied to the reflected shock wave to determine the conditions in region (5).

The equation of state is complicated by the presence of reacting gases, or gaseswith degrees of freedom other than those of translation and rotation. If thermodynamic equilibrium is assumed in determining the equation of state, the solution of the system of shock wave equations will yield flow parameters which are strictly correct

only at locations where thermodynamic equilibrium is actually obtained. This condition may not be reached until the gas has passed an appreciable distance behind the abrupt pressure jump which is usually associated with the shock wave. In some experiments mentioned in Part II, for example, equilibrium ionization of chromium was obtained only at positions at least 10 cm behind the reflected shock wave. The state of the gas in the "relaxation region", where thermodynamic equilibrium is not established, can only be determined by direct measurement or a consideration of the various reaction rates, which are usually poorly known.

Many investigators have used the shock tube to measure vibrational relaxation, chemical reaction and ionization rates of gases by using dilute mixtures with inert gases. At temperatures below about 10,000°K the inert gases have only translational degrees of freedom, and these are equilibrated within a few collisions (i.e., within the width of the shock wave). For sufficiently dilute mixtures, the enthalpy is negligibly affected by the degree of reaction or relaxation of the reacting component(s); in this case an accurate 'translational temperature' may be computed by using the conservation equations together with the equation of state of the inert gas. This temperature will be only slightly lowered as translational energy is converted to other degrees of freedom, so that observed reaction rates can be converted to useful isothermal cross sections.

For our gf-value measurements, $Cr(CO)_6$ concentrations of less than one part in 10^4 of argon were used, and results were based

upon measurements of Cr II radiation behind the reflected shock after it had reached a steady value which was assumed to indicate thermodynamic equilibrium. The amount of chromium ionization, as computed by means of the Saha equation, was greater than 99 percent for all runs. For the highly dilute mixtures which we used, computation of the pressure and temperature behind the reflected shock wave required only minor corrections to values obtained from analytic expressions for a gas of specific heat ratio $\gamma = 5/3$. The accurately computed temperatures (which were obtained by considering the effects of dissociation and all degrees of freedom for $Cr(CO)_6$, CO, C, O, and Cr) never differed by more than 1/2% from temperatures computed from the simple $\gamma = 5/3$ formula.

B. Theory of Radiant Emission Measurements

According to Equation (24), it is possible to determine the gf-value for a spectral line by measuring the absolute amount of radiation emitted by atoms undergoing transitions from the higher to the lower of the two energy levels involved. In order to obtain accurate gf-values by such an experiment, it is first necessary to verify that the assumptions of local thermodynamic equilibrium and negligible self-absorption, which were made in deriving Equation (24), are in fact justified; it is also necessary to consider the distortion of spectral line profiles caused by the non-monochromatic response function (slit function) of the radiation-detecting apparatus. These problems are discussed in the remainder of this section.

1. The Local Thermodynamic Equilibrium Assumption

For our purposes, local thermodynamic equilibrium (LTE) is

defined as a condition which exists whenever the local chemical composition and the relative populations of the various energy levels available to each chemical species are the same as would be obtained in a gas in complete (i.e., chemical, mechanical, thermal and radiative) thermodynamic equilibrium at a certain pressure and temperature. The LTE condition differs from complete thermodynamic equilibrium in that temperature and pressure gradients may exist, and the radiant energy distribution,

$$I_\nu(\nu, \theta, \phi, x, y, z),$$

may be anisotropic and completely different from the Planck black body function,

$$B_\nu(T) = \frac{2h\nu^3}{c^2} \frac{1}{\left[\exp(h\nu/kT)-1\right]} . \tag{34}$$

When LTE is obtained, the relative population of any two energy levels, E_1 and E_2, with respective degeneracies of g_1 and g_2, is given by the Boltzmann relation

$$\frac{n_1}{n_2} = \frac{g_1 e^{-E_1/kT}}{g_2 e^{-E_2/kT}} , \tag{35}$$

where T is the local temperature. The ratio of the population, n_i, in energy level E_i, to the total population, n, of a particular chemical species is then

$$\frac{n_i}{n} = \frac{g_i e^{-E_i/kT}}{\sum g_j e^{-E_j/kT}} = \frac{g_i e^{-E_i/kT}}{Q(T)} \quad , \tag{36}$$

where Q(T) is the partition function or "sum-over-states".

Deviations from LTE may occur in gases which are at low pressures and not in equilibrium with the radiation field, even though the level populations may have reached steady state values. In such a situation, spontaneous emission may be the dominant process by which a given excited state is depopulated. The inverse process of induced absorption (less induced emission) will not be in detailed balance with spontaneous emission unless the steradiancy everywhere is given by the Planck function. In a shock tube emission experiment, for example, the steradiancy is everywhere much less than that corresponding to the Planck function at the (translational) temperature of the gas, and the rate of radiative transitions from an upper state to a lower state, $E_u \rightarrow E_\ell + h\nu$, far exceeds the rate of the inverse process, $E_\ell + h\nu \rightarrow E_u$. The various collision reactions will be in detailed balance, however (provided the distribution of translational, rotational, and vibrational energy can be characterized by a unique temperature, as we shall assume). As a result, it is quite possible that inelastic collisions may be dominant in populating a certain electronically excited state, while spontaneous emission is most effective in depopulating it. The resulting distribution of excited state populations will differ markedly from Equation (36). The radiation is then said to be "collision limited". Such a situation is

quite familiar in astronomy, since it explains the appearance of forbidden lines in nebulae, aurora, and the solar corona.[50]

The possibility of collision limited excitation in a shock tube has been considered by Keck et. al.[51] in their experiments on the emissivity of heated air. By varying the density (and hence the collision frequency) over a wide range while holding the temperature constant, and noting that the relative populations of excited electronic states with respect to the ground state did not change appreciably, they concluded that LTE was obtained in their experiments. Similar conclusions were reached by Doherty.[52]

Suppose for simplicity that a monatomic gas, X, has only two energy levels, E_u and E_ℓ (=0), and that neither is degenerate. The upper state will have a radiative lifetime of

$$\tau_r = \frac{1}{A_{u\ell}} \approx 10^{-8} \text{ sec}, \tag{37}$$

and we shall assume that the radiation density is so low that absorption is negligible. Inelastic collisions in which the energy of X atoms is raised or lowered will be represented by the generalized reaction

$$X_\ell + Y \underset{k_r}{\overset{k}{\rightleftharpoons}} X_u + Y ,$$

where X_ℓ and X_u represent X atoms in the ground and excited states, respectively, and Y is any colliding particle. The forward reaction takes place at a rate $k n_{X_\ell} n_Y$ ($cm^{-3} sec^{-1}$), and the reverse reaction at a rate $k_r n_{X_u} n_Y$. The forward and reverse reaction rate constants, k and k_r, are related according to detailed balance requirement,

$$\frac{k}{k_r} = e^{-E_u/kT} \quad . \tag{38}$$

The differential equation governing the population of the energy levels is

$$\frac{dn_{X_\ell}}{dt} = -\frac{dn_{X_u}}{dt} = k_r n_{X_u} n_Y - k n_{X_\ell} n_Y + n_{X_u} A_{u\ell} \tag{39}$$

$$= k_r n_Y (n_{X_u} - n_{X_\ell} e^{-E_u/kT}) + n_{X_u} A_{u\ell} \quad . \tag{40}$$

When a steady state is obtained, the ratio of populations of energy levels E_u and E_ℓ is

$$\frac{n_{X_u}}{n_{X_\ell}} = \frac{1}{1 + \frac{A_{u\ell}}{k_r n_Y}} e^{-E_u/kT} \quad , \tag{41}$$

which differs appreciably from the LTE value of $\exp(-E_u/kT)$ if the radiative de-excitation rate, $A_{u\ell} n_{X_u}$, is of the same order as or greater than the collisional de-excitation rate, $k_r n_Y n_{X_u}$.

In reality, of course, atoms and ions possess very large numbers of energy levels. These are spaced, on the average, a few electron volts apart near the ground state and progressively closer together near the ionization limit. For LTE to be obtained, the total collisional depopulation rate must greatly exceed the net radiative depopulation rate for each energy level. Because of the large number of reactions which must be considered, and the lack of accurate cross sections for inelastic collision processes (especially at thermal velocities), it is often difficult to say on a theoretical basis whether

or not LTE will be obtained in a given experiment.

In the shock tube measurements presented here, temperatures behind the reflected shock wave were typically 8000°K, and electron number densities were approximately 10^{14} cm^{-3} once ionization equilibrium had become established. On the basis of an experimental investigation of ionization and electronic excitation relaxation processes under these conditions (cf. Part II), it was concluded that inelastic collisions of CrI with electrons occur with a frequency which is either greater than, or approximately equal to, the frequency of inelastic collisions of CrI with other (chiefly argon) atoms. This estimate is consistent with an order-of-magnitude calculation of the relative cross sections for electron-atom and atom-atom excitation cross sections, based upon the experimental measurements of inert gas ionization rates by Weymann[53] and Harwell.[54] The reasoning is as follows: At a given energy just above threshhold, electrons are 10^{2}-10^{3} times more effective than atoms in causing excitation. Also, because of their lower mass, the electrons have velocities about 300 times larger than argon atoms of the same energy. As a result, collisional excitation (or de-excitation) of atomic energy levels will be mainly due to collisions with electrons whenever the ratio of the number densities of electrons and atoms exceeds a value of about 10^{-5}. Electrons were approximately $4 . 10^{-5}$ times as plentiful as atoms in the gas which we used for gf-value measurements, and therefore electron-atom inelastic collisions should have occurred at a rate somewhat greater than atom-atom inelastic collisions.

We now inquire whether local thermodynamic equilibrium was obtained in our experiments. It will be assumed that only collisions with electrons are effective in de-exciting electronic levels of chromium. It has recently been demonstrated that inelastic cross sections for electron-atom collisions can be computed with an accuracy of about 50% by means of a classical theory due to Gryzinski.[55] According to this theory, incident electrons are scattered by means of the Coulomb interaction with atomic electrons, which are assumed to move in circular Bohr orbits. For our purposes it is sufficient to consider some results of this theory which are of rather general validity: (1) collisional de-excitation rates are nearly independent of the electron temperature, T_e, if kT_e is not much larger than the change of kinetic energy for relative translation. (2) The cross section for collisions in which the electron energy changes by an amount greater than or equal to U falls off as U^{-n}, where $2 < n < 3$. (3) At low energies of the incident electron, transitions which are optically forbidden or which involve a change in multiplicity are not unimportant in comparison with transitions for which gf-values are large, i.e., optical selection rules do not apply in collision processes.

Because energy level separations are largest for low-lying transitions, colliding electrons must undergo large energy changes in order to de-excite levels near the ground state. Such collisions will be relatively infrequent. Radiative depopulation, on the other hand, is usually most rapid for allowed transitions between low-lying levels and the ground state. For hydrogenic atoms, for example, the

radiative lifetime of excited states varies approximately as the 9/2 power of the principal quantum number, n.[56] The ratio of radiative to collisional de-excitation, which according to Equation (41) determines whether or not LTE is obtained, is likely to be largest in Cr I for the group of electronic levels in the vicinity of the $3d^5 4s\ ^7P^o$ state (E=2.90 ev). The dominant radiative transitions involved are shown on the energy level diagram of Fig. 2(a).

The widest separation of Cr I terms occurs between the a^5D (E=1.0 ev) and a^5G (E=2.53) terms. It is quite possible that the relative population of these terms will differ significantly from the LTE value. On the other hand, rapid collisional transitions between the closely spaced terms <u>above</u> 2.53 ev, and between weakly bound levels and the free electron continuum, will tend to cause the relative populations of free electrons and excited Cr I levels above 2.53 ev to obey the LTE relationship[50]

$$\frac{n_e^2}{n_{0,i}} = \frac{(2\pi mkT)^{3/2}}{h^3} \frac{2Q_1(T)}{g_{0,i}} e^{-(I-E_i)/kT_e}, \qquad (42)$$

where $n_{0,i}$, $g_{0,i}$ and E_i denote, respectively, the number density, statistical weight, and energy of the i^{th} level of Cr I; I represents the ionization potential of Cr I, $Q_1(T)$ the partition function of Cr II, and T_e is the electron temperature. Equation (42) is known as the "combined Boltzmann-Saha equation", and we have written it with the assumption that the number of electrons equals the number of chromium ions.

In considering whether or not the relative populations of excited levels and the ground state correspond to thermodynamic equilibrium,

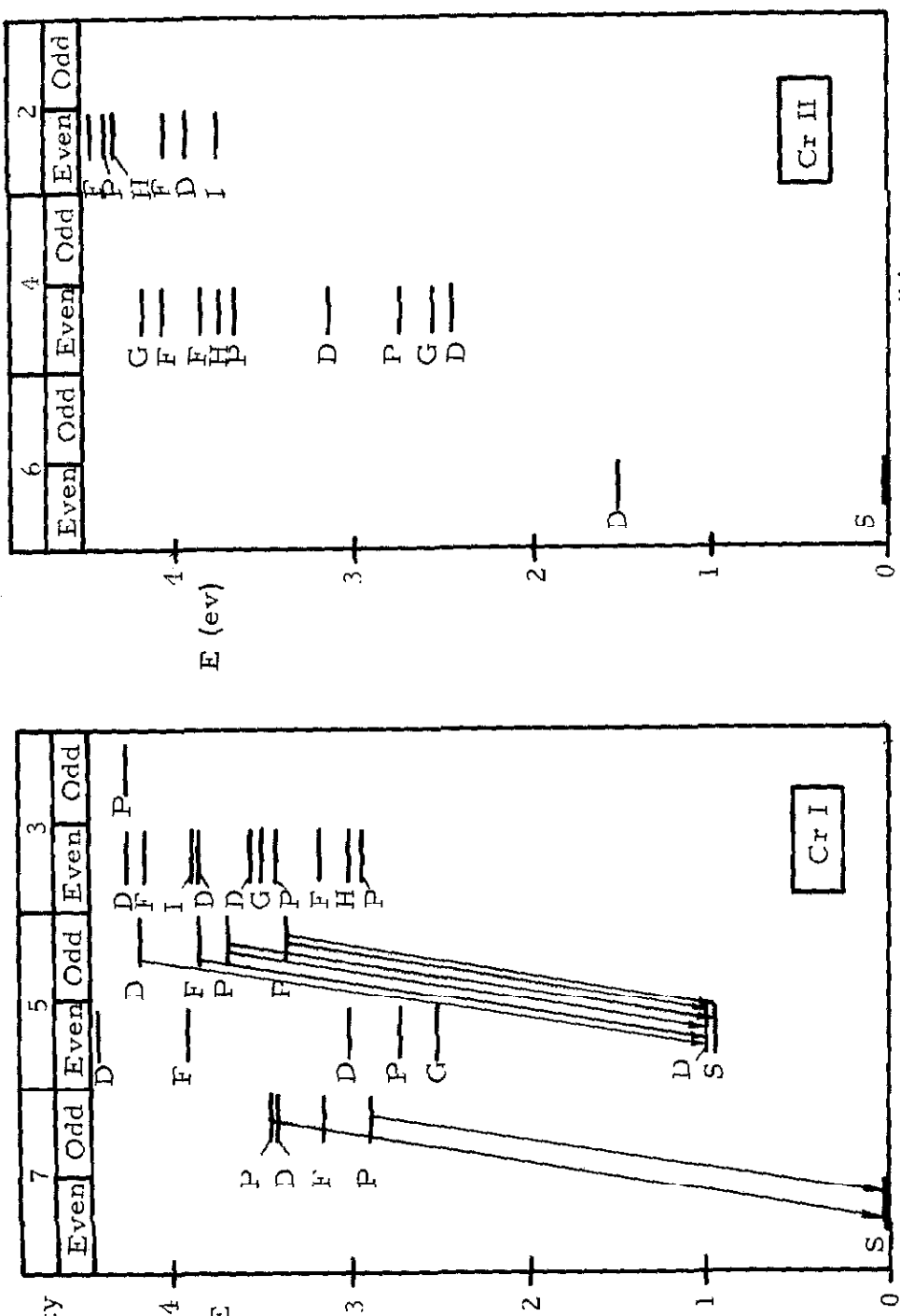

Fig. 2. Low-lying energy levels of Cr I (a) and Cr II (b). Spectroscopic terms are represented as single levels and designated in L-S notation, with the multiplicity and parity directly above and the term value indicated by the adjacent letter. The arrows in (a) indicate strong (i.e. L-S permitted) radiative transitions. Several infrared and intercombination transitions are not shown. All terms in (b) are of even parity, and therefore metastable.

it will be helpful to simplify the problem by "lumping together" all energy levels of Cr I for which the energy lies in the ranges 0-1 and 2.5-3.5 ev, and averaging the relative collisional and radiative transition rates between these two "sets" of levels. Since about two-thirds of the multiplets in the excited "set" are metastable and lifetimes of non-metastable upper levels are typically of the order of 10^{-8} sec, the average reciprocal radiative lifetime for the upper set will be about $\frac{1}{3} \cdot 10^{8}$ sec^{-1}. The radiative lifetime can be effectively extended by several orders of magnitude by means of the trapping of resonance radiation (i.e., self-absorption) as discussed by Weymann,[53] but at the low chromium concentrations used in our experiments it is not likely that the resulting increase in the effective radiative lifetime was much greater than a factor of 3.* We therefore take 10^{7} sec^{-1} as the effective reciprocal radiative lifetime of the upper set.

The relative populations of Cr I levels, with respect to the population of the ground state, will be determined by the relative frequencies of radiative and collisional transitions from the set of

---

* This factor may be estimated as follows: Let ℓ be a characteristic dimension of the heated gas (i.e., a few inches in our experiment). The integrated intensity of the emitted line radiation leaving the gas volume, if self absorption were not present, would be

$$I' = gf \frac{2\pi he^2}{m\lambda^3} \frac{n\ell}{Q} e^{-E_u/kT}$$

as noted in Equation (24). The actual intensity is some value which is less than I', and which we shall denote by I. The value of I can be determined from a study of the curves of growth (see Section III. B. 2). The lifetimes of upper states may be considered effectively increased by a factor I'/I, which is the ratio of the rate of radiant energy emission to the rate at which energy leaves the gas volume, for the spectral line in question.

terms between 2.5 and 3.5 ev to the set of three terms between 0 and 1 ev. The effects of radiative and three-body recombination of electrons and ions in populating the levels which make up these sets can be ignored at the temperatures and electron densities of interest here. In order to estimate the mean de-excitation rate of the upper set of levels, we make use of recent calculations of de-excitation probabilities for hydrogen by Byron, Stabler, and Bortz.[57] The mean separation of our two Cr I sets, 2.5 ev, approximates the separation of the n=3 and n=2 levels of H. At an electron density of $n_e = 10^{14} cm^{-3}$, the mean collisional de-excitation probability of the n=3 state is 2.10^7 sec^{-1}. Since this is only slightly greater than the mean radiative transition probability of 10^7 sec^{-1}, it is possible that our equilibrium ratios of Cr I excited state to ground state populations, $n_{0,i}/n_{0,0}$, may be smaller than LTE values.

The effect of collision-limited excitation upon the equilibrium degree of ionization can be determined in the following manner: The ratio of excited state to ground state populations will be some fraction η of the corresponding LTE ratio, i.e.,

$$\frac{n_{0,i}}{n_{0,0}} = \eta \frac{n_{0,i}^{(e)}}{n_{0,0}^{(e)}} \qquad (\eta \leq 1) \qquad (43)$$

where the superscript (e) denotes LTE values. According to the arguments presented in the preceding paragraph, η was probably somewhere between 0.1 and 1.0 under the conditions of our experiments. The value of η will be nearly the same for all levels above 2.53 ev.

At temperatures below 10,000°K, over 99% of the Cr I atoms will be in the a^7S ground state or in the metastable a^5D and a^5S terms at about 1.0 ev, which have LTE populations with respect to the ground state. The ratio $n_{0,0}/n_{0,0}^{(e)}$ can therefore be written

$$\frac{n_{0,0}}{n_{0,0}^{(e)}} \cong \frac{1-\alpha}{1-\alpha^{(e)}} \tag{44}$$

where α is the degree of ionization of Cr I, and $\alpha^{(e)}$ is the LTE ionization value, as predicted by the Saha equation. Since the values of $n_{0,i}$ for highly excited states must obey Equation (42) whether or not there is LTE with respect to the ground state, we may also write

$$\frac{\left(n_e^{(e)}\right)^2}{n_{0,i}^{(e)}} = \frac{n_e^2}{n_{0,i}} = f(T) ,$$

and

$$\frac{n_e^2}{\left(n_e^{(e)}\right)^2} = \frac{n_{0,i}}{n_{0,i}^{(e)}} = \frac{\alpha^2}{\left(\alpha^{(e)}\right)^2} . \tag{45}$$

Combining Equations (43-45) we obtain

$$\eta = \frac{\alpha^2}{\left(\alpha^{(e)}\right)^2} \frac{1-\alpha^{(e)}}{1-\alpha} , \tag{46}$$

which implicitly gives the degree of ionization, α, in terms of the "underpopulation factor" η.

Under the conditions of our experiments, the degree of ionization predicted by the Saha equation was $\alpha^{(e)} = 0.9990$. In this case, it may be readily verified that the values of α, n_e and $n_{0,i}$ are changed

by less than 1% if there are factor-of-ten deviations of the ratios $n_{0,i}/n_{0,0}$ from LTE values (i.e., $0.1 < \eta < 1.0$). We may therefore conclude that LTE calculations of the number densities for highly excited states of Cr I, and of the degree of ionization, should be accurate even though the computed ground state population of Cr I may be too low by some factor between one and ten.

The accuracy of the Cr II gf-values presented here depends mainly upon our assumed values for the populations of Cr II excited states. It has just been demonstrated that, although deviations from thermodynamic equilibrium population ratios for Cr I may occur, the degree of ionization as calculated by the Saha equation remains quite accurately determined. It remains to be demonstrated whether or not LTE population ratios for Cr II levels are obtained. A consideration of the Cr II energy level diagram in Fig. 2(b) reveals that all of the low-lying electronic levels, which are likely to have slow collisional de-excitation rates, are metastable. Their radiative lifetimes are therefore approximately 10^{-2} sec, and it appears quite safe to assume that LTE is obtained for Cr II.

On the basis of the theoretical arguments just presented, it does not seem likely that the gf-values presented here are systematically in error because of deviations from local thermodynamic equilibrium. This question has been discussed at length here because it arises as a possible explanation of the factor-of-nine discrepancy of our gf-values with those of Corliss and Bozman.[1]

It is clear that LTE should never be taken for granted in shock tube studies, as it often is, and that some experimental verification of

the assumption, such as noting the effects of a large variation in the electron density, is desirable.

2. The Curve of Growth

In order to obtain accurate gf-values by means of emission measurements, it is necessary to measure the absolute amount of radiation emitted by a known number of excited atoms, in the frequency interval corresponding to the transition involved. Under certain conditions, a significant fraction of the emitted radiation may be reabsorbed by atoms in the lower state of the transition, before it can escape the gas and be measured. The amount of radiation which is self-absorbed in this manner depends critically upon the spectral line shape and the optical depth.

As in Equations (22-24), let $I = \int_{\text{line}} I_\nu d\nu$ represent the steradiancy emergent from a column of heated gas, integrated over the frequency range corresponding to a single spectral line. A plot of I, as a function of the number of atoms of the emitting species per unit area along the line of sight, is known as a "curve of growth". Such a curve can be obtained theoretically by performing the integrations indicated in Equation (22), if the spectral line shape, $P(\nu)$, the number densities for the upper and lower states, and the gf-value, are all known.

For the case of pure Doppler broadening, the line shape function, $P(\nu)$, is given by

$$P(\nu) = \frac{1}{\sqrt{\pi}\Delta\nu_D} \exp\left[-\left(\frac{\nu - \nu_o}{\Delta\nu_D}\right)^2\right] \qquad (47)$$

$$\Delta\nu_D = \nu_o \left(\frac{2RT}{\sigma c^2}\right)^{1/2} , \qquad (48)$$

where ν_o is the frequency at the line center, σ the molecular weight of the radiating species, and R is the molar gas constant.

The combined effects of collisions and the finite lifetimes of excited states can usually be treated by making a Fourier analysis of a wave train which is damped and which undergoes phase shifts at each collision. The resulting line profile can be described by means of a dispersion formula,

$$P(\nu) = \frac{\Delta\nu_s/\pi}{(\nu-\nu_o)^2 + (\Delta\nu_s)^2} \qquad (49)$$

where $\Delta\nu_s$ is the "dispersion half-width". An accurate determination of $\Delta\nu_s$ usually requires either a direct experimental measurement or a consideration of the statistical and quantum mechanical aspects of the collision phenomena. Recent contributions to the theory of collision broadening have been described in the book by Breene.[58]

In general both Doppler and dispersion broadening are important. In this case $P(\nu)$ is a convolution of the functions given in Equations (47) and (49), i.e.,

$$P(\nu) = a\pi^{-3/2} \int_{-\infty}^{\infty} \frac{e^{-x^2}\,dx}{a^2 + (b-x)^2} , \qquad (50)$$

where

$$a = \frac{\Delta\nu_s}{\Delta\nu_D} \qquad \text{and} \qquad b = \frac{\nu-\nu_o}{\Delta\nu_D} .$$

Curves of growth which result from this combined type of broadening have been computed by van der Held.[59] Penner and Kavanagh[60] later extended these calculations over a wider range of broadening parameters. The integrated intensity, I, and the optical depth, $n\ell$, are conveniently nondimensionalized by introducing the quantities

$$C = \frac{\sqrt{\pi}\, e^2}{\Delta\nu_D mc} \frac{n\ell}{Q(T)} gf \left[1-\exp(-h\nu_o/kT)\right] \exp(-E_\ell/kT) \tag{51}$$

and

$$J(C, a) = \frac{I}{\Delta\nu_D B_{\nu_o}(T)} . \tag{52}$$

The reader is referred to the literature for graphical representations of the function J(C, a). For $C \ll 1$, J becomes a linear function of C and independent of the line broadening ratio, a. The spectral line is then said to be in the "linear portion of the curve of growth". This is another way of saying that self-absorption is negligible. In this case the integrated intensity is independent of the line shape function and one obtains, after some manipulation, the relation

$$I = gf \frac{2\pi he^2}{m\lambda^3} \frac{n\ell}{Q(T)} e^{-E_u/kT} . \tag{24}$$

At larger values of C, the curves of growth asymptotically approach a $C^{1/2}$ dependence for fixed values of $a(>0)$. In this case, it is impossible to obtain gf-values from intensity measurements unless the quantity, $a = \Delta\nu_s/\Delta\nu_D$, is accurately known in advance. Although $\Delta\nu_D$ is easily computed, $\Delta\nu_s$ is usually not reliably known. It is therefore imperative that gf-value measurements be made using lines

which are seen in the linear portion of the curve of growth.

Since a theoretical prediction of whether or not a line is observed in the linear region would depend upon prior knowledge of the gf-value (in order to compute the parameter C), an experimental verification of linearity is required. Wilkerson[2] demonstrated linearity by making a large number of runs at different densities and temperatures. The experimental scatter of data can make it difficult to establish the slope of the curve of growth by this method. Charatis[3] succeeded in determining the shape of the curve of growth in a single experiment by means of a multiple path technique. In our experiments, radiation emitted axially from the end wall of the shock tube was measured. Since the reflected shock travels (ideally) with constant speed away from the end wall, the observed optical depth increases linearly with time. By using photomultiplier pickups, direct observations of the curve of growth were thus obtained (cf. Section V). All gf-value measurements were based upon experiments in which the observed curve of growth was linear.

3. The Slit Function

A monochromator, such as the ones used in our experiments, actually measures a weighted average of the intensity of radiation in a small wavelength interval. The width of the wavelength interval to which a monochromator will respond, when set to record radiation at a particular wavelength, depends upon the dispersion of the instrument and the width of the entrance and exit slits. The weighting function is known as the slit function (see, for example, Chapter 5 of Ref. (61)).

If the instrument is set at λ' and light of intensity $I_\lambda(\lambda)$ is incident upon the entrance slit, the recorded signal will be

$$S(\lambda') = K(\lambda') \int_0^\infty g(\lambda-\lambda')I_\lambda(\lambda)d\lambda , \tag{53}$$

where $g(\lambda-\lambda')$ is the slit function* and $K(\lambda')$ is an experimental proportionality factor. Usually the slit function is zero except within a narrow wavelength interval defined by $|\lambda-\lambda'| \leqq \Delta\lambda^*$, in which case we may write

$$S(\lambda') = K(\lambda') \int_{\lambda'-\Delta\lambda^*}^{\lambda'+\Delta\lambda^*} g(\lambda-\lambda')\, I_\lambda(\lambda)d\lambda \tag{54}$$

The units in which $K(\lambda')$ is expressed are of no interest, since only the ratio of the signal to that due to a standard light source is of importance; one may therefore arbitrarily normalize $g(\lambda-\lambda')$ so that $g_{max}=1$. The shape of the slit function may be determined by varying the setting, λ', in the vicinity of a single narrow line of wavelength λ_o, and observing the response of a linear detecting device located behind the exit slit.

The wavelength setting of our instrument (a Perkin-Elmer Model 98 monochromator) is adjusted by means of an arbitrarily calibrated dial which controls the rotation of the Littrow mirror.

---

* The value of the slit function also depends upon the wavelength setting (λ') and the widths of the entrance and exit slits; however, since these parameters are constant during a shock tube run, only the dependence upon $\lambda-\lambda'$ is indicated.

The true value of λ' corresponding to a certain dial setting will be defined as that wavelength to which the instrument is most sensitive; hence

$$g(\lambda - \lambda' - 0) = g_{max} = 1.$$

In practice, λ' was determined by calibrating the instrument at a series of known wavelengths and interpolating between points at which calibrations had been made. Performing this calibration as accurately as possible, there was still an uncertainty of from 1/2 to 2 Å in the value of λ' corresponding to a particular dial setting.

The choice of slit widths depended upon the line(s) being investigated. The slits had to be narrow enough to minimize contributions from background radiation and exclude nearby multiplets, and yet wide enough to admit sufficient light and minimize the error in $g(\lambda - \lambda')$ due to the uncertainty in λ'. At wide slit openings (> 100 microns) the slit functions were nearly of the triangular form expected for instruments of the type used, while for narrower slit widths the functions took on a somewhat Gaussian form. Representative slit functions are shown in Fig. 3.

To monitor radiation from a single spectral line of wavelength λ_o, the monochromator dial is set at $\lambda' = \lambda_o$ (within the limits of accuracy of the wavelength calibration). In our experiments, the width of the slit function base, $2\Delta\lambda^* \approx 20$ Å, was many times larger than the characteristic widths of spectral lines investigated ($\approx 10^{-1}$ Å); it was therefore possible to approximate $g(\lambda - \lambda')$ by a constant value $g(0) = 1$ over the width of the line. Equation (53) then becomes

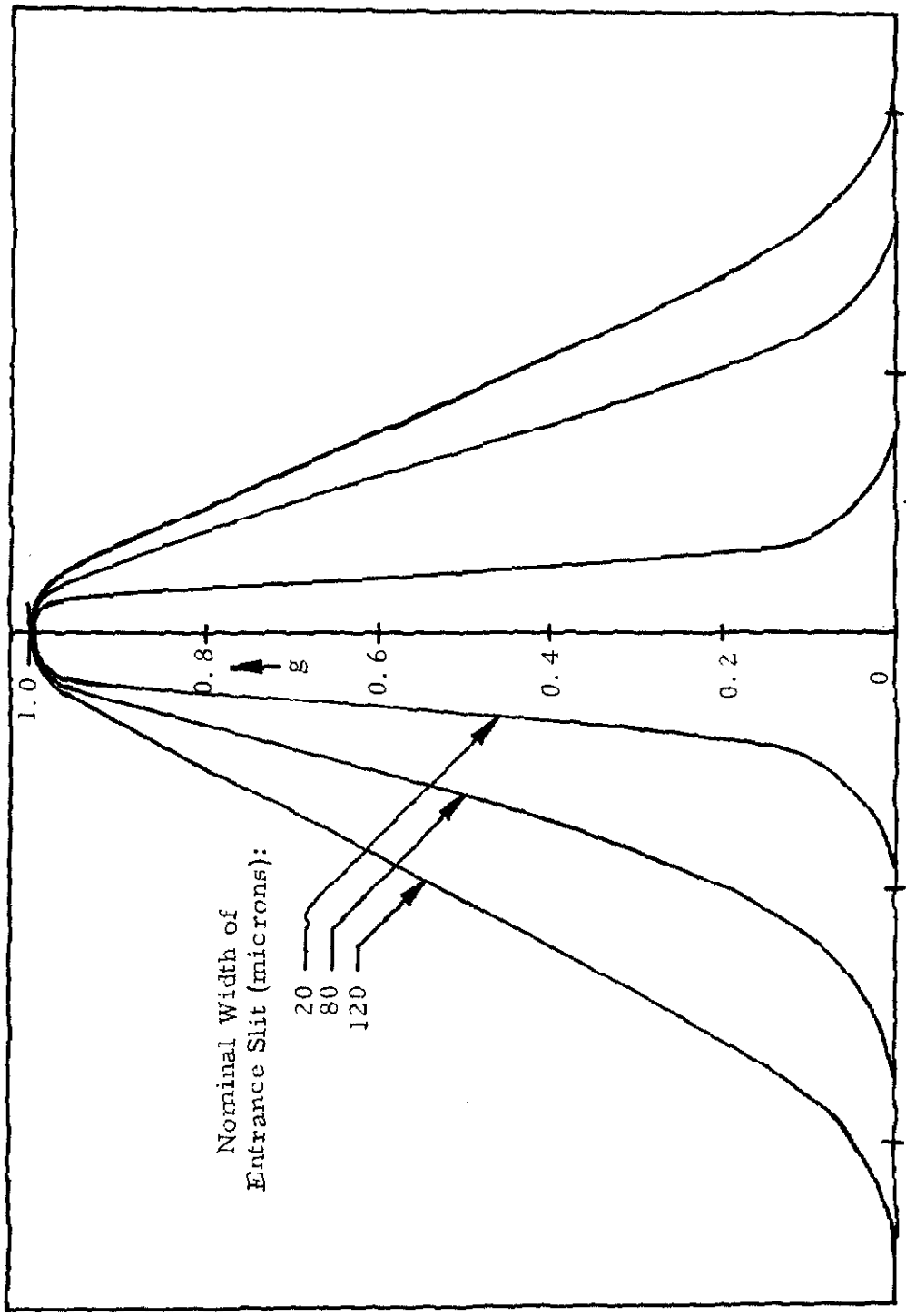

Fig. 3. Typical slit functions, $g(\lambda-\lambda')$, for a Perkin-Elmer Model 98 Monochromator utilizing a LiF prism, as determined by scanning the λ3341 line of Hg.

$$S_{Line}(\lambda') = K \int_{Line} I_\lambda(\lambda)d\lambda = K \int_{Line} I_\nu d\nu = KI_L, \tag{55}$$

where I_L is the integrated steradiancy of the line. If the monochromator is left at the same settings and the detector sensitivity, K, is unchanged, the response to a continuum source of steradiancy $I_{\lambda,c}(\lambda)$ will be given by

$$S_c(\lambda') = K \int_{\lambda'-\Delta\lambda^*}^{\lambda'+\Delta\lambda^*} I_{\lambda,c}(\lambda)\, g(\lambda-\lambda')d\lambda \ . \tag{56}$$

When the steradiancy of the continuum is approximately constant over the $2\Delta\lambda^*$ width of the slit function base, Equation (56) becomes simply

$$S_c(\lambda') = K I_{\lambda,c} \int g(\lambda-\lambda')d\lambda \tag{57}$$

Comparing Equations (55) and (57),

$$\frac{S_{Line}(\lambda')}{S_c(\lambda')} = \frac{I_L}{I_{\lambda,c}\int g(\lambda-\lambda')d\lambda} \ . \tag{58}$$

An absolute measurement of the integrated intensity of a line is therefore possible if a calibrated continuum source is available and the integral of the slit function is known.

The technique may be extended in a straightforward manner to the case where radiation from several lines falls within the width of the slit function. If the relative strengths of the lines are known in advance, the contribution of each line to the net signal can be weighted by the relative intensity and the slit function value. By performing

an absolute calibration, the relative line strengths can be put on an absolute basis. This method is suitable for the measurement of gf-values for close multiplets, for which relative line strength measurements are usually available, and is discussed further in Section V. C.

IV. APPARATUS

A. The Shock Tube and Spectroscopic Equipment

A schematic diagram of the shock tube and the equipment for radiation measurements is shown in Fig. 4. The shock tube is the same one that was used previously by Watson[6, 49, 62] to measure temperatures and the electronic f-value for a band system of OH. The reader is referred to his dissertation or to his open-literature publications for a discussion of details omitted here.

In preliminary work, a Hilger Medium Quartz Spectrograph was used to record survey spectra of the radiation emitted near the shock tube end wall, in the wavelength range 2500-5500 Å. These spectra, although not time-resolved, aided in the identification of impurities, and in the selection of operating conditions and lines to be investigated. For the determination of gf-values, radiation emitted along the shock tube axis was split into two beams and monitored by means of two Perkin-Elmer Model 98 single-pass prism monochromators. Each monochromator was set to record the radiation of a single line or close multiplet. Although only one monochromator is essential for an experiment of this type, the availability of two made it possible to gather more data with each shock tube run. A view of the shock tube and optical equipment is presented in Fig. 5. The calibrated light source (discussed in part B of this section) is at the opposite end of the tube and not visible in this figure.

The shock tube was of the conventional, pressure-driven type

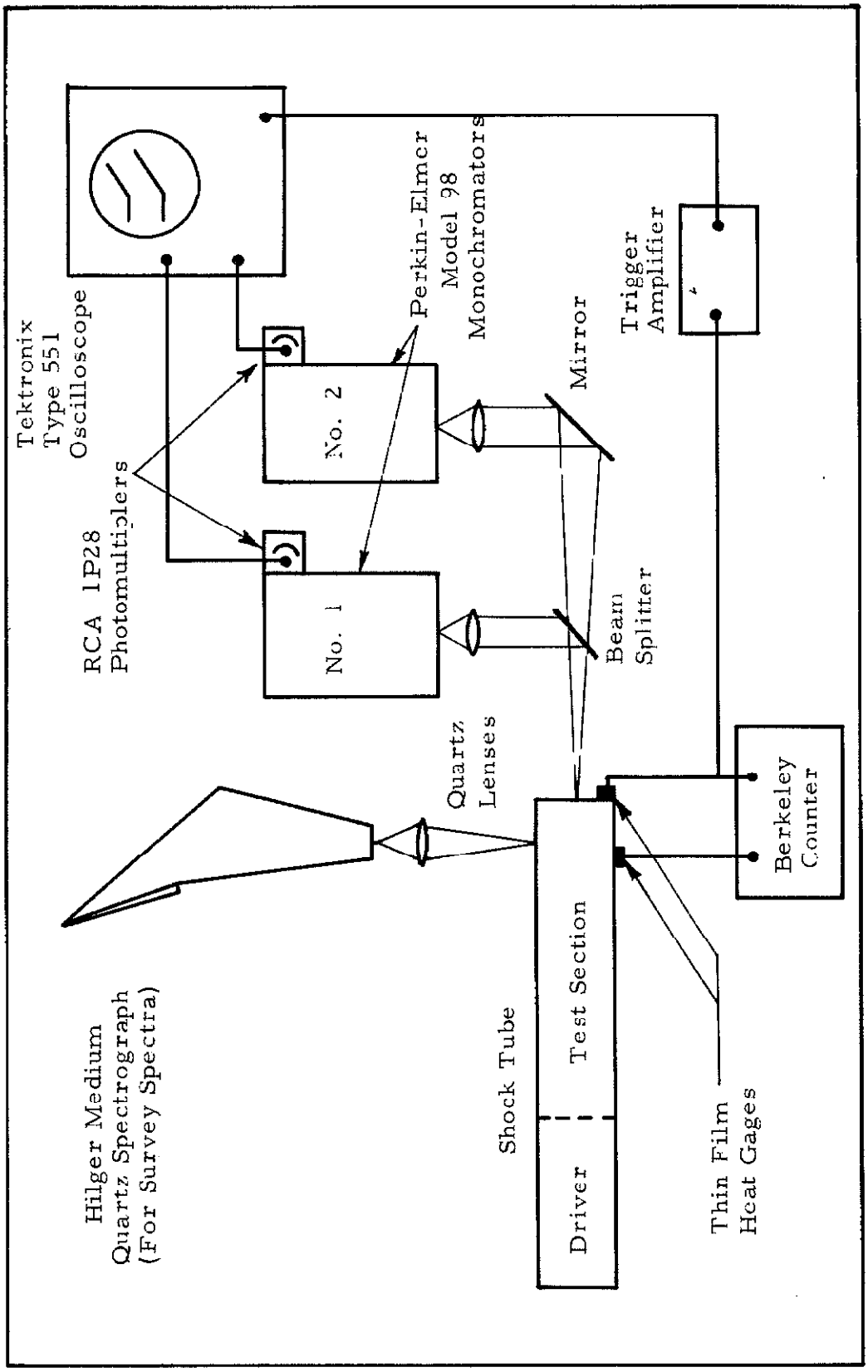

Fig. 4. Schematic diagram of the shock tube and equipment for radiation measurements.

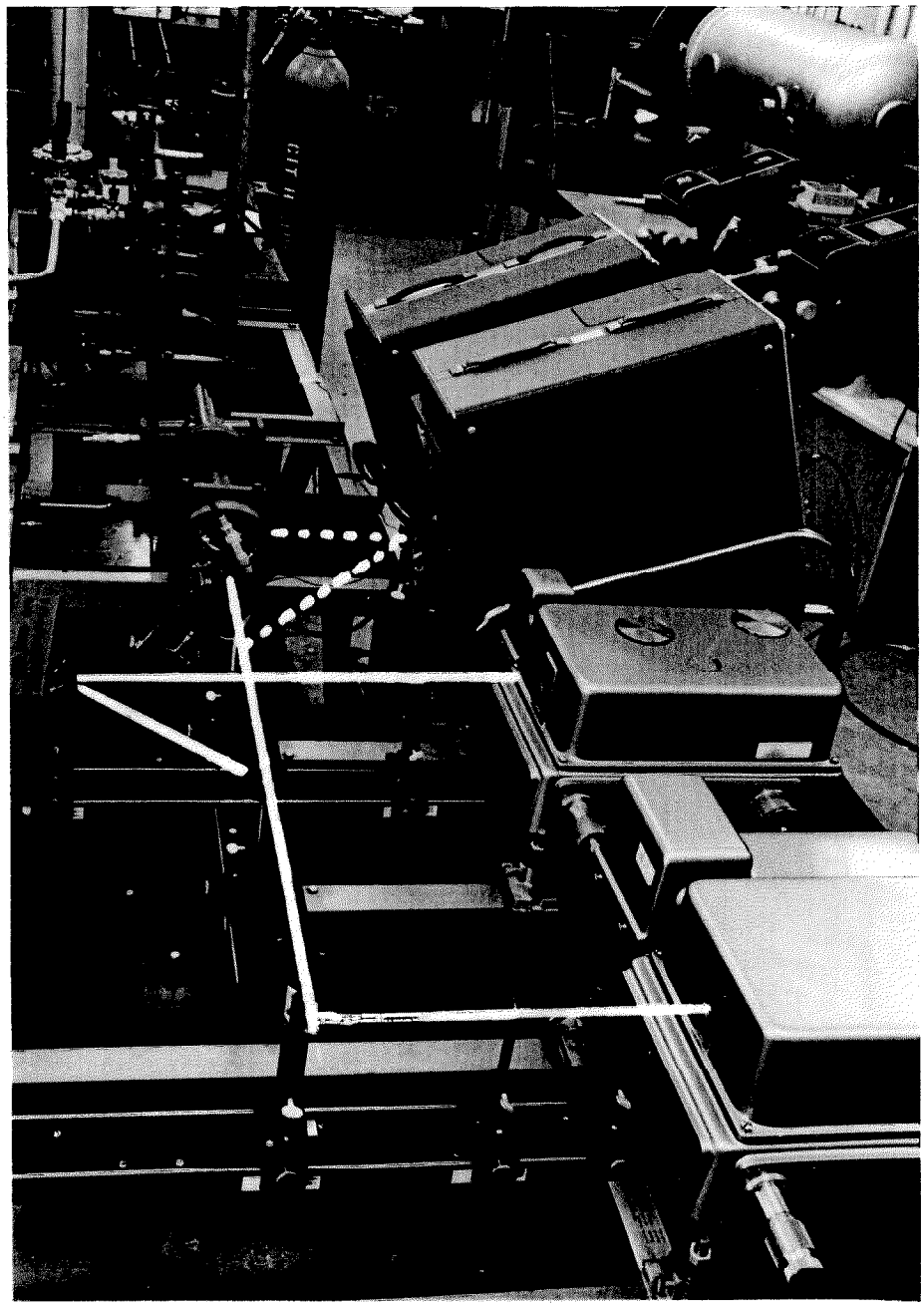

Fig. 5. Shock tube and dual monochromator arrangement for measuring emission at two wavelengths. The solid line shows the optical path of light emitted along the tube axis for gf-value measurements. By adding two mirrors, light emitted normal to the tube axis, along the dotted line, can be monitored for relaxation studies (described in Part II).

without area change at the diaphragm. The test section was 6 feet in length and constructed from mild steel tubing, honed to an internal diameter of 3.079 ± .001 inches with a surface finish of RMS 20 micro-inches. The high pressure section was five feet long and fabricated from the same type of tubing, but was not honed. Mylar diaphragms were used to separate the two sections. By using a two-inch diameter diffusion pump, together with a liquid nitrogen cold trap, the test section could be evacuated, in a few hours, to a pressure of 0.1 micron Hg with an indicated leak rate of approximately one micron per hour. A General Electric type 101 Quartz window, of 1/4 inch thickness, was located in the center of the shock tube end plate. A second quartz window of 3/16 inch thickness was located in the side of the shock tube, 1.80 inches from the end wall. Both windows had effective apertures of 1 cm.

Incident shock velocity measurements were made with two platinum thin film heat gages, one of which was mounted in the end plate while the other was imbedded in the wall of the shock tube 454 mm from the end. The elapsed time for shock passage between these two gages was recorded by means of a Berkeley counter. The heat gage in the end wall also served to trigger the oscilloscope when the incident shock wave was reflected.

Each monochromator was equipped with an RCA 1P28 photo-multiplier tube. Light leaving the monochromator exit slits was focused onto the photocathodes of these tubes by means of quartz condensing lenses. A regulated voltage of between 400 and 1000V,

depending upon the gain desired, was applied to the voltage divider network of each tube. The anode current of each tube passed through a 10K load resistor and the resulting voltage signals were recorded by means of a Tektronix 551 dual beam oscilloscope. The output voltage of each photomultiplier detection system was found to be a linear function of the intensity of incident radiation, provided the ratio of anode current to voltage divider current did not exceed the value of 0.1 recommended by the manufacturer. The time constant for the detection systems was approximately 0.5 μsec, being mainly the result of the combined effects of the 10K load resistors and the distributed capacitance of the coaxial cables connecting them to the oscilloscope. Since the available testing time for these experiments was about 100 μsec, the response was more than adequately fast.

B. Absolute Intensity Calibration Equipment

An absolute intensity calibration was performed by forming an image of a continuous light source of known steradiancy at the shock tube exit window, and observing the resulting responses of the photomultipliers. The calibrated light source and the image-forming lenses were located at the opposite end of the shock tube from the exit window. The optical arrangement is shown schematically in Fig. 6; for simplicity only one monochromator is represented in the diagram.

A GE 30A/T24/6 Volt tungsten strip lamp was used as the calibrated light source. The steradiancy of this lamp was determined by a comparison with another lamp of the same type which had been calibrated by the National Bureau of Standards. For operation at 35.0

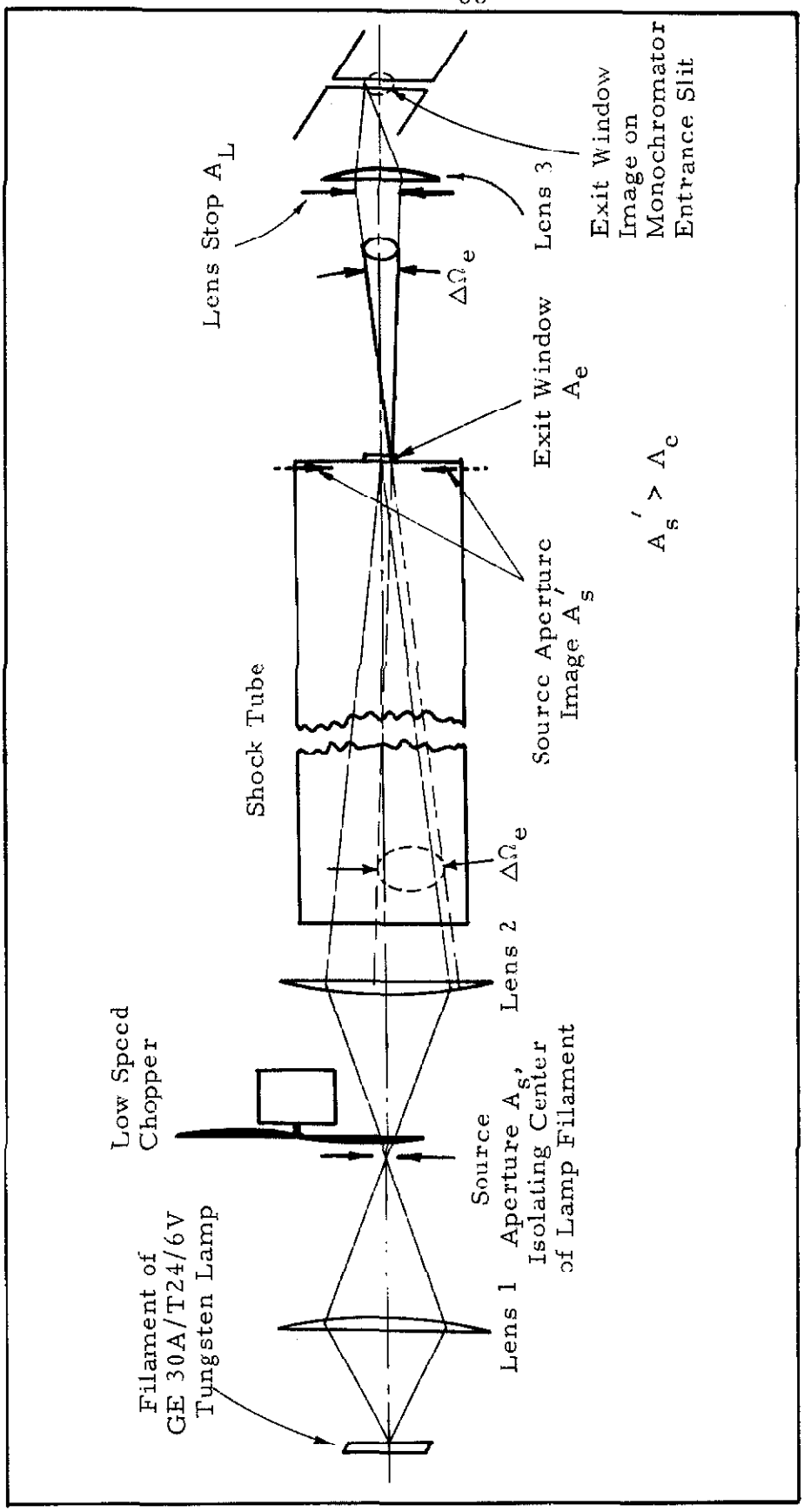

Fig. 6. Schematic representation of optical arrangement for absolute intensity calibration. Lens 3 is stopped down to area A_L to cause the solid angle $\Delta\Omega_e$, subtended by A_L from each portion of the exit window, to intercept an area completely within the aperture of lens 2 when extended to the left along dashed lines. This ensures that all illuminated portions of the slit receive the same solid angle of light from the source. The same solid angle is collected during a shock tube run.

amperes (rms AC), the NBS had measured steradiancy values for the latter lamp at wavelengths between 2500 and 7500 Å. Since the radiative characteristics of tungsten lamps are subject to slow changes when operated at high currents for a few hours, the NBS lamp was used only briefly to calibrate the second lamp as a "working standard". A Leeds and Northrup optical pyrometer was used to ensure that the brightness temperature of the working standard lamp (at 6500 Å) was equal to that of the NBS lamp operating at the specified current. By interchanging the lamps in the calibration optical system and comparing their intensities at other wavelengths, it was found that their steradiancies differed by less than 5% at all wavelengths between 3000 and 6500 Å, provided their brightness temperatures, as determined by the optical pyrometer, were in agreement.

The lamp current was supplied by a regulating stepdown transformer, the input voltage of which was adjusted by means of a variable autotransformer. A small portion of the lamp filament was isolated as a source by imaging the filament on a square aperture of 0.0232 cm^2 area (A_s in Fig. 6). This source aperture was then imaged at the shock tube exit window by means of a second lens. Light from the calibrated source was chopped at a frequency of 50 c/sec so that the intensity could be measured as an AC signal on the oscilloscope.

Further details concerning the intensity calibration procedure are discussed in Section V. C.

C. The Gas-Handling System

A flow system was constructed which permitted argon to be mixed with chromium carbonyl in controllable proportions, and flushed through the shock tube test section for ten minutes prior to each run (see Fig. 7). The flushing procedure was adopted in order to permit the walls of the shock tube and the flow system to reach adsorption equilibrium with the gas mixture.

Gas mixing was accomplished by passing Ar of 99.998% purity through a packed column of $Cr(CO)_6$ crystals. By making use of mass transfer data of Wilke and Hougen,[64] the column dimensions and the flow rates were chosen so as to ensure that the gas mixture leaving the mixing column would be completely saturated with $Cr(CO)_6$. Saturation of the gas mixture was also indicated by the fact that variations in the flow rate through the column had no noticeable influence upon the experimentally determined gf-values.

The column consisted of a commercial Corning type 39530 gas dispersion tube of 0.2 in I.D., having a coarse fritted glass permeable diaphragm at one end. The diaphragm end of this tube was packed with three inches of $Cr(CO)_6$. Since the pore size of the diaphragm ($50\,\mu$) was about 10^3 times larger than the mean free path of $Cr(CO)_6$ molecules in the column, it is unlikely that the gas composition was appreciably altered by preferential diffusion through the diaphragm.[65] The composition was calculated from $Cr(CO)_6$ vapor pressure data of Wilkerson[2] and a measurement of the total pressure in the mixing flask (the pressure drop across the porous diaphragm was negligible

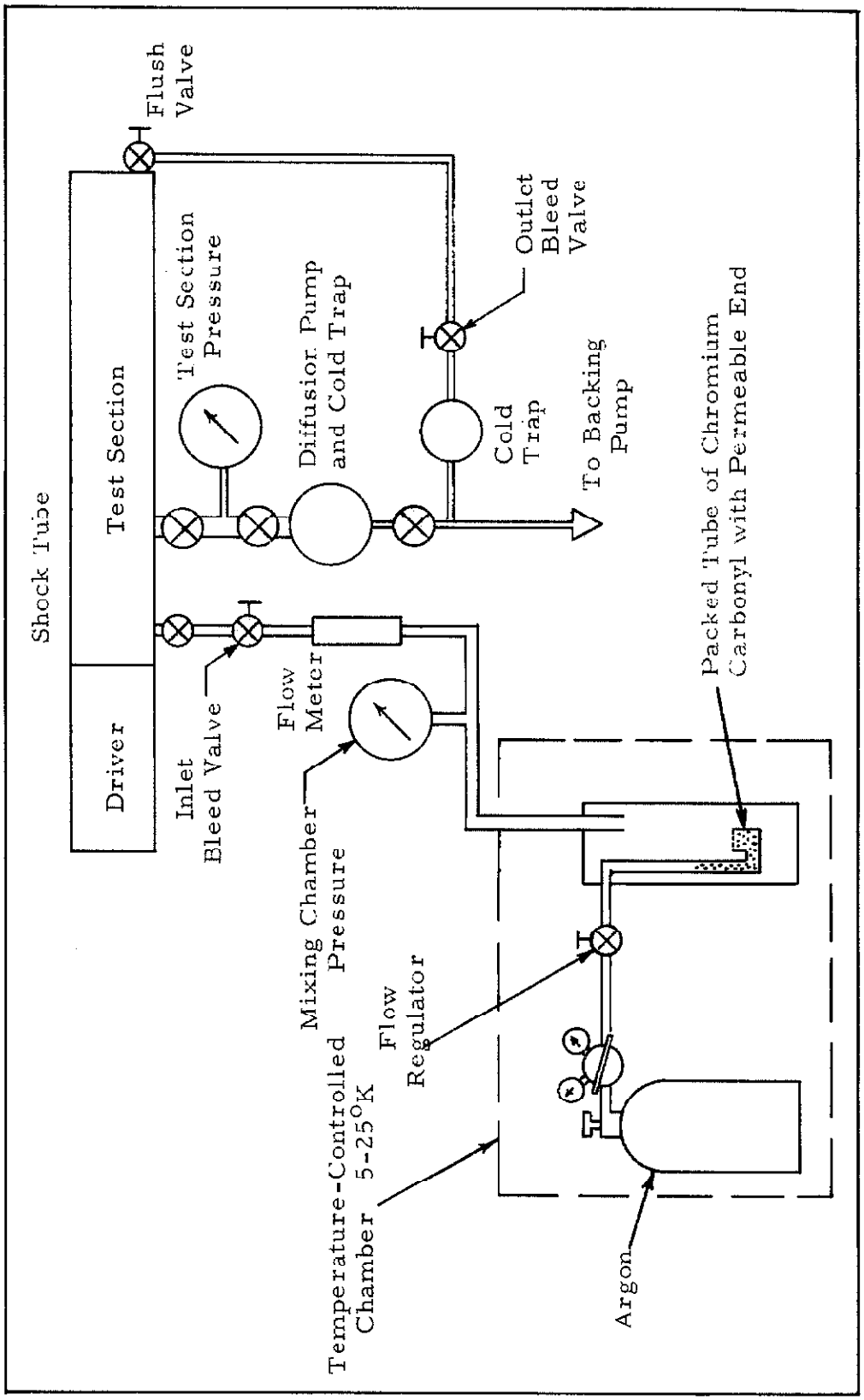

Fig. 7. Schematic diagram of shock tube and gas handling system.

at the flow rates employed).

The argon bottle and mixing apparatus were enclosed in a thermally insulated chamber. A thermostat-controlled air conditioner permitted the temperature within the chamber to be varied between 5°C and 25°C, with fluctuations of less than 1°C. This provided a sensitive control of the vapor pressure of chromium carbonyl. The flushing rate, mixing system pressure and test section pressure were controlled by simultaneous adjustment of a flow regulator and two bellows-sealed bleed valves located at opposite ends of the test section. The test section pressure was measured with a Wallace and Tiernan mercury manometer.

A special "flush" valve, designed by Watson and described in his dissertation, was used to seal off the end of the test section before each run. The end of the valve stem was designed to be flush with shock tube end wall when the valve was closed, thus eliminating flow disturbances.

The temperature of the gas downstream of the flush valve was measured with a thermocouple probe and found to be within 1°C of room temperature, regardless of the temperature of the gas mixing system.

V. EXPERIMENTAL PROCEDURE

A. Preliminary Spectral Measurements

Before the gf-value measurements were carried out, it was necessary to examine the spectra of shock-heated $Cr(CO)_6$-Ar mixtures in the wavelength region of interest (2400-5500 Å), for the purpose of selecting those lines of Cr I or Cr II which were suitable for analysis. Only lines or multiplets which could be isolated by the monochromators, and which were visible in optically thin layers, were ultimately chosen. Preliminary time-resolved measurements of the intensities of Cr I and Cr II lines were also made, in order to assess relaxation effects and non-ideal shock tube behavior, and to determine the optimum operating conditions for observing specific transitions.

1. Discussion of the Spectra

Spectra were photographed with a Hilger Medium Quartz Spectrograph, using 103-O UV-sensitive plates. The spectrograph was positioned to collect radiation from the side window of the shock tube, located 1.80 inches from the end wall (see Fig. 4).

A series of spectra taken under different conditions is shown in Fig. 8. For each spectrum, the incident shock Mach number and the temperature and pressure behind the reflected shock wave are listed. The radiation which the spectrograph collected during a shock tube run was actually emitted by gas under a variety of conditions, because of the relaxation effects and the several shock wave interactions; hence no unique temperature and pressure can be ascribed to the conditions under which spectra were taken. The highest temperature attained by

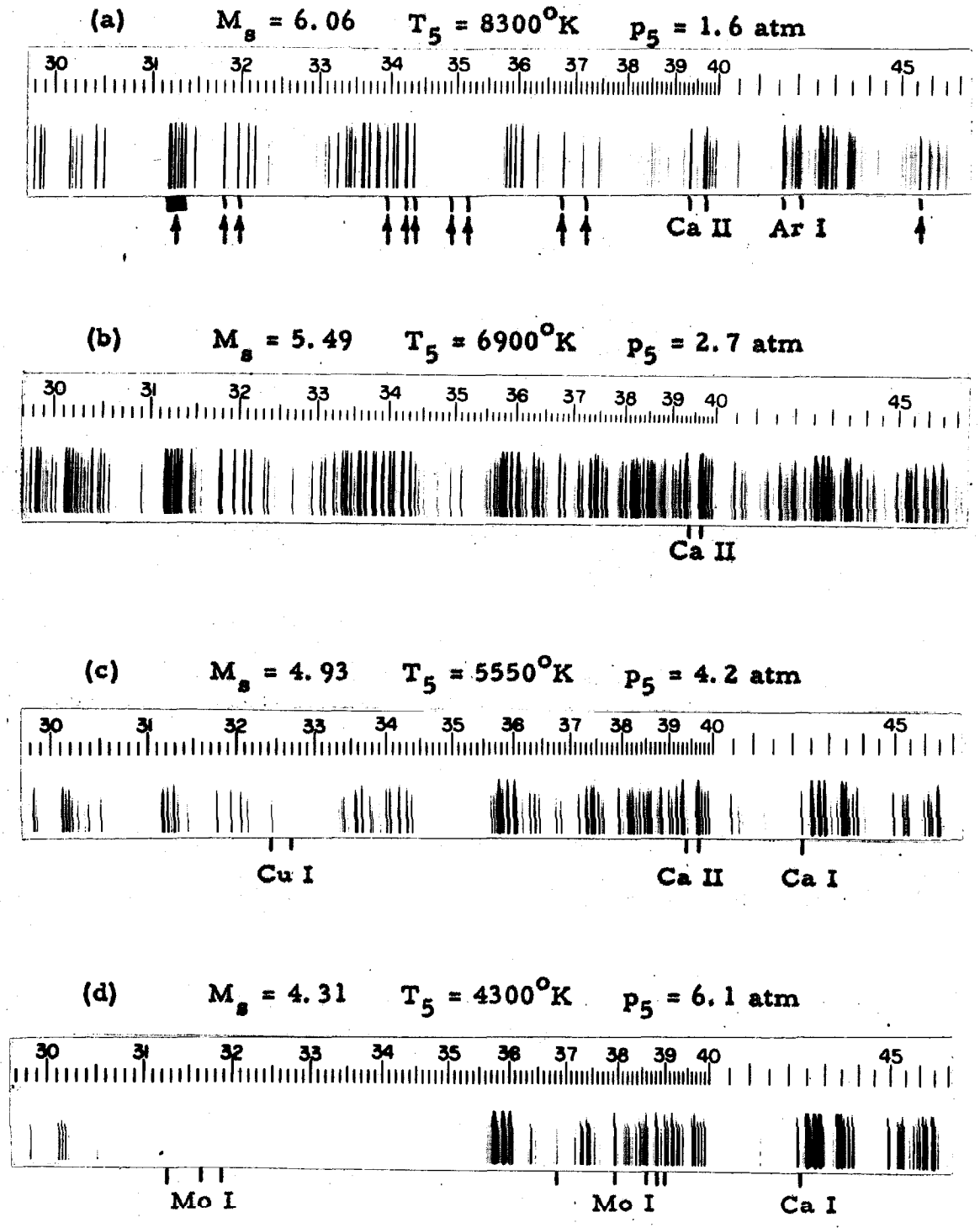

Fig. 8. Time-integrated spectra of shock-heated mixtures of $Cr(CO)_6$ and Ar. The incident shock Mach number, M_s, and the temperature and pressure behind the reflected shock, are listed above each spectrum. Spectral lines are due to Cr I and Cr II, with the exception of those noted. Arrows in spectrum (a) designate Cr II lines or multiplets for which gf-value measurements were made.

the gas was equal to the temperature T_5 behind the reflected shock for those cases where multiple reflections did not occur (i.e., for incident shock Mach numbers below the "tailoring" value of 4.1*); for stronger shocks the gas reached a temperature somewhat higher than T_5. Since most radiation is emitted by the most highly heated gas, T_5 is a fair indication of the temperature of the gas producing the spectra.

The spectrum for which $T_5 = 4300^{\circ}K$ shows mostly Cr I transitions, although several resonance lines of Mo I are also visible. Evidently the $Cr(CO)_6$ vapor contained approximately one part per thousand of chemically similar $Mo(CO)_6$. The λ4227 resonance line of CaI also appears. Since calcium lines were also present in pure argon shocks, it is believed that it may have been introduced in the decomposition of Mylar diaphragm fragments by the heated gas. This opinion was given further basis by later time-resolved measurements of Ca II resonance lines, which showed that most of this radiation comes from the region of the reflected shock-contact surface interaction.

Both Cr I and Cr II lines are present in the T_5-5500°K spectrum. According to the Saha equation, the chromium would be about 70% ionized at equilibrium behind the reflected shock wave for this case. The Mo I lines are still faintly visible, and impurity resonance lines of Ca I, Ca II (λ3934, 3968), and Cu I (λ3248, 3274) are also in evidence. The source of the Cu lines was probably the copper tubing in the gas-handling system.

---

* "Reflected shock tailoring" is a term often used to describe the condition where the reflected shock passes through the contact surface, leaving it stationary.

The T_5=6900°K and T_5= 8300°K spectra are completely dominated by Cr II lines; however, the resonance lines of Cr I (λ 4254, 4275, 4290; 3575, 3593, 3605) and a few others, are visible. The two Ca II lines are still strong and, at T_5= 8300°K, a few ArI lines appear. Subsequent time-resolved measurements of the argon lines revealed that these were actually only excited behind multiple reflected shocks (see Fig. 1) where the temperature was a few thousand degrees higher than T_5. The carbon line λ 2479 was also observed at the higher temperatures, but this region of the spectrum is not shown in Fig. 8.

In selecting lines for gf-value measurement, it was necessary to choose those which were separated by at least 10 Å from nearby lines of other multiplets, because of the limited resolution of the monochromators. This meant that only a relatively small number of the observed lines could be used. At the higher temperatures, only Cr II lines were suitable; those which were ultimately chosen are designated in the T_5= 8300°K spectrum of Fig. 8. At these temperatures, the Cr I lines display a strong "population overshoot" at the reflected shock front which dominates the radiation viewed along the shock tube axis. The overshoot phenomenon was first noticed by Wilkerson[2] and is further discussed in the following paragraphs and in Part II of this dissertation. The overshoot and the proximity of Cr I lines to other lines rendered them unsuitable for gf-value measurements at temperatures above 5500°K by the technique which we employed.

2. Preliminary Time-Resolved Measurements

Time-resolved measurements of the radiation from selected lines of Cr I and Cr II were performed by focusing light from the side window of the shock tube onto the monochromator entrance slits, as illustrated in Fig. 5. A typical oscilloscope record of the simultaneous intensities of the Cr II λ3421, 3423 and the Cr I λ3977, 3984, 3994 line groups is shown in Fig. 9. Both sets of lines were seen at low optical depths, so that the oscilloscope deflections are directly proportional to the number densities of atoms in the upper states of the corresponding transitions. The temperature behind the reflected shock wave, as computed from the incident shock velocity, was 7150°K for the run shown. The traces indicate that ionization and electronic excitation processes reached equilibrium within 60 μsec after the gas had passed through the reflected shock wave, and that the intensities of Cr I and Cr II lines remained steady for another 60 μsec thereafter, after which further heating due to the contact surface interaction occurred. The relaxation processes were faster for stronger shocks and for mixtures containing more $Cr(CO)_6$ (cf. Part II). At temperatures below about 5500°K, it was not possible to reach a state of equilibrium behind the reflected shock wave before further shock interactions occurred. Furthermore, according to the arguments presented in Section III. B, the electron densities produced by much weaker shocks would probably be too low to bring about LTE excited state populations for Cr I, even if the shock tube testing times were infinitely long.

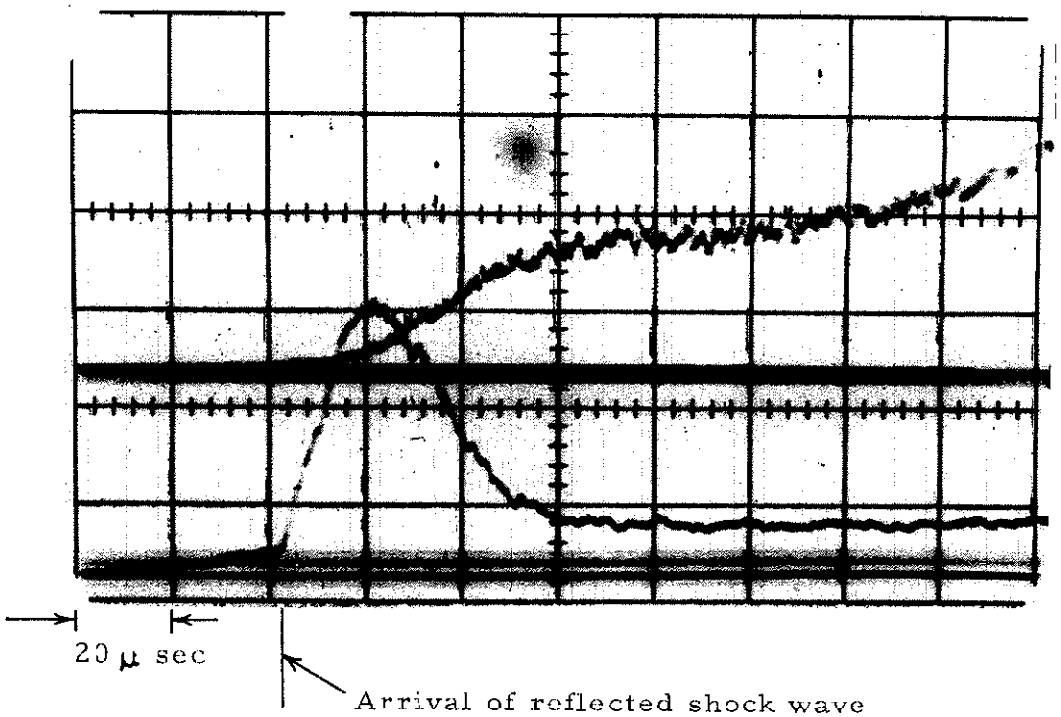

Upper trace:
Cr II λ3421.2, 3422.7
(E_u = 6.0 ev, E_ℓ = 2.4 ev)

Lower trace:
Cr I λ3976.7, 3983.9, 3991.7
(E_u = 5.6 ev, E_ℓ = 2.5 ev)

T_5 = 7150°K p_5 = 2.8 atm

Cr concentration 0.0043%

Fig. 9. Oscilloscope record of the intensities of Cr I and Cr II transitions, showing relaxation effects. The observation was made looking across the shock tube at a point 1.80 inches from the end wall. The abrupt rise in the lower (Cr I) trace indicates passage of the reflected shock wave past the observation window. For approximately 120 μsec thereafter the gas is at the temperature T_5 and pressure p_5 listed above. During this interval equilibrium levels of ionization and electronic population are attained. At the end of the upper (Cr II) trace a second rise occurs, as a result of an interaction with the contact surface.

On the basis of these preliminary studies, it was decided that Cr I gf-values could not be reliably measured without a major modification of the experimental equipment. At the high temperatures required to bring about thermodynamic equilibrium within the available testing time, the nonequilibrium "overshoot" region contributed most of the Cr I radiation as seen looking along the shock tube axis (as the gf-value measurement experiment had been set up). In addition, the monochromators could not adequately separate the Cr I lines from nearby Cr II and continuum radiation at these temperatures. We therefore decided to make gf-value measurements for Cr II lines only, using reflected-shock heated gas mixtures at about 8000°K.

B. Shock Tube Radiation Measurements

The preliminary operations described in the preceding paragraphs made possible the selection of Cr II transitions for which intensity measurements could be made, and demonstrated that fairly steady excited state populations could be achieved behind the reflected shock wave under suitable shock tube operating conditions. Following the preliminary operations, the optical system was rearranged for the purpose of verifying the linearity of the curves of growth for the selected lines, and ultimately measuring their gf-values.*

---

* We also intended to confirm the validity of ideal shock theory by measuring the temperature spectroscopically, using observed relative intensities of Cr II lines together with relative gf-values of Corliss and Bozman to determine relative populations of electronic levels (see, for example, p. VI of Ref. (1)). This technique makes use of the $\exp(-E_u/kT)$ dependence of excited state populations upon the energy E_u; in our case, however, the values of E_u for the usable Cr II lines were not sufficiently different from each other to enable temperature determinations to be made by this method.

Images of the quartz window in the shock tube end plate were formed at the monochromator entrance slits by means of quartz condensing lenses. The apertures of these lenses were stopped down so that the solid angle, $\Delta\Omega_e$, which they collected could be completely filled by radiation from the calibrated source (see Fig. 6). The value of $\Delta\Omega_e$ was approximately $3 \cdot 10^{-5}$ steradians for both lenses.

Besides the eleven lines and line groups which were chosen for gf-value measurements (see Fig. 8), two dozen other transitions in the wavelength region 2600-3100 Å were judged to be of sufficient intensity and spectral purity to be included in the investigation. These had to be ruled out, however, because of the scattering of light of longer wavelengths inside the monochromators during the absolute intensity calibration. With the tungsten strip lamp as light source and a monochromator adjusted to record the intensity at 3000 Å, approximately 90% of the observed signal was due to scattered visible light, with an undetermined fraction of the remainder of the signal being caused by scattered UV light; the situation rapidly became worse at shorter wavelengths. This problem has been discussed in detail by Watson in Ref. (62). The situation can be greatly improved by making the light pass through a filter which is opaque to visible radiation. A filter of this type (Corning 7-54 glass) was used by us to permit absolute intensity calibrations to be carried out in the wavelength interval 3100-3500 Å. For $\lambda \lesssim 3100$ Å, scattered radiation transmitted by the filter still accounted for an appreciable but not accurately known fraction of the observed signal; for $\lambda \gtrsim 3500$ Å no filter was necessary. When the filter was used, it was positioned just past the shock tube exit window and left in place during both the shock

tube run and the absolute intensity calibration.

In preparation for shock tube radiation measurements, the temperature-controlled chamber in which the Ar-$Cr(CO)_6$ mixtures were prepared (see Fig. 7) was cooled down to a uniform temperature. Argon was then passed through the $Cr(CO)_6$ column at about 1 atm abs and a flow rate of 400 cc/min, throttled down to the test section pressure of 5.0 mm Hg, and flushed through the shock tube. The mole fraction of $Cr(CO)_6$, was $4.3 \cdot 10^{-5}$ for the runs from which gf-value determinations were obtained. When concentrations of $4 \cdot 10^{-4}$ were used, self-absorption of the more intense lines was observed after the reflected shock had traveled a few inches from the end wall.

The reliability of the continuous flushing technique as a means of controlling the composition of H_2O-Ar mixtures in shock tubes has been demonstrated by the analyses of Watson[6] and Patch[66] in this laboratory. A flushing procedure is often necessary to replenish molecules which leave the gas phase and become adsorbed on the walls of the shock tube and the gas-handling system. Although no quantitative analysis of the $Cr(CO)_6$-Ar mixtures was carried out in our experiments (because of the extremely low concentrations involved), the fact that there was no observed dependence of the experimental results upon the amount of gas flushed through the shock tube may be interpreted as an indication that adsorption equilibrium was rapidly obtained, and that the composition of the gas in the test section before

each run was the same as that of the gas leaving the mixing system. Approximately two minutes elapsed between the end of the flushing procedure and the firing of the shock tube. According to the indicated shock tube leak rates, an impurity mole fraction of approximately 0.003% was added to the gas in the test section during this interval.

Helium was used as the driver gas. Mylar diaphragms of 0.010 in thickness were used to separate the two sections of the shock tube, with bursting occurring at a driver pressure of about 145 psia. The resulting temperatures T_5, as determined from incident shock velocity measurements and ideal shock theory, had values between 7920 and 8730°K. Under these conditions, all but about 0.1% of the chromium atoms should have been in the singly ionized form at equilibrium behind the reflected shock.

Each monochromator was set at the wavelength of one Cr II line or line group. The oscilloscope was triggered by a signal from the heat gage in the end plate, and began recording the emitted radiation within 1 μsec after reflection of the incident shock wave. A typical oscilloscope record is shown in Fig. 10. After a relaxation time of approximately 50 μsec, during which the chromium attains equilibrium ionization and electronic level population, the emitted intensity shows a linear increase with time due to the linear increase in optical depth as the reflected shock wave travels away from the end wall at constant speed. The linearity of the oscilloscope traces demonstrates the uniformity of the conditions behind the reflected shock wave and the absence of self-absorption.

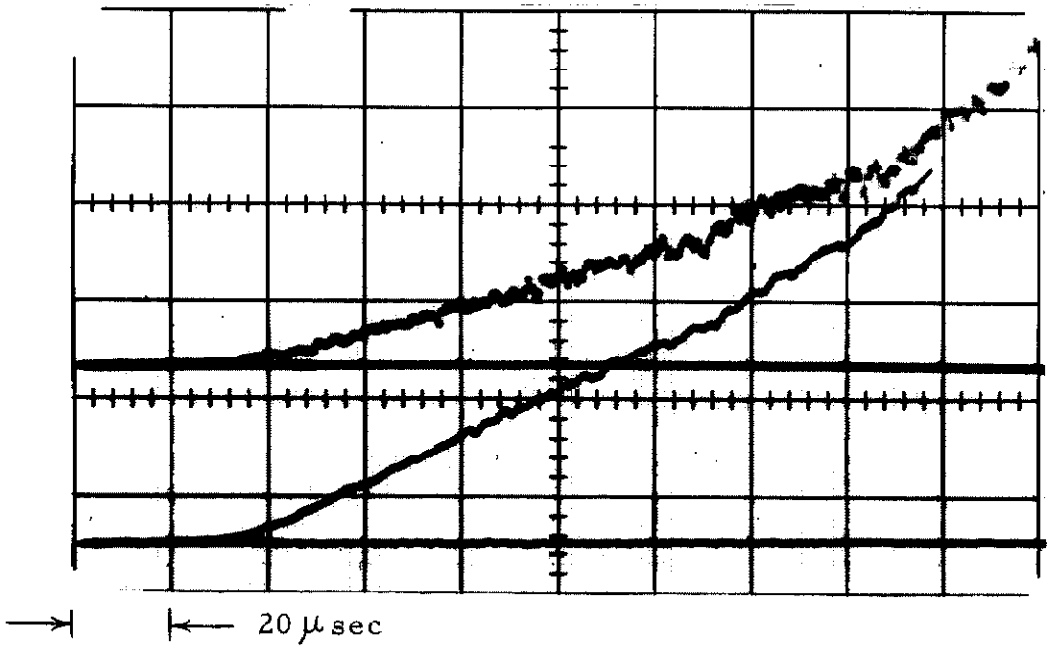

Upper trace: Cr II λ3392, 99, 3393. 84, 3394. 30

Lower trace: Cr II λ3421. 21, 3422. 74

Fig. 10. Oscilloscope record of the intensities of two groups of Cr II lines. The observation was made looking along the axis of the shock tube. The oscilloscope sweep was triggered by the reflection of the incident shock wave. Radiation was emitted by the lengthening volume of gas behind the reflected shock wave, for which T_5= 8250°K and p_5 = 1. 62 atm. The 50 μsec time delay before a constant slope was attained is due to relaxation effects. After 170 μsec an interaction with the contact surface occurred.

The contribution of background radiation to the observed signal was estimated by monitoring the radiation in wavelength intervals adjacent to some of the spectral lines. In the worst cases, the ratio of line radiation to nearby background radiation was about 3 to 1. The difficulty in estimating background intensities is a clear disadvantage of the photoelectric measurement technique which we used.

C. The Absolute Intensity Calibration

After each shock tube radiation measurement, the end plate of the high pressure section and the broken diaphragm were removed, and the standard lamp was turned on. The lamp current was set at the value for which the lamp had been calibrated. By means of the optical system described in Section IV. B (see Fig. 6) an image of the central portion of the tungsten strip was thus formed at or near the shock tube exit window.

According to a fundamental result from geometrical optics (see, for example, pp. 153-155 of Ref. (67)), the steradiancy of the image in the direction of any ray which can be traced back to the source is equal to the source steradiancy, diminished by the transmission and reflection losses of the intervening lenses, provided the source and image are located in a non-absorbing, non-scattering medium of constant refractive index. Since the transmission of the GE type 101 quartz lenses which we used is greater than 0. 998 for the wavelengths employed, almost all of the reduction in image intensity was due to reflection losses at the four air-quartz interfaces of the calibration

optical system (the reflection losses at the lamp window had already been taken into account in the NBS calibration). The reflection losses were estimated by means of the Fresnel normal-incidence formula

$$r = \left(\frac{n_1 - n_2}{n_1 + n_2} \right)^2 , \qquad (59)$$

where r is the fractional reflection loss due to a single interface, and n_1 and n_2 are the refractive indices of quartz and air, respectively. The net transmission of the two lenses was therefore $(1-r)^4$, which is equal to 0.856 at 3000 Å and 0.865 at 4500 Å. The light losses associated with the remainder of the optical equipment were the same for both the shock tube experiment and the absolute intensity calibration, and need not be considered.

The photomultiplier signals for both monochromators due to the chopped light from the lamp was measured by means of the dual beam oscilloscope, with the monochromator wavelength settings, slit widths and photomultiplier voltages identical to the corresponding values which had been used for the preceding shock tube radiation measurement. In addition to the oscilloscope preamplifiers, a Tektronix type 122 40 KC bandpass preamplifier with a calibrated gain of 100 ± 1 was used to amplify the rather weak calibration signals from the lamp and to smooth out the statistical noise due to the low photon flux. Calibration signals were typically 10^3 - 10^4 times weaker than the signals due to Cr II radiation which were obtained in the shock tube experiments.

The basic formulae involved in the absolute intensity calibration were derived in Section III. B. 3, in conjunction with the discussion of

the slit function. The signal, $S_c(\lambda')$ due to the calibrated lamp is given by

$$S_c(\lambda') = K(\lambda')\, I_{\lambda,c} \int_{\lambda'-\Delta\lambda^*}^{\lambda'+\Delta\lambda^*} g(\lambda-\lambda')d\lambda \qquad (60)$$

where $K(\lambda')$ is the instrument response factor and $I_{\lambda,c}$ is the steradiancy at the source image. This steradiancy is equal to the known steradiancy of the lamp, multiplied by the lens transmission factor $(1-r)^4$. The slit function integral $\int g \cdot d\lambda$ was obtained by a direct measurement, as described in Section III. B. 3. The absolute calibration measurement thus enables one to calculate the response factor, $K(\lambda')$, which relates the signals obtained from shock tube experiments to the integrated intensities (and hence the gf-values) of the observed lines. With the reflected shock traveling away from the end wall at a velocity U_{rs} (computable from ideal shock theory), the rate of increase for the observed signal due to a group of lines is

$$\frac{dS}{dt} = \frac{1}{U_{rs}} \frac{dS}{d\ell}$$

$$= \frac{1}{U_{rs}} \frac{d}{d\ell} \left[K(\lambda') \int_{\lambda'-\Delta\lambda^*}^{\lambda'+\Delta\lambda^*} \sum_i I_\lambda^i(\lambda)\, g(\lambda-\lambda')d\lambda \right], \qquad (61)$$

where I^i is the steradiancy of the i^{th} line and the summation is taken over all lines within the width of the slit function, $2\Delta\lambda^*$. Because the characteristic line widths were much less than $\Delta\lambda^*$, an average value g^i may be associated with the i^{th} line, so that the preceding relation

becomes

$$\frac{dS}{dt} = \frac{1}{U_{rs}} \frac{d}{d\ell} \left[K(\lambda') \sum_i I^i g^i \right], \tag{62}$$

where I^i is the integrated intensity for the i^{th} line. Since the intensity is proportional to the gf-value at low optical depths (provided all lines belong to a single multiplet, as is the case here), we may define an average slit function value $\bar{g}$ for the line group, viz.,*

$$\bar{g} = \frac{\sum_i g^i (gf)_i}{\sum_i (gf)_i} . \tag{63}$$

The determination of $\bar{g}$ involves only relative gf-values of the various lines of the multiplet with respect to each other. In cases where line groups rather than single lines were used, values of $\bar{g}$ were computed using measured slit function values g^i for each line together with Cr II gf-values of Corliss and Bozman, [1] whose relative values within a given multiplet are expected to be correct to within a few percent.

After local thermodynamic equilibrium has become established behind the reflected shock, one may make use of Equations (24), (62), and the definition of $\bar{g}$ to obtain

$$\frac{dS}{dt} = \frac{1}{U_{rs}} K(\lambda') \bar{g} \sum_i (gf)_i \frac{2\pi he^2}{m\lambda^3} \frac{n}{Q} e^{-E_u/kT} . \tag{64}$$

---

* Care must be taken to avoid confusing the statistical weight and the slit function, both of which are represented by the symbol g.

where n and Q are the number density and partition function for Cr II, respectively (the radiation from the non-equilibrium region just behind the reflected shock wave remains constant as the shock wave moves down the tube, and therefore does not contribute to dS/dt). When single lines were observed, the monochromator was adjusted so that $g(\lambda - \lambda') = 1$, in which case the above expression becomes

$$\frac{dS}{dt} = \frac{1}{U_{rs}} K(\lambda') gf \frac{2\pi he^2}{m\lambda^3} \frac{n}{Q} e^{-E_u/kT} . \qquad (65)$$

The two preceding expressions were used in the calculation of gf-values from our data, with $K(\lambda')$ being given by the absolute intensity calibrations.

VI. RESULTS OF EXPERIMENTS

A. Measurement of gf-values for Cr II

Measurements of Cr II radiation from the gas behind the reflected shock wave were converted to gf-values by performing the required absolute intensity calibrations, as described in Section V. C. The radiation measurements were made at eleven narrow wavelength intervals, with each interval including from one to six Cr II lines (see spectrum (a) of Fig. 8). Groups of more than one line, belonging to a single multiplet, were observed in cases where the lines were too closely spaced to be resolved individually by the monochromators. In these cases measurements yielded values for the sum of all gf-values, $\sum gf$, for those lines within the wavelength interval under investigation. These were subsequently converted to individual gf-values for each line using relative intensity data of Corliss and Bozman.[1] Altogether, gf-values for 21 lines of Cr II were measured. The experimental results are summarized in Table I.

The first column of Table I lists the designation of the multiplet to which each spectral line belongs, according to the numbering scheme of the Revised Multiplet Table (RMT) of C. E. Moore.[69] The second column lists the wavelength in $\mathring{A}$; the wavelengths are also taken from the RMT and differ in some cases by a few hundredths of an $\mathring{A}$ from those listed in the transition probabilities compilation of Corliss and Bozman.[1] The measured gf-values are listed in the third column. In cases where more than one line was monitored by the mono-

TABLE I

Cr II gf-VALUES

Multiplet No. (RMT)	Wavelength (Å)	Measured gf-Values		Previous gf-Value * Measurements (Corliss & Bozman)	
		gf	Σgf	gf	Σgf
2	3495.37	0.015±0.007		0.62	
2	3511.84	0.022±0.011		0.64	
3	3421.21	(0.75 ± 0.33)	1.8±0.8	3.2	7.7
3	3422.74	(1.05 ± 0.46)		4.5	
3	3433.30	0.29± 0.10		2.3	
5	3118.65	(0.46 ± 0.14)		4.7	
5	3120.37	(0.86 ± 0.26)		8.7	
5	3124.98	(0.96 ± 0.29)		9.7	
5	3128.70	(0.24 ± 0.07)	4.1±1.2	2.4	41.4
5	3132.06	(1.28 ± 0.38)		13.	
5	3136.68	(0.29 ± 0.09)		2.9	
5	3147.23	1.4 ± 0.4		3.0	
9	3197.12	1.7 ± 0.5		4.9	
12	3677.69	(0.038±0.013)		0.65	
12	3677.86	(0.048±0.016)	0.09±0.03	(0.74)	0.98 1.53
12	3677.93	(0.014±0.005)		(0.24)	
12	3712.97	0.063±0.021		1.3	
21	3393.00	(0.41 ± 0.12)		2.0	
21	3393.84	(0.54 ± 0.15)	1.4±0.4	2.6	6.7
21	3394.32	(0.44 ± 0.13)		2.1	
44	4558.66	0.13 ± 0.04		1.3	

* Corliss and Bozman list 0.98 for the gf-value of a single line at λ3677.89, which is probably a combination of the two lines λ 3677.86 and λ 3677.93 (see RMT). We have divided the gf-values among the two lines by using the relative intensity tables of White and Eliason. (68)

chromators, the various rows corresponding to each of the lines are grouped together and the measured value of $\sum gf$ is presented in the fourth column, with proportionately divided gf-values for each line indicated within parentheses in the third column. For comparison, electric arc measurements of gf-values taken from Ref. (1) are listed in column 5. Our experimentally measured values of gf (or $\sum gf$ for line groups) are plotted in Fig. 11 as a function of the corresponding values from Ref. (1). It is apparent from the figure that the gf-values which we obtained are, on the average, a factor of about nine below the latter measurements. The indicated margins of error represent the rms deviations from mean values which were obtained by repeating the measurements two or three times. The possibility of additional systematic errors is discussed in the remainder of this section.

B. Discussion of Results

It is useful to consider the accuracy of our measured gf-values in two respects: as relative values for each line with respect to the others, and as absolute values. Some of the possible reasons for errors in our relative gf-values are the following: 1. Since no more than two lines or line groups could be observed during each shock tube run, random experimental errors in the determination of the temperature and mixture composition, in the absolute intensity calibration, and variations in impurity level affect the relative gf-values of the various lines. Errors of this nature were responsible for the 25%-50% standard deviations in our gf-value measurements for a given line or

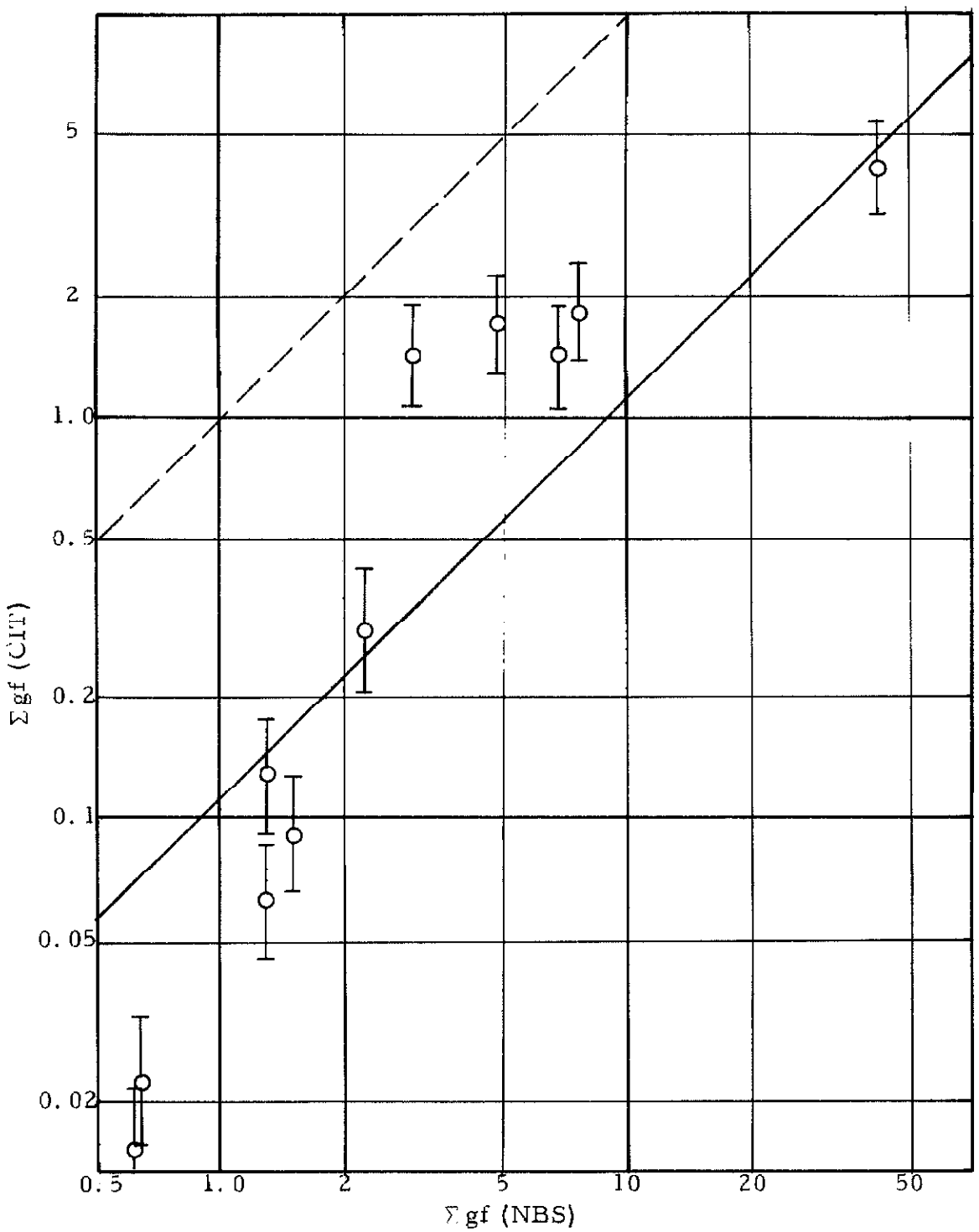

Fig. 11. A comparison of the Cr II gf-values measured here, Σgf(CIT), with previous measurements from Ref. (1), Σgf(NBS). Circles represent the sum of gf-values for all lines within each of the 11 wavelength intervals which we used. The separation of the solid and dashed diagonal lines represents the average deviation of our absolute values from those of Ref. (1).

group of lines. 2. Monochromators are subject to wavelength calibration errors which introduce uncertainties in the value of the slit function for the line(s) under study (see Section III. B. 3). This is particularly troublesome when narrow wavelength intervals must be used. We estimate the probable error due to this cause to be about ±20% in our experiment. 3. One cannot be certain, on the basis of a photomultiplier signal, of just how much of the signal is contributed by the spectral line(s) of interest. Approximate background corrections to our data were made by repeating the shock tube measurements with the monochromators set at wavelength intervals near to, but not including, the spectral line(s) being studied. The probable error due to background radiation is difficult to assess, but may have been about ±20% for the weaker lines and somewhat less for the stronger lines.

To the author's knowledge, the only other absolute gf-value measurements for the Cr II lines which we observed are those of Corliss and Bozman.[1] These authors based their values upon measurements of the emission spectra from a copper arc, the electrodes of which contained trace amounts (0.1%) of the element under study (seventy different elements were investigated). An effective arc temperature was established by means of relative intensity measurements for a large number of lines, using relative gf-value data obtained at five other laboratories. An effective electron density was also determined, using calculated degrees of ionization based upon relative intensities of neutral and ionized spectra of

eleven elements for which gf-values, of about factor-of-five accuracy, for both the neutral and singly ionized species are available. Although no direct measurements of either the atom concentration or of the absolute emitted intensity were performed, the known relative concentrations for arcs consisting of different trace elements enabled them to establish an absolute scale for their gf-values by using experimental absolute gf-values for lines of certain neutral elements which had been obtained by other investigators (in most instances using anomalous dispersion or atomic beam techniques).

As is evident from Fig. 11, the values of log gf which we obtained are, on the average, 0.95 lower than those of Ref. (1). This corresponds to a factor of nine in the gf-values. The standard deviation of our log gf-values from mean values 0.95 below those of Ref. (1) (i.e., the solid diagonal line in Fig. 11) is 0.36, corresponding to relative gf-value fluctuations by a factor of 2.4. It will be noted that the discrepancy between our gf-values and values listed in Ref. (1) tends to be larger for the weaker lines. No reason for this effect is apparent. Corliss and Bozman state that their relative gf-values may be expected to deviate from correct values by 40 to 50% if the upper state energies lie between 1.9 and 6.2 ev above the ground state, and by a somewhat larger amount for other lines. The upper state energies of the lines which we investigated are between 6.00 and 6.76 ev. As a consequence of the sources of random error listed at the beginning of this discussion, we expect our gf-values to be correct in a relative sense to within ±60%. The factor-of-2.4 fluctuations of our relative

gf-values with respect to those of Corliss and Bozman is slightly greater than would be expected from the combined estimates of relative gf-value errors presented by the respective authors.

The comparative accuracies of the absolute values presented here and other available measurements will now be discussed. Barring some unknown source of systematic error, our absolute gf-values are expected to be correct to within a factor of three. Corliss and Bozman have stated in Ref. (1) that their absolute gf-values are expected to be correct to within a factor of about two for neutral atoms, and perhaps a somewhat larger factor for ionized atoms. Wilkerson[2] and Charatis[3] have also measured gf-values for some lines of Cr II, using a shock tube. These authors obtained time-resolved spectra of Cr I and Cr II by means of a drum camera spectrograph. Absolute intensity calibrations were performed using a carbon arc as radiation standard. The lines for which they have presented gf-values have not been analyzed by us, as they were either too weak or not resolvable by our monochromators. Unfortunately, none of the Cr II lines which they used are tabulated in the compilation of Corliss and Bozman. However, one of the transitions measured by Wilkerson, 4634.11 Å, belongs to the same multiplet as the 4558.66 Å line studied both by us and by Corliss and Bozman, and the gf-values can be approximately related by means of the L-S coupling tables of White and Eliason.[68] According to these tables, the 4558.66 line ($b^4F_{9/2}$–$z^4D_{7/2}^o$) should be 100/28.0 times as intense as the 4634.11

line ($b^4F_{3/2}$-$z^4D_{1/2}^o$). Since Wilkerson quotes a gf-value of 0.28 ± 0.04 for the latter line, a gf-value of 1.00 ± 0.14 is indicated for the former line. This is to be compared with the value of 0.13 ± 0.04 measured by us and 1.3 listed by Corliss and Bozman.

It should also be mentioned that the Cr I gf-values of Wilkerson are, on the average, about 60% higher as those of Corliss and Bozman and that the Cr I gf-values of Charatis agree with values obtained by the latter authors to within ± 30%. The Cr I gf-values presented by Corliss and Bozman are in good agreement with atomic beam measurements of Bell et. al.,[70] since the latter values were used in establishing their absolute scale, and are about 25% lower than recently revised anomalous dispersion measurements of Ostrovskii and Penkin.[31]

The absolute scales of the various available experimental determinations of log gf-values for Cr I and Cr II are compared in Table II. The numerical entries represent the average deviation of the log gf-values from values tabulated in Ref. (1) for all lines which may be compared. The choice of the gf-values of Ref. (1) as the basis of comparison was made not because they are expected to be the most reliable, but rather because of the greater number of tabulated values which may be compared with other measurements. The anomalous dispersion Cr I gf-value measurements of Ostrovskii and Penkin[71] have recently been revised downward by 33%,[31] while the previously published Cr I atomic beam measurements of Bell et. al.[70] have been revised upward by about 45%.[72] The revisions bring the two sets of Cr I resonance line measurements into an agreement within better

TABLE II

COMPARISON OF AVAILABLE $\log_{10}$ gf-VALUES FOR Cr I AND Cr II

Measurement Technique		Shock Tube (Emission)			Arc (Emission)	Anomalous Dispersion	Atomic Beam (Absorption)
	Reference	Present Experiment	Ref. (2) (Wilkerson)	Ref. (3) (Charatis)	Ref. (1) (NBS)	Ref. (31) (Penkin)	Ref. (72) (Lawrence, Hill & King)
Cr I	$\left[\log \frac{gf}{(gf)_{NBS}}\right]_{mean}$	--	+0.22	+0.01	(0.00)	-0.08	+0.10
	Number of Lines Compared	--	17	6	--	34	6
Cr II	$\left[\log \frac{gf}{(gf)_{NBS}}\right]_{mean}$	-0.95	-0.11	--	(0.00)	--	--
	Number of Lines Compared	22	1*	**	--	--	--

* Wilkerson has performed gf-value measurements for 8 lines of Cr II, one of which may be compared with Ref. (1) by making use of L-S coupling tables of White and Eliason.(68) The other lines belong to a multiplet not investigated elsewhere.

** Charatis has measured gf-values for 17 lines of Cr II, but none of these lines have been measured by other investigators.

than 20%. The entries in Table II corresponding to these two measurement techniques represent the revised gf-values. It now appears that the absolute gf-values for low-lying transitions of Cr I are known to within about ±50%. The rather good agreement of the Cr I gf-values of Corliss and Bozman with other measurements does not necessarily imply comparable accuracy for their Cr II gf-values, since the relative magnitudes of the Cr I and Cr II values is critically dependent upon the calculated degree of ionization of Cr within their arc (50.5%), which may have been subject to a systematic error.

Possible sources of systematic error in our measured gf-values are the following: 1. There may have been errors in the computed temperature behind the reflected shock wave, due to non-ideal shock effects. If the calculated temperatures were 3% high at 8000°, the computed upper state Cr II populations would be too high by about 25%, causing the calculated gf-values to be too low by this amount. 2. Departures from local thermodynamic equilibrium would tend to decrease the population of excited Cr II levels, thus yielding gf-values which would be low. According to the discussion of Section III. B. 1, this effect is not likely to have been a significant factor in our experiments. 3. Light scattering within the monochromators during the absolute intensity calibration may have increased the calibration signals somewhat, even though most of the extraneous light was removed by a filter (cf. Section V-B). A calibration signal which is too high, due to the inclusion of scattered light of other wavelengths, would cause the calculated gf-values to be too low. Such errors would tend to be greatest at shortest

wavelengths; however, no such trend was noted. 4. Errors in the steradiancy of the standard lamp would tend to be of a systematic character. The steradiancy values for our lamp, as quoted by the National Bureau of Standards, were about 30% higher than values obtained from measurements made with an optical pyrometer, calibrated by Leeds and Northrup. The former values are expected to be the more accurate. 5. The computed composition of the $Cr(CO)_6$-Ar mixtures may have been in error as a result of incorrect $Cr(CO)_6$ vapor pressure data (the measurements of Wilkerson, which we used, have been confirmed by Charatis and are probably correct to within ±5%); systematic errors due to adsorption were probably negligible because of the continuous flushing technique employed (see Section V. B). 6. Systematic errors of unknown origin are always a possibility in measurements of this type. Previous intensity measurements for the $OH\ ^2\Sigma - ^2\Pi$ band system made by R. Watson, using the same tube which we employed and substantially the same experimental procedure, yielded f-values which are a factor of three higher than previously accepted values.

It is the author's opinion that the correct gf-values of Cr II lie somewhere between those presented here and those of Corliss and Bozman. Our results are believed to be correct to within a factor of three, and it is interesting to note that Corliss and Bozman quote approximately the same probable accuracy for their absolute values. There is obviously still a great need for data on Cr II, even if they are only accurate to within a factor of two. Some suggestions for improvements in the shock tube experiment are presented in the next section.

VII. CONCLUSIONS

The results of our measurements of the intensity of 21 Cr II lines indicate gf-values that are about a factor of nine lower than the previous arc measurements of Corliss and Bozman. It is believed that our measurements are correct to within a factor of three.

The limits of error in shock tube measurements of transition probabilities will remain in doubt unless independent determinations of temperature and electron density can be made. The shock tube impurity level can be reduced to better than one part per million through the use of very high purity gases and flushing systems which shut off automatically just before firing of the shock tube. Problems of alignment of the calibration optical system could be minimized by making provisions for accurate positioning of the calibrated light source at the location of the shock tube exit window. Chromatographic analyses of the gas mixtures, performed after the shock tube has been flushed for varying lengths of time, would be useful in determining the reliability of the gas-handling procedure. Measurements should be made over a wide range of temperatures and densities to demonstrate that the local thermodynamic equilibrium assumption is valid. The linearity of the curves of growth should be verified directly by varying the optical depth; the technique of observing radiation along the tube axis, which we used, is a simple means for demonstrating this linearity when the reflected wave region is used.

It is the author's belief that gf-values of about ± 10% accuracy for neutral and singly ionized lines of about a dozen metals with volatile or gaseous compounds could be obtained from shock tube measurements if the preceding measures were taken. For a further discussion of shock-tube instrumentation problems, the reader's attention is called to the recent shock-tube measurements by Patch[66] of the absorption coefficient for the 2.7 micron band of water vapor. Patch's measurements were made in reflected-shock-heated Ar-H_2O mixtures, using both emission and absorption techniques; both methods yielded absorption coefficients which are within 20% of accepted values.

REFERENCES FOR PART I

1. C. H. Corliss and W. R. Bozman, Experimental Transition Probabilities for Spectral Lines of Seventy Elements. National Bur. Stand., Washington, Monograph 53 (1962).

2. T. Wilkerson, U. of Mich., O.R.A. Report No. 02822-3T, AFOSR 1151 (1961); Ph. D. Thesis (1961).

3. G. Charatis, Ph. D. Thesis, U. of Mich. (1962).

4. S. H. Bauer, Unpublished work at Cornell Univ. (1961).

5. A. G. Gaydon and I. R. Hurle, Proc. Roy. Soc. 262A, 38 (1961).

6. R. Watson, Rev. Sci. Instr. 10, 1113 (1962).

7. E. U. Condon and G. H. Shortley, The Theory of Atomic Spectra, Cambridge University Press (1953).

8. P. A. M. Dirac, The Principles of Quantum Mechanics, Second Edition, Clarendon Press, Oxford (1958).

9. A. Messiah, Quantum Mechanics, Vol. II, Ch. XXI, John Wiley and Sons, New York (1962).

10. W. Heitler, The Quantum Theory of Radiation, Second Edition, Oxford University Press (1944).

11. C. W. Allen, M.N.R.A.S. 121, 299 (1960).

12. C. W. Allen and C. H. Corliss, M.N.R.A.S. 126, 37 (1963).

13. T. M. Helliwell, Ph. D. Thesis, Calif. Inst. of Tech. (1962).

14. J. C. Slater, Quantum Theory of Atomic Structure, Vol. II, McGraw-Hill, New York (1960).

15. D. R. Hartree, Proc. Cambridge Phil. Soc. 24, 89, 111, 426 (1928); 25, 310 (1929).

16. V. Fock, Z. Physik 61, 126 (1930).

17. T. M. Helliwell, Ap. J. 133, 566 (1961).

18. G. D. Bell and R. B. King, Ap. J. 133, 718 (1961).

19. S. F. Boys, Proc. Roy. Soc. London A200, 542 (1950); A217, 136, 235 (1953).

20. E. A. Hylleraas, Z. Physik 106, 395 (1937).

21. L. Goldberg, E. A. Muller, and L. H. Aller, Ap. J. Supplement 5, No. 45 (1960).

22. B. M. Glennon and W. L. Wiese, Bibliography on Atomic Transition Probabilities, National Bur. Stand., Washington, Monograph 50 (1962).

23. H. N. Olsen, J. Quant. Spectr. Radiat. Transfer 3, 305 (1963).

24. H. Maecker, Z. Naturf. 11a, 32 (1956).

25. L. Huldt and A. Lagerquist, J. Opt. Soc. Amer. 42, 142 (1952).

26. R. B. King and A. S. King, Ap. J. 82, 377 (1935).

27. H. Kopfermann and G. Wessel, Z. Physik 130, 100 (1951).

28. R. B. King, J. Quant. Spectr. Radiat. Transfer 3, 299 (1963).

29. S. A. Korff and G. Breit, Rev. Mod. Phys. 4, 471 (1932).

30. Optical Transition Probabilities. A Collection of Russian Articles. 1924-1960. Israel Program Scientific Translations, Jerusalem (1962). Available from the Office of Technical Services, U. S. Department of Commerce, Washington.

31. N. P. Penkin, J. Quant. Spectr. Radiat. Transfer 4, 91 (1964).

32. M. Weingeroff, Z. Physik 67, 679 (1931).

33. G. Stephenson, Proc. Phys. Soc. London A64, 458 (1951).

34. K. Ziock, Z. Physik 147, 99 (1957).

35. R. G. Bennett and F. W. Dalby, J. Chem. Phys. 32, 1716 (1960).

36. E. B. Turner and O. Laporte, U. of Mich. Eng. Research AFOSR TN-56-150, ASTIA Document No. AD 86309 (1956).

37. E. L. Resler, S. C. Lin, and A. Kantrowitz, J. App. Phys. 23, 1390 (1952).

38. J. K. Wright, Shock Tubes, Methuen and Co., Ltd., London (1961).

39. D. R White, J. Fluid Mech. 4, 585 (1958).

40. R. E. Duff, Phys. Fluids 2, 207 (1959).

41. A. Roshko, Phys. Fluids 3, 835 (1960).

42. W. J. Hooker, Phys. Fluids 4, 1451 (1961).

43. H. Mirels, Test Time in Low Pressure Shock Tubes, Aerospace Corp. Report No. TDR-169 (3230-12) TN-5, El Segundo, Calif. (1962); Phys. Fluids 6, 1201 (1963). Shock Tube Test Time Limitation Due to Turbulent Wall Boundary Layer, Aerospace Corp. Report No. TDR-169 (3230-12) TR-3, El Segundo, Calif. (1963).

44. J. P. Toennies and E. F. Greene, J. Chem. Phys. 26, 655 (1957).

45. H. Mark, NACA Technical Memorandum 1418 (1958); J. Aero. Sci. 24, 304 (1957).

46. R. A. Strehlow and A. Cohen, J. Chem. Phys. 30, 257 (1959).

47. G. B. Skinner, J. Chem. Phys. 31, 268 (1959).

48. T. A. Brabbs, S. A. Zlatarich, and F. E. Belles, J. Chem. Phys. 33, 307 (1960).

49. R. Watson, J. Quant. Spectr. Radiat. Transfer 3, 255 (1963).

50. L. H. Aller, Astrophysics. The Atmospheres of the Sun and Stars, Second Edition, Ronald Press, New York (1963).

51. J. C. Keck, J. C. Camm, B. Kivel and T. Wentink Jr., Annals of Physics 7, 1 (1959).

52. L. R. Doherty, Ph. D. Thesis, U. of Mich. (1961).

53. H. D. Weymann, University of Maryland Institute for Fluid Dynamics and Applied Mathematics TN BN-144 (1958).

54. K. E. Harwell, Ph. D. Thesis, Calif. Inst. of Technology (1963); K. E. Harwell and R. G. Jahn, Phys. Fluids 7, 214 (1964).

55. M. Gryzinski, Phys. Rev. 115, 374 (1959).

56. H. A. Bethe and E. E. Salpeter, Quantum Mechanics of One- and Two-Electron Atoms, Academic Press, New York (1957), p. 269.

57. S. Byron, R. D. Stabler, and P. I. Bortz, Phys. Rev. Letters 8, 376 (1962).

58. R. G. Breene, The Shift and Shape of Spectral Lines, Pergamon Press, Oxford (1961).

59. E. M. F. van der Held, Z. Physik 70, 508 (1931).

60. S. S. Penner and R. W. Kavanagh, J. Opt. Soc. Amer. 43, 385 (1953).

61. S. S. Penner, Quantitative Molecular Spectroscopy and Gas Emissivities, Addison-Wesley, Reading, Mass. (1959).

62. R. Watson, Ph. D. Thesis, Calif. Inst. of Tech. (1963).

63. R. Watson, J. Quant. Spectr. Radiat. Transfer 4, 1 (1964).

64. C. R. Wilke and O. A. Hougen, Amer. Inst. Chem. Engrs. Transactions 41, 445 (1945).

65. R. W. Patch, private communication.

66. R. W. Patch, Ph. D. Thesis, Calif. Inst. of Tech. (1964).

67. L. C. Martin, Geometrical Optics, Philosophical Library, New York (1956).

68. H. E. White and A. Y. Eliason, Phys. Rev. 44, 753 (1933).

69. C. E. Moore, A Multiplet Table of Astrophysical Interest (Revised Edition), National Bur. Stand., Washington, Technical Note 36 (1959).

70. G. D. Bell, M. H. Davis, R. B. King, and P. M. Routly, Trans. I. A. U. 10, 221 (1958).

71. Yu. Ostrovskii and N. P. Penkin, Optika i Spektrosk. 3, 193 (1957).

72. G. M. Lawrence, J. K. Link, and R. B. King, Ap. J. (in press).

PART II: EXPERIMENTAL INVESTIGATION OF THE APPROACH TO EQUILIBRIUM IONIZATION AND ELECTRONIC EXCITATION IN SHOCK-HEATED MIXTURES OF CHROMIUM AND ARGON

I. INTRODUCTION

The rather interesting relaxation phenomena associated with the ionization and electronic excitation of chromium which were noted during our shock tube measurements of Cr II gf-numbers (cf. Part I, Section V. A. 2) raised questions concerning the mechanism of the ionization process and the validity of the assumption of local thermodynamic equilibrium. The latter question arose as a result of the observation that relaxation times of about 50 μsec were required for the degree of ionization and excited-state populations to reach steady values, thus causing suspicion that collisional de-excitation rates might be slower than spontaneous radiative transition rates. This matter has been discussed in Section III. B. 1 of Part I. Additional questions regarding the relaxation phenomena which interested us were the relative importance of electron-atom and atom-atom processes in causing excitation and ionization, whether most ionization takes place from the ground state or excited states of Cr I, and the reason for the "population overshoot" of the Cr I excited states. Since the photomultiplier-equipped monochromators which were used for gf-value measurements also provided a convenient means for determining the populations of various excited states of Cr I and Cr II during the relaxation period following the passage of the reflected shock wave,

it was decided to make a series of time-resolved observations of the simultaneous populations of selected Cr I and Cr II excited states over a range of temperatures and Cr concentrations. These measurements should be useful toward elucidating various features of the ionization mechanism.

Time-resolved line radiation measurements, such as those which will be described here, are among the techniques which have been used by shock-tube workers in recent years for the purpose of studying ionization phenomena in shock-heated gases. Petschek and Byron[1] investigated the approach to equilibrium ionization behind strong shock waves in argon, using a diffusion potential probe, together with measurements of the continuum radiation due to recombination. Line broadening and shift due to the Stark effect has been used by Petschek et. al.[2] and by Turner[3] to measure ion densities. Lin, Resler, and Kantrowitz[4] employed a magnetic-induction probe to measure the electrical conductivity of shock-heated gases (the electrical conductivity can be related to the electron density if electron-atom collision cross sections are known). The technique of optical interferometry has been shown by Alpher and White[5] to be useful for measuring electron concentrations above about 10^{16} cm^{-3}. A microwave reflection technique has been used by Lin, Neal and Fyfe[6] to measure ionization rates in air, and by Harwell[7] in similar measurements using argon, krypton, and xenon. It is not our intention to discuss the details and relative merits of the various techniques just mentioned, nor to speculate about the lack of agreement of various

investigators concerning the relative effectiveness of atom-atom collisions, impurity reactions, wall reactions, and precursor radiation in promoting the initial ionization in shock-heated noble gases.[1, 7-10]

Because of the high ionization potentials of inert gases, shock tube studies of these gases have been limited to degrees of ionization below 30%. Previously, Wilkerson[11] and Haught[12] have observed ionization relaxation phenomena in shock tubes, using mixtures of inert gases with small amounts of more easily ionized elements. Wilkerson employed mixtures of neon and chromium carbonyl and obtained time-resolved spectra of chromium under conditions where the ionization of chromium proceeds nearly to completion. His results indicated the same type of relaxation behavior which we noted in Part I of this dissertation, namely, (1) an initial overshoot of the intensity of Cr I lines above their final equilibrium intensities, during which time very little Cr II radiation is observed, followed by (2) a period during which Cr I radiation decreases while Cr II radiation increases in intensity, until, finally, equilibrium intensities are simultaneously attained for both types of spectral lines. Wilkerson noted that the time required to reach equilibrium ionization behind the reflected shock wave depended inversely upon the computed equilibrium electron density behind the incident shock, but as he did not vary the temperature and chromium density independently, the mechanism of the approach to equilibrium was not determined. A. F. Haught[12] has also observed a radiation overshoot due to Cr I

lines during the ionization of cesium behind incident shock waves in mixtures of argon and cesium vapor. His relaxation time measurements were based upon time-resolved photographs of the total radiation behind the incident shock wave, and therefore did not provide information concerning the populations of specific excited states. On the basis of his photographs, Haught defined two relaxation times, the first being related to the time required for the overshoot to occur, and the second being a measure of the additional time required for the attainment of equilibrium. The observed dependence of both of these two relaxation times upon the temperature indicated an activation energy of 1.43 ± 0.06 ev which coincides, within experimental error, with the energy of the first excited state of neutral cesium; however, the two delay times differed in their dependence upon the concentration of cesium, and neither dependence was explained in terms of a model for the reaction mechanism.

The use of chromium carbonyl-inert gas mixtures in a shock tube provides a convenient means for studying ionization kinetics. The activation energy for Cr ionization is lower than that required for the ionization of inert gases, and thus impurity reactions, wall reactions, and the presence of precursor electrons and photons ahead of the shock wave are not expected to exhibit the disturbing effects noted in high-enthalpy studies of pure inert gases. The use of alkali metal vapor in a shock tube, on the other hand, requires a complicated procedure for the preparation of the test section. For example, Haught found that a total of one week was required to prepare the shock tube for a single run with cesium.

The experiments described in the following sections consist of time-resolved photoelectric measurements of the radiation from selected excited states of Cr I and Cr II behind reflected shock waves in $Cr(CO)_6$-Ar mixtures. The temperature and chromium concentration behind the reflected shock wave were independently varied in order to shed further light upon the ionization kinetics. A discussion of the physical foundations of the experiment is presented in the following section; the experimental techniques are described in Section III (some of the details of the experimental equipment and procedure have already been described in Part I and are omitted in the present discussion). Our results are presented and analyzed in Section IV. Section V contains a summary of the conclusions drawn from these experiments and suggestions for possible future investigation.

II. THEORETICAL CONSIDERATIONS

A. Description of the Experiment

Mixtures of chromium carbonyl and argon were heated to temperatures between 6170° and 8600°K behind reflected shock waves in a conventional pressure-driven shock tube. Radiation emitted normal to the shock tube axis was analyzed with two monochromators in order to provide a record of the populations of Cr I and Cr II excited states.

Before being compressed and heated by the reflected shock wave, the gas mixture in the test section of the shock tube was first heated to a temperature between 3000° and 4000°K by the incident shock wave. Since the dissociation reaction

$$Cr(CO)_6 \rightarrow Cr + 6(CO)$$

goes virtually to completion at temperatures above 700°K for the $Cr(CO)_6$ partial pressures which we employed (Ref. 11, Appendix B), the chromium carbonyl is expected to have been completely dissociated into atomic chromium and carbon monoxide by the incident shock wave. The amount of Cr ionization which occurred behind the incident shock wave is not known, and cannot be calculated from the Saha equation since our time-resolved radiation measurements indicate that ionization equilibrium was not attained during the $\approx 60\mu$ sec interval of time between passage of incident and reflected shock waves past the observation window. The degree of Cr ionization obtained ahead of the reflected shock wave is expected to be less than equilibrium values predicted by the Saha equation. The calculated equilibrium degree of

Cr ionization ahead of the reflected wave was between 1% and 20% for the experimental conditions which we used. The fact that the degree of ionization, and therefore the electron density, is not accurately known ahead of the reflected shock wave is one of the disadvantages of working with the reflected wave region in experiments of this type.

It will be helpful to present at this point a qualitative description of the ionization relaxation process, as evidenced by our results. The degree of Cr ionization ahead of the reflected shock front was, as previously mentioned, not accurately known, but probably not more than a few percent. After passage of the reflected wave, the rate of ionization increased steadily until approximately one half of the Cr was ionized, and then decreased as the reaction proceeded to completion. The tendency of the ionization process to accelerate initially was interpreted as an indication that the reaction was autocatalytic in nature, being dominated by collisions between Cr atoms and electrons which had previously been removed from other atoms. It is known that, at comparable temperatures and number densities, inelastic collisions with electrons are approximately 10^5 times more effective than similar collisions with atoms in causing ionization.[7, 8] Since the ionization and excitation rates which are obtained immediately downstream of the reflected shock wave are critically dependent upon the (unknown) electron density of the gas upstream of the shock wave, it was not considered advisable to attempt a quantitative interpretation of the initial reaction rates behind the reflected wave. Had we wished to measure the very small excitation and ionization cross sections of atom-atom

collisions, it would have been necessary to make measurements behind the incident shock wave, since for this case the gas entering the shock wave is not expected to contain free electrons. The shock tube which we employed was, however, not capable of producing sufficiently high temperatures behind the incident shock wave to bring about thermodynamic equilibrium within the available testing time; it was therefore necessary to restrict our relaxation studies to an investigation of the later stages of the ionization and electronic excitation processes behind the reflected shock wave. These processes, as has been mentioned, are believed to have been dominated by collisions between chromium atoms and free electrons released in prior ionization of chromium.

B. Interpretation of Radiant Emission Measurements

The radiant emission from a heated gas, due to a single spectral line which is not self-absorbed, is given by (cf. Part I, Eq. 23)

$$I = \frac{h\nu A_{u\ell} n_u \ell}{4\pi} \quad , \tag{1}$$

where I is the steradiancy integrated over the spectral line width, $h\nu$ the energy of the emitted photons, $A_{u\ell}$ the spontaneous transition probability, n_u the number density of atoms in the initial state of the transition considered, and ℓ the length of the heated gas along the line of sight. If n_u varies along the line of sight, the product $n_u \ell$ must be replaced by $\int_0^\ell n_u ds$, where ds is an elemental path length. Since the observed radiation was emitted in a direction normal to the shock tube axis in our experiments, n_u was uniform along the optical path, except

within the wall boundary layer, and ℓ was equal to the diameter of the shock tube.

The error introduced by assuming $\int_0^{\ell} n_u ds = n_{u,o}\ell$, where $n_{u,o}$ is the free stream upper state number density and ℓ the shock tube width, is given approximately by

$$\frac{\ell n_{u,o} - \int_0^{\ell} n_u ds}{\ell n_{u,o}} = 1 - \frac{2\delta n_{u,m} + (\ell - 2\delta) n_{u,o}}{\ell n_{u,o}}$$

$$= \frac{2\delta(n_{u,o} - n_{u,m})}{\ell n_{u,o}} ,$$

where $n_{u,m}$ is an effective mean value of n_u for the boundary layer and δ is a characteristic boundary layer thickness. Because of the exponential dependence of n_u upon E_u/kT,

$$n_{u,o} >> n_{u,m},$$

so that

$$\frac{n_{u,o}\ell - \int_0^{\ell} n_u ds}{n_{u,o}\ell} \approx \frac{2\delta}{\ell} . \qquad (2)$$

According to available information on shock tube boundary layer transition,[20] the boundary layer in front of the reflected shock was laminar when the reflected shock passed by the observation window. An order-of-magnitude estimate for δ is then $\delta \approx (\tau \nu_m)^{1/2} \approx 10^{-2}$ in, where τ is the interval between passage of the incident and reflected shock waves past the observation window and ν_m is the kinematic viscosity of the

gas at a mean temperature. For our three-inch diameter shock tube the error due to neglecting the boundary layer, $2\delta/\ell$, is therefore only of the order of one per cent.

In Part I of this dissertation measurements of the emitted intensity were combined with local thermodynamic equilibrium predictions of n_u to determine, in effect, values of $A_{u\ell}$ for various lines. Since Eq. 1 is valid whether or not local thermodynamic equilibrium is obtained, one may also make use of the equation to determine values of n_u for various excited levels during the relaxation interval before thermodynamic equilibrium is established. Although it is in principle possible to measure n_u by means of an absolute measurement of the emitted radiation if $A_{u\ell}$ is known, the uncertainty of most available $A_{u\ell}$ values and the difficulties inherent in an absolute intensity calibration are likely to cause the value of n_u thus obtained to be in error by an order of magnitude or more. It is much more practical to make use of the fact that the emitted intensity is proportional to n_u, and to establish the proportionality factor by making measurements over a sufficiently long period to permit thermodynamic equilibrium to be obtained. The value of n_u can then be calculated and related to the corresponding value of the emitted intensity, and relative intensity values can be used to establish the variation in n_u during the relaxation period. The need for both an absolute intensity calibration and accurate knowledge of $A_{u\ell}$ is thereby eliminated.

For the experiments which we performed, the temperature and pressure of the gas behind the reflected shock wave, at the location of the observation window, remained nearly constant during a "testing

time" of approximately 100 μsec after the reflected wave passed by the window; after this interval further heating due to the interaction of the reflected wave with the contact surface occurred (cf. Part I, Fig. 1). The time required for equilibrium populations of Cr I and Cr II to become established behind the reflected shock wave varied between 12 and 60 μsec for the range of shock strengths and mixture compositions which we used. Since thermodynamic equilibrium was always obtained within the testing time interval, the relationship between the observed intensities and the upper state populations was easily determined.

For a detailed description of the relaxation toward ionization and excitation equilibrium, it would of course be advantageous to perform simultaneous population measurements for a large number of excited states of Cr I and Cr II, as well as for the corresponding ground states and for free electrons. Ground state population measurements would require an absorption, rather than an emission, technique. Several methods for determining electron densities directly have been mentioned in Section I. However, the primary purpose of the experiments described here was to gather sufficient data with our available equipment to permit us to obtain some understanding of the basic kinetics of the relaxation processes. To accomplish this purpose, we limited our experiments to emission measurements, using two groups of Cr I lines and one group of Cr II lines.

C. Possible Reactions Involving Excitation, De-excitation and Ionization of Chromium

In the remainder of this section a summary of the various inelastic collisions involving chromium atoms or ions is presented. On the basis of available theoretical and experimental information, some of the possible reactions will be shown to have had a negligible influence under the conditions of our experiment. A comparison of the reactions which are likely to have been important, and of the effect of these reactions upon the observed relaxation behavior, is deferred until Section IV, where the experimental results are analyzed.

The gas which was used in the shock tube test section consisted of 1 part Ar to η parts of $Cr(CO)_6$ (by volume) with $4.3 \times 10^{-5} \leq \eta \leq 3.6 \times 10^{-4}$, depending upon the operating conditions. The gas mixture entering the reflected shock wave, having already passed through the incident shock wave, was composed mainly of Cr atoms, CO molecules, and Ar atoms. According to the specified purity of the argon which we used and the indicated leak rate of the shock tube, an impurity concentration of about 5×10^{-5} was also present in the test section when the shock tube was fired. The impurity molecules were probably mainly N_2, O_2 and H_2O. Pump oil vapors were kept out of the shock tube by means of a liquid nitrogen cold trap. As previously mentioned, a small but unknown percentage of the Cr atoms entering the reflected shock wave had already been ionized at the 3000-4000°K temperature behind the incident shock wave. The populations of the various levels of Cr I and Cr II, after passage of the reflected shock wave, were thus affected to a greater or lesser degree by the following reactions:

1. Collisions with atoms

The atoms with which a Cr atom or ion would be most likely to collide inelastically are argon atoms, because of their greater number in the gas mixtures which we used. Such reactions may be of the following types:

(1a) excitation of a certain level of neutral Cr, Cr_u, from a lower level, Cr_ℓ: $Cr_\ell + Ar \rightarrow Cr_u + Ar$

(1b) the reverse (superelastic) de-excitation from a higher Cr level to a lower level: $Cr_u + Ar \rightarrow Cr_\ell + Ar$

(1c) excitation of an excited level of singly ionized Cr, Cr_u^+, from a lower level, Cr_ℓ^+: $Cr_\ell^+ + Ar \rightarrow Cr_u^+ + Ar$

(1d) the reverse of (1c): $Cr_u^+ + Ar \rightarrow Cr_\ell^+ + Ar$

(1e) ionization of neutral Cr: $Cr + Ar \rightarrow Cr^+ + Ar + e^-$

(1f) three-body recapture of electrons (the reverse of (1e)): $Cr^+ + Ar + e^- \rightarrow Cr + Ar$

Of the preceding reactions, (1f) should have been much less frequent than (1e) during the relaxation period, since the number densities of free electrons and Cr^+ ions are then less than the final equilibrium values. Ionizing collisions (1e) may either involve a direct transition from a Cr I level to a Cr II level, or a Cr I atom may be excited to an unstable level above its ionization limit and subsequently lose an electron by autoionization.

A calculation of the rates of excitation reactions of the types 1a, 1c and 1e, for a Maxwell-Boltzmann distribution of atomic velocities, would require accurate cross section data for all inelastic collisions

for which the total initial kinetic energy in center-of-mass coordinates exceeds the threshold energy of the reaction. Because of the difficulty in preparing monoergic atomic beams with energies in the range of a few electron volts and because of the tendency of the relatively more efficient collisions with electrons and impurity molecules to dominate the observed rates, very few data are available. Recent shock-tube measurements by Harwell[7] of atom-atom ionization rates in shock-heated Ar, Kr, and Xe indicate that the rate-controlling step in the ionization of these gases is the excitation of ground state atoms to the first excited states, at 11.55, 9.92, and 8.32 ev, respectively. Although the variation of the excitation cross sections with the relative velocity of the colliding atoms was not established by Harwell, his measurements indicate that cross sections for the reactions which he observed are typically of the order 10^{-19}-10^{-20} cm^{2}* for $0.5 < kT < 0.8$ ev. Lacking further information, one might guess that cross sections for the excitation of Cr I and Cr II excited states from the respective ground states by means of Cr-Ar collisions may be of a similar magnitude. The rates of de-excitation reactions of types (1b) and (1d) may be obtained from estimates of rates of the corresponding excitation reactions by making use of the principle of detailed balancing.

2. Collisions with electrons

Although free electrons were only about 10^{-4} times as abundant

* The cross sections quoted here represent average values for all collisions in which the available kinetic energy exceeds the threshold energy, weighted by the Maxwell-Boltzmann distribution of relative velocities.

as heavy particles under our experimental conditions, the greater cross sections and velocities of electrons, as compared with atoms at the same temperature, make it likely that collisions with electrons dominate the ionization and excitation processes whenever the relative abundance of electrons and atoms, n_e/n_{Ar}, exceeds a value of about 10^{-5} (cf. p. 44 and Ref. 7). The main source of electrons behind the reflected shock wave is expected to have been the ionization of chromium, although ionization of impurity atoms and molecules[1,7] and ionization of carbon atoms (from $Cr(CO)_6$) may also have contributed significantly.

The list of inelastic collisions involving free electrons and Cr atoms or ions is similar to the previous list of collisions involving Ar atoms, i.e.,

(2a) excitation from a lower level to a higher level of neutral Cr:

$$Cr_\ell + e^- \rightarrow Cr_u + e^-$$

(2b) the reverse of (2a): $Cr_u + e^- \rightarrow Cr_\ell + e^-$

(2c) excitation of a higher level of singly ionized Cr^+:

$$Cr_\ell^+ + e^- \rightarrow Cr_u^+ + e^-$$

(2d) the reverse of (2c): $Cr_u^+ + e^- \rightarrow Cr_\ell^+ + e^-$

(2e) ionization of neutral Cr: $Cr + e^- \rightarrow Cr^+ + e^- + e^-$

(2f) three-body recapture of electrons:

$$e^- + e^- + Cr^+ \rightarrow Cr + e^-$$

Although three-body recapture plays a major role in populating Cr I levels near the ionization limit once equilibrium is obtained,[13] the frequency of such processes is expected to be negligible in comparison

with that of the corresponding forward reaction (2e) during most of the relaxation period, since the number of free electrons is then much smaller than the equilibrium value.

It is important to the interpretation of our relaxation rate measurements that it be established whether or not an "electron temperature" exists and, if so, whether or not this temperature is expected to be approximately equal to the translational temperature of the heavier particles. During the relaxation period the supply of highly energetic electrons is constantly being depleted by inelastic collisions of types (2a), (2c) and (2e), and since there are insufficient reactions of the reverse type to replenish the energy loss until equilibrium is obtained, there must be a net transfer of kinetic energy from heavy particles to electrons by means of elastic collisions. The electron velocity distribution may be expected to be of a Maxwellian form if the time required for an electron to acquire an energy kT by means of "collisions" with other electrons is less than the time required for an electron to collide $\sim 10^5$ times with atoms and ions (the factor $10^5 \sim m_e/m_{Ar}$ accounts for the relatively small amount of energy transferable is such collisions). Assuming reasonable values for the cross sections involved, the criterion for the existence of a Maxwellian electron velocity distribution is that the electron number density, n_e, should exceed 10^{10} cm^{-3}, a condition that was met as soon as about 0.01% of the Cr became ionized.

The electron temperature is expected to be somewhat less than the temperature of the atoms and ions during the relaxation period, in order for there to be a net transfer of energy from atoms and ions to

the electrons by elastic collisions. The electron temperature obeys the electron energy equation,[1]

$$Q_{e\ell} - Q_{in} = \frac{3}{2} n_e k \frac{dT_e}{dt} \quad , \tag{3}$$

where $Q_{e\ell}$ represents the net rate of energy transfer from atoms and ions to electrons by means of elastic collisions, and Q_{in} the net rate at which electrons lose energy in inelastic collisions. The quantity $Q_{e\ell}$ is proportional to the difference $T_a - T_e$ between the temperatures of heavy particles and electrons. Although $Q_{e\ell}$ can be estimated from available electron diffusion data, a determination of Q_{in}, and hence T_e, requires information concerning the mechanism of excitation and ionization. This matter is discussed further in the next section.

3. Collisions with ions

Inelastic collisions in which chromium atoms or ions are excited by colliding with other ions (chiefly Cr^+) are not expected to have been significant in comparison to either chromium-atom or chromium-electron collisions. Cross sections for excitation of atoms by ions are of the same order of magnitude as for similar collisions with atoms,[14] and since atoms were about 10^4 times more abundant than ions in our experiments, the frequency of Cr-atom inelastic collisions must have exceeded that of Cr-ion collisions by about the same factor. Similarly, although the number densities of ions and electrons are about equal, the greater velocity and inelastic cross section of electrons, compared with ions of comparable energy,

results in a greater inelastic collision frequency for electrons than for ions.

4. Collisions with molecules

The most abundant molecular species present behind the reflected shock wave should have been CO, formed by dissociation of $Cr(CO)_6$ behind the incident shock wave. According to chemical equilibrium computations, the degree of CO dissociation should have proceeded from a low value at the reflected shock wave to a final equilibrium value greater than 95%. No measurements of the relaxation time for CO dissociation were performed. Since diatomic molecules are known from radiation quenching measurements to be more effective than atoms in de-exciting excited atomic levels, it follows that inelastic cross sections for excitation of Cr I and Cr II upper levels by CO molecules should be larger than corresponding Ar-Cr cross sections. Previous measurements[15] indicate that CO is about 200 times more effective than Ar for quenching Hg resonance radiation, and 4 times more effective than for similar quenching of Tl radiation. The relative abundance of Ar and CO (before CO dissociation) was between 400 and 4000 under our experimental conditions, making it unlikely that inelastic collisions between CO and Cr were of importance.

5. Reactions involving photons

Since our measurements were made at low optical depths, reactions involving absorption of photons, i. e.,

(5a) Cr I absorption: $Cr_\ell + h\nu \rightarrow Cr_u$

(5b) Cr II absorption: $Cr_\ell^+ + h\nu \rightarrow Cr_\ell^+$

(5c) photoionization: $Cr + h\nu \rightarrow Cr^+ + e^-$

must have been negligible in comparison to rates of the corresponding reverse reactions:

(5d) Cr I spontaneous emission: $Cr_u \rightarrow Cr_\ell + h\nu$

(5e) Cr II spontaneous emission: $Cr_u^+ \rightarrow Cr_\ell^+ + h\nu$

(5f) radiative recombination: $Cr^+ + e^- \rightarrow Cr + h\nu$.

Spontaneous emission from Cr I upper levels quite possibly was of importance in determining the relative populations of Cr I upper levels and the ground state, since radiative lifetimes of upper states near 3 ev were of the same order as lifetimes for collisional de-excitation to lower levels (see Section III. B. 1 of Part I). Spontaneous emission of Cr II is not likely to have been important since all excited levels less than 5. 8 ev above the ground state (i. e., the only levels likely to have had collisional de-excitation lifetimes longer than characteristic radiative lifetimes)are metastable.

The rate of the radiative recombination process (5f) may be calculated from the equation[16]

$$a_R \approx 3 \times 10^{-10} Z^2 T_e^{-3/4} \qquad (4)$$

where a_R denotes the recombination coefficient (cm^3 sec^{-1}), Z the effective nuclear charge, and T_e the electron temperature (^oK). Taking Z=1 as the effective nuclear charge of a Cr^+ ion, one obtains for the characteristic lifetime for radiative recombination of a Cr^+ ion (at $T_e = 5000^oK$ and $n_e = 10^{14}$ cm^{-3}) the value

$$\tau_r \approx (a_R n_e)^{-1} = 2 \times 10^{-2} \text{ sec},$$

which is about 1000 times longer than the observed times required for neutral Cr to become ionized. Radiative recombination may therefore be neglected as long as $n_{Cr}/n_{Cr^+} \gtrsim 0.001$, that is, until the degree of chromium ionization reaches 99.9%. Since the degree of ionization was less than this value during most or all of the relaxation period, radiative recombination processes certainly could not have had any appreciable influence upon the observed relaxation rates.

III. EXPERIMENTAL PROCEDURE

Mixtures of $Cr(CO)_6$ and argon were prepared by passing argon (99.998% pure) through a packed column of $Cr(CO)_6$ crystals, with the argon supply and column being enclosed within a temperature-controlled chamber which was cooled down to a temperature between 5° and $25^{\circ}C$ (see Fig. 7 of Part I). The $Cr(CO)_6$ partial pressure in the gas leaving the mixing column was equal to vapor pressure of this substance at the temperature of the chamber. By adjusting the pressure of the argon in the packed column and the temperature of the chamber, the $Cr(CO)_6$ mole fraction for the gas mixture could be varied between 3×10^{-5} and 10^{-3} in a convenient manner. The mixture was bled into and flushed through the shock tube at the desired test section pressure for ten minutes prior to each run, to permit adsorption equilibrium with the walls of the shock tube and gas-handling system to become established.

The shock tube which we used has been described in detail in Part I; we reiterate here that the test section was six feet in length and fabricated from mild steel tubing of 3 inch internal diameter. The temperature and pressure behind the reflected wave were computed from measurements of the incident shock speed and one-dimensional shock theory.

Radiation measurements were made in the region of gas located near the end wall, before and after passage of the reflected shock wave. The heated gas was observed through a quartz window, located

in the side wall of the shock tube at a point 1.80 inches from the end wall. The observed radiation, which was emitted in a direction normal to the shock tube axis, was split into two beams and analyzed by means of two Perkin-Elmer Model 98 monochromators (see Part I, Fig. 5). Each monochromator was equipped with an RCA 1P 28 photomultiplier tube, the signal from which was recorded on one beam of a Tektronix Model 551 dual beam oscilloscope.

Images of the observation window were focused on the monochromator entrance slits. The time resolution of the detection system was determined by two factors: (1) the $\approx 1/2\ \mu$sec time constant associated with the photomultiplier load resistors and the distributed capacitance of the lead-in cables and (2) the $\approx 2\ \mu$sec required for the reflected shock wave to pass across the narrow pencil of light rays ultimately collected by the monochromators. The overall time resolution of our measurements was therefore approximately $3\ \mu$sec, which was entirely adequate for our purposes, since relaxation phenomena were typically of 10-60 μsec duration.

The slit widths and wavelength settings of the monochromators were adjusted so that only radiation from a single line or multiplet of Cr I or Cr II would be measured by each. For all but one of the measurements, one monochromator was used to collect radiation due to the λ3421.2 and 3422.7 Å transitions of Cr II, while the other monochromator simultaneously monitored radiation from the λ 3976.7, 3983,9 and 3990.0 Å transitions of Cr. I.

In order to convert intensity measurements to quantitative

information about the populations of the excited levels responsible for the radiation, knowledge of the extent of self-absorption is required (see, for example, Section III. B. 2 of Part I). According to our previous gf-value measurements for the Cr II lines (cf. Part I) and available gf-value measurements for the Cr I lines,[17,18] all of the spectral lines previously mentioned were free from self-absorption under the conditions of our experiment. The observed intensities were therefore proportional to the number density of Cr I and Cr II atoms in the upper levels of the corresponding transitions. A single relaxation measurement was made using the λ4254.4 resonance line of Cr I. Insufficient line broadening data are available to permit an accurate calculation of the extent of self-absorption to be made for the latter line; nevertheless, the qualitative features of the observed intensity variation during the relaxation period were useful in our analysis of the excitation and ionization kinetics.

IV. RESULTS OF EXPERIMENTS

A. Presentation of Data

The raw data from the experiments consisted of oscilloscope traces showing the intensities of selected Cr I and Cr II lines before and after passage of the reflected shock wave. A representative oscilloscope record is shown in Fig. 1 (a similar record was presented in Fig. 9 of Part I). The deflection of the upper trace in Fig. 1 is proportional to the combined intensities of the Cr II lines at λ 3421.2 and 3422.7 Å; the lower trace deflection is proportional to the intensities of the λ3976.7, 3983.9, and 3991.7 Å lines of Cr I. Since both of these line groups are known to have been free from self-absorption, the trace deflections should also be proportional to the populations of the upper states involved in the corresponding transitions. However, there is the possibility that part of the observed radiation may have been due to nearby weaker lines of other transitions and continuum background radiation. To minimize this background contamination, the lines which were selected for analysis were those which, on the basis of photographs of the spectra (see Fig. 8, Part I), appeared to have the greatest spectral purity.

The striking features of the relaxation phenomena which occurred after passage of the reflected shock wave are the initial linear increase and the overshoot of the Cr I radiation, the gradual initial increase of the Cr II radiation, and the tendency of both Cr I and Cr II line intensities to reach nearly steady values at approximately the same time. The interpretation of the oscilloscope records is

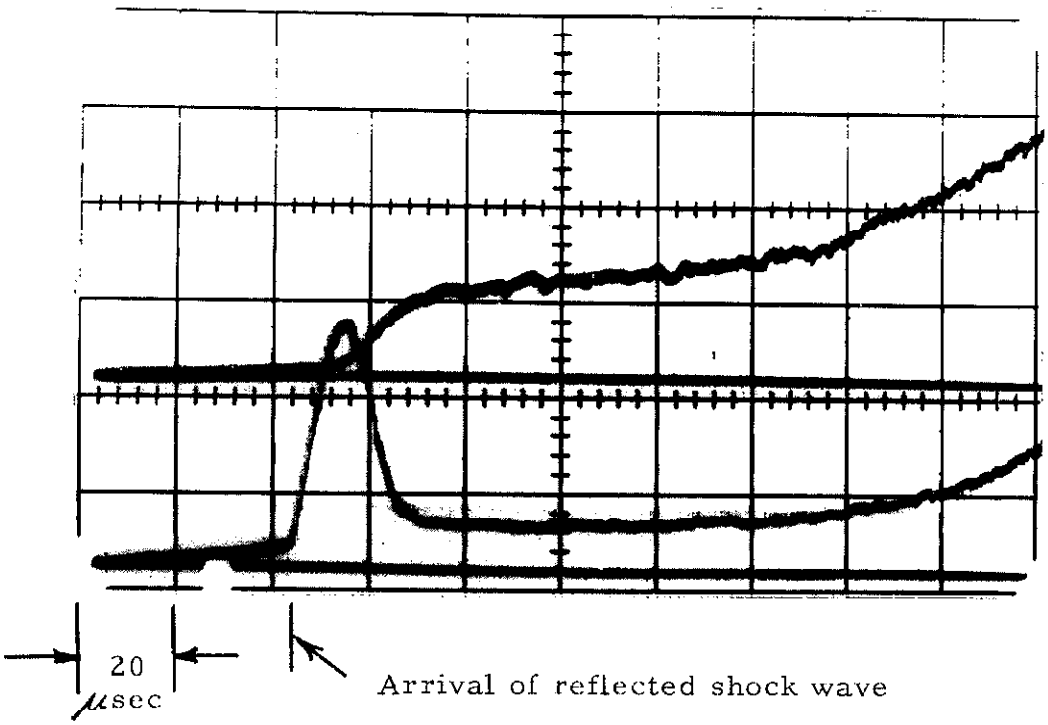

Upper trace: λ3421.2, 3422.7 Å

Lower trace: λ3976.7, 3983.9, 3991.7 Å

T_5 = 8140°K p_5 = 1.61 atm

Cr concentration $\eta = 1.5 \times 10^{-4}$

Fig. 1. Oscilloscope record of the intensities of Cr I lines (lower trace) and Cr II lines (upper trace) before and after passage of the reflected shock wave through the observed gas. The temperature and pressure behind the reflected wave and the wavelengths of the observed transitions are listed above. The reflected shock wave passed by the observation window 40 μsec after the oscilloscope was triggered. The intensities of both groups of lines attain quasi-steady values approximately 30 μsec after passage of the reflected wave. The rise in both traces near the end is caused by additional compression of the gas due to an interaction with the contact surface.

complicated somewhat by the fact that the gas behind the reflected shock wave is not exactly at rest and at a uniform temperature and pressure, as predicted by ideal shock theory (cf. Part I, Section III.A). Instead of being brought to rest by the reflected wave, the gas retains a component of velocity in the direction of the end wall,[11] and subsequently undergoes additional compression and heating. This non-ideal behavior is probably responsible for the steady increase in Cr II intensity after the $\approx 30\mu$sec required for completion of the relaxation processes. Approximately 110 μsec after passage of the reflected shock wave by the observation window, a secondary compression wave, resulting from an interaction of the reflected shock wave with the diffuse "contact surface", caused an increase in both upper and lower traces in Fig. 1. The various phenomena to which we have referred are shown more clearly on the somewhat idealized sketch of typical intensity-vs.-time behavior in Fig. 2.

A characteristic "relaxation time" for the approach to equilibrium behind the reflected wave may be arbitrarily defined. For reasons which will become clear in the remainder of this section, we chose to define a characteristic ionization relaxation time τ_i which is based upon the maximum rate of increase of Cr II radiation (see Fig. 2). In column 5 of Table I there are presented values of τ_i for shock tube runs for which the same groups of Cr I and Cr II lines were observed. These runs were made using initial $Cr(CO)_6$ concentrations $\eta = 4.3 \times 10^{-5}$, 1.5×10^{-4} and 3.6×10^{-4}. Since $Cr(CO)_6$ molecules were completely dissociated into Cr and CO by the incident shock wave, η is also very

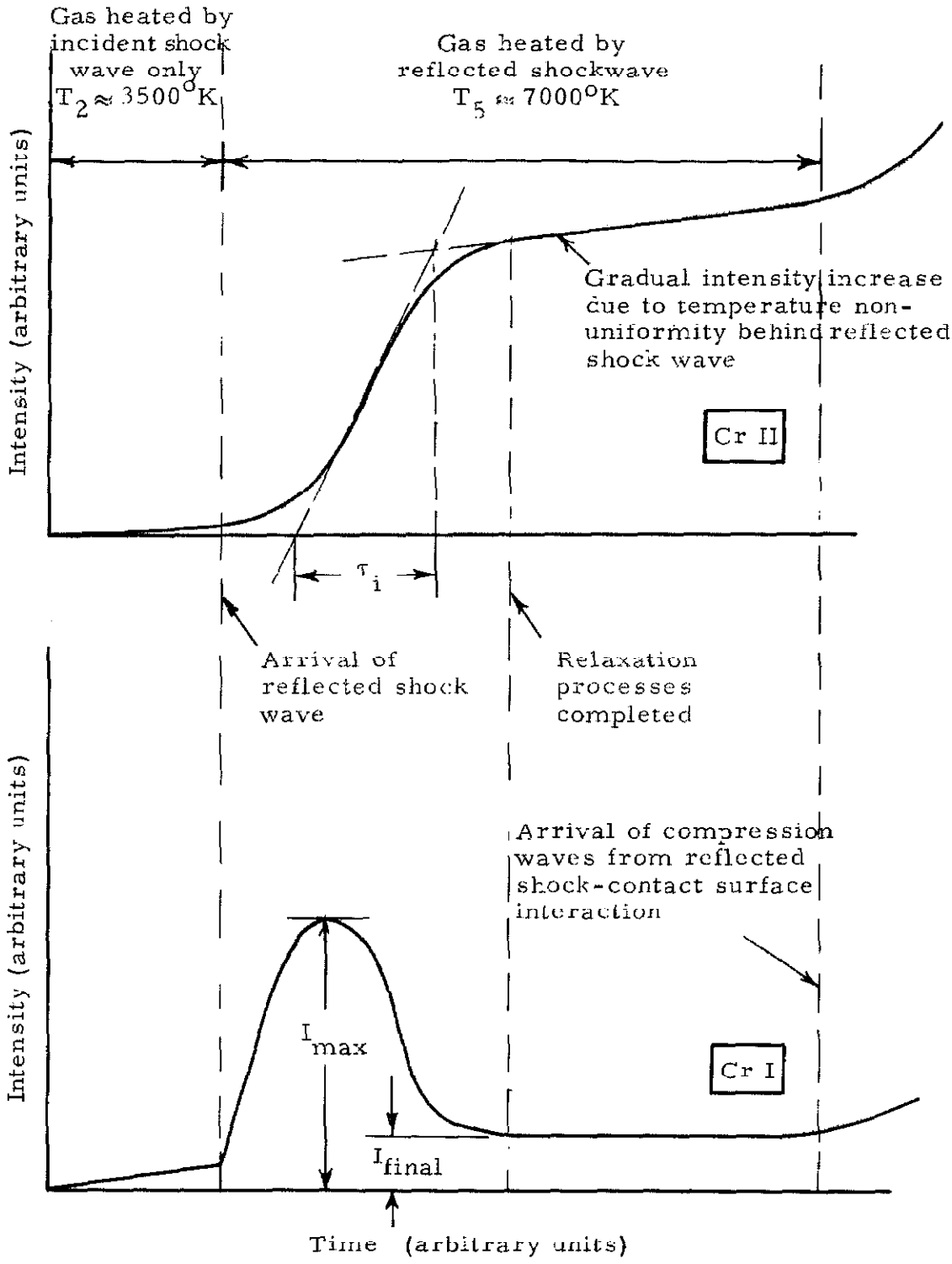

Fig. 2. Representation of a typical oscilloscope record, with an explanation of the important features and the means by which τ_i, I_{max} and I_{final} are defined.

TABLE I

Tabulation of experimental relaxation time and overshoot data.

Run No.	$Cr(CO)_6$ concentration in initial gas mixture, η	Temperature behind reflected shock, T_5 ^oK	Pressure behind reflected shock, p_5 atm	Relaxation time, τ_i μsec	Relative Cr I overshoot intensity $\left(\frac{I_{max}}{I_{final}}\right)_{Cr\ I}$
1	4.3×10^{-5}	8200	1.61	37+9	7
2	4.3×10^{-5}	7150	2.75	40±3	6
3	4.3×10^{-5}	6170	3.30	56±4	1.7
4	1.5×10^{-4}	8140	1.61	15±2	5
5	1.5×10^{-4}	6740	2.59	20±2	2.0
6	3.6×10^{-4}	8600	1.71	10±2	2.7
7	3.6×10^{-4}	6700	2.59	14+3	1.0

nearly equal to the relative abundance of Cr (atoms + ions) and Ar in the shock-heated gases. The temperature behind the reflected wave, T_5 (computed using ideal shock theory), was varied between 6170 and 8600°K.

The "relative height" of the Cr I radiation overshoot, as indicated by the relative values of the maximum and final steady-state intensities, $(I_{max}/I_{final})_{Cr\ I}$ (see Fig. 2), was less for those runs which were made at lower values of T_5 and higher values of η, that is, for those runs in which the final equilibrium degree of Cr ionization was least. No Cr I overshoot was observed in the run for which the equilibrium degree of Cr ionization behind the reflected wave (as computed from the Saha equation) was 92%. Values of $(I_{max}/I_{final})_{Cr\ I}$ are listed in column 6 of Table I.

In Fig. 3 an oscilloscope record of the simultaneous intensities of two sets of Cr I lines is shown. The lower trace indicates the combined intensity of the λ 3976.7, 3983.9 and 3991.7 lines, which were also used in the previously described measurements. These transitions originate from a term which is 5.6 ev above the ground state, and terminate at a term which is 2.5 ev above the ground state. The upper trace shows the simultaneous intensity of the Cr I resonance line, λ 4254.4 Å, which is produced by a transition from an excited level at 2.90 ev to the ground state. Although this line was probably self-absorbed, it is interesting to note that the record indicates the populations of both excited terms showed qualitatively the same "overshoot" behavior, and reached their maximum values at the same time. The significance of this fact, and of the other observations, is discussed in the following part of this section.

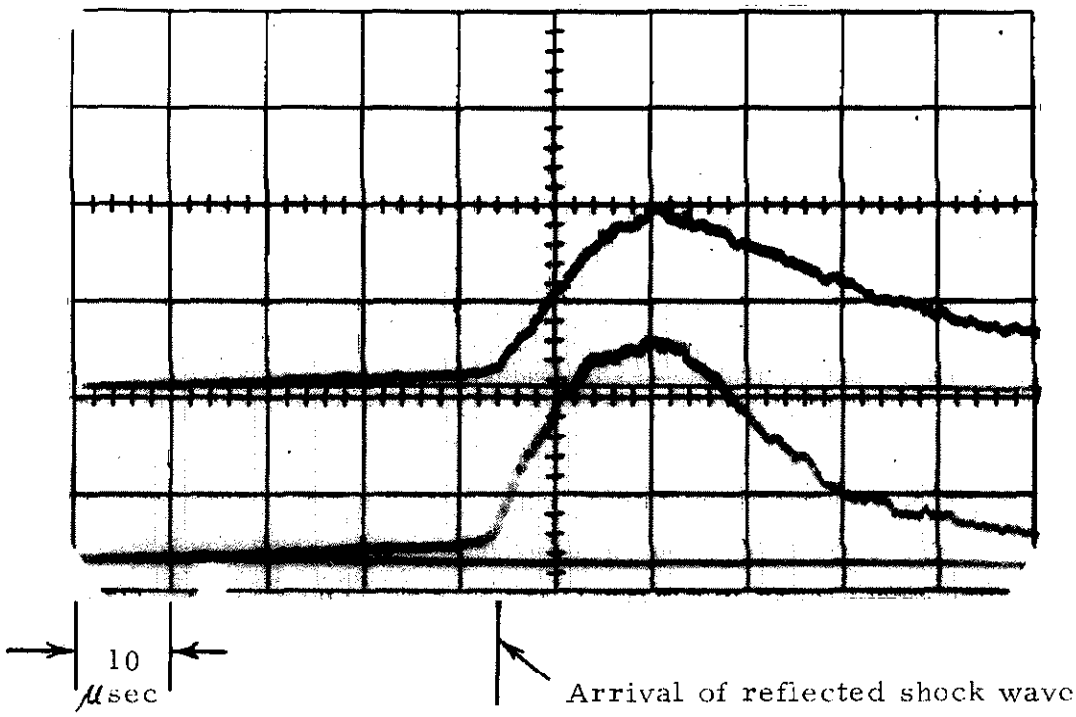

$T_5 = 8260^{\circ}K$

$p_5 = 1.61$ atm

Cr concentration $\eta = 4.3 \times 10^{-5}$

Fig. 3. Oscilloscope record of the intensity of the $\lambda 4254.4$ Å resonance line of Cr I (upper trace) and of the combined intensities of the Cr I lines $\lambda 3976.7$, 3983.9, and 3991.7 Å (lower trace).

B. DISCUSSION OF RESULTS

Before attempting to interpret the data in Table I in terms of a simplified model for the excitation and ionization processes, it will be helpful to make some preliminary approximate calculations of the frequencies of the various reactions which are believed to be of importance. In making these calculations, the following typical values for the pertinent kinetic parameters will be employed:

translational temperature of heavy particles : $T_a = 7000^{\circ}K$

electron temperature : $T_e = 7000^{\circ}K$

argon number density : $n_{Ar} = 2 \times 10^{18}\ cm^{-3}$

electron density : $n_e = 10^{14}\ cm^{-3}$

mean electron velocity : $c_e = (8kT_e/\pi m_e)^{1/2} = 5 \times 10^7\ \frac{cm}{sec}$

mean relative velocity of Cr and Ar : $c_a = (8kT_a/\pi\mu)^{1/2} = 2.5 \times 10^5\ \frac{cm}{sec}$

$\left(\mu = \frac{m_{Ar} m_{Cr}}{m_{Ar} + m_{Cr}}\right)$

The mean "time-of-flight" of an electron between elastic collisions with Ar atoms is given, approximately, by $\tau_{e\text{-}Ar}^{el} \approx (n_{Ar} c_e \sigma_{e\text{-}Ar}^{el})^{-1} \approx 5 \times 10^{-11}$ sec, where we have used the value $\sigma_{e\text{-}Ar}^{el} = 2 \times 10^{-16}\ cm^2$ for the mean electron-argon elastic cross section.[21] The choice of a mean cross section for this process is complicated by the strong energy dependence due to the Ramsauer effect and uncertainties in available experimental cross sections.

The stated value is probably correct to within a factor of three. In our notation, the first subscript denotes the species the flight time of which is being considered, while the second subscript identifies the colliding particles; hence $\tau^{el}_{e\text{-}Ar} \neq \tau^{el}_{Ar\text{-}e}$.

The time between elastic collisions of electrons and Cr^+ ions is, approximately,

$$\tau^{el}_{e\text{-}Cr^+} \approx (n_{Cr^+} \cdot c_e \cdot \sigma^{el}_{e\text{-}Cr^+})^{-1} = (n_e c_e \sigma^{el}_{e\text{-}Cr^+})^{-1} \approx 2.5 \times 10^{-10} \text{ sec}$$

if

$$\sigma^{el}_{e\text{-}Cr^+} \approx 2\pi \left(\frac{e^2}{mc_e^2} \right) \ell n \left[9(kT_e)^3 / 8\pi n_e e^6 \right] = 8 \times 10^{-13} \text{ cm}^2$$

is an appropriate energy-transfer cross section for the $e\text{-}Cr^+$ interaction with Debye shielding taken into account.[1] It is apparent that electrons were more likely to collide elastically with Ar atoms than with Cr^+ ions under the experimental conditions which we encountered.

An average radiative lifetime of 10^{-7} sec for excited states of Cr I has been estimated in Part I (p. 48). In arriving at this estimate, the effects of self-absorption and nearby metastable states were taken into account in an approximate way. Denoting this quantity by $\tau^{rad}_{Cr'}$,

$$\tau^{rad}_{Cr'} \approx 10^{-7} \text{ sec.}$$

The population of a Cr I excited level, Cr', during the relaxation period is determined by the following competing processes:

(1) spontaneous radiative depopulation: $Cr' \xrightarrow{\tau^{rad}_{Cr'}} Cr + h\nu$

(2) inelastic collisional excitation from lower levels: $Cr + X \longrightarrow Cr' + X$
(X may be either an atom or an electron)

(3) collisional de-excitation to lower levels: $Cr + X \longleftrightarrow Cr' + X$

(4) collisional excitation or ionization from the excited state:
$$\begin{cases} Cr' + X \longrightarrow Cr'' + X \\ Cr' + X \longrightarrow Cr^{+} + X + e^{-} \end{cases}$$

A characteristic lifetime for de-excitation of Cr excited states with energies about 3 ev above the ground state by collisions with electrons may be estimated, as in Part I, by a comparison with de-excitation rates for the n = 3 level of hydrogen.[19] Assuming the de-excitation rates to be about equal, we obtain for a typical collisional de-excitation lifetime of Cr' the value

$$\tau^{inel}_{Cr'-e}\left(Cr' \underset{\sim 3ev}{\longrightarrow} Cr_{ground}\right) \approx 2 \times 10^{-7} \text{ sec}$$

The characteristic time required for the reverse process (excitation of a ground-state Cr atom to a level near 3 ev), $\tau^{inel}_{Cr-e}\left(Cr_{ground} \longrightarrow Cr'_{\sim 3ev}\right)$, may be related to $\tau^{inel}_{Cr'-e}\left(Cr'_{\sim 3ev} \longrightarrow Cr_{ground}\right)$ by requiring that the forward and reverse reaction rates be equal when the population ratio $n_{Cr'}/n_{Cr}$ equals the local thermodynamic equilibrium value $(n_{Cr'}/n_{Cr})_{eq}$, viz.,

$$\frac{\tau^{inel}_{Cr'-e}}{\tau^{inel}_{Cr-e}} \approx \left(\frac{n_{Cr'}}{n_{Cr}}\right)_{eq} \approx \exp(-3ev/kT) \approx 10^{-2};$$

hence

$$\tau^{\text{inel}}_{\text{Cr-e}}\,(\text{Cr}_{\text{ground}} \longrightarrow \text{Cr}'_{\sim 3\text{ev}}) \approx 2 \times 10^{-5} \text{ sec},$$

which is of the same order as the relaxation times, τ_i, which we observed. A possible explanation of this agreement is that the mechanism of ionization involved excitation of ground-state Cr atoms to levels about 3 ev above the ground state, from which ionization occurred within a time shorter than the de-excitation lifetime, $\tau^{\text{inel}}_{\text{Cr'-e}} \approx 2 \times 10^{-7}$ sec. Such a mechanism would necessarily require that ionization cross sections increase rapidly with the electronic energy of the initial atomic state, a situation that is consistent with the classical theory of inelastic collisions.[22] Further evidence that the ionization proceeded by this mechanism was provided by the dependence of the relaxation rates upon the temperature behind the reflected shock wave, which is discussed at the end of this section.

Because of the current lack of adequate information concerning atom-atom inelastic collision cross sections, it is not possible to predict with certainty which type of inelastic collisions, Cr-Ar or Cr-electron, contributed most to the excitation and ionization of chromium. A crude estimate of the relative cross sections for these processes (cf. p. 44) suggests that electrons are the more important when the relative abundance of electrons and atoms exceeds about 10^{-5}. Assuming this value to be reliable and Cr atoms to be the main source of electrons, the degree of chromium ionization, α, required for the predominance of Cr-electron collisions would then be 25% for the

lowest Cr concentrations and 3% for the highest concentrations which were used. The possibility that easily ionized impurities may have also contributed significantly to the number of free electrons increases the likelihood that electrons were sufficiently abundant to dominate the excitation and ionization rates.

Experimental evidence that inelastic collisions with electrons were dominant was provided by the observed dependence of the relaxation times upon the Cr concentration, as well as by the form of the time variation of Cr I line intensities. The two types of evidence will now be discussed individually.

1. Dependence of relaxation time upon the chromium concentration

If Cr-Ar inelastic collisions were the dominant means of excitation and ionization of Cr, the observed relaxation time, τ_i, would have depended only upon the temperature and argon number density behind the reflected shock wave; however, a strong dependence upon the Cr concentration, η, was also noted. Since only three different values of η were employed in these experiments, the dependence of τ_i upon η could not be determined in detail; the relation $\tau_i \sim \eta^{-\gamma}$, with $\gamma = 0.6 \pm 0.1$ was found to describe the dependence upon η fairly well at a given temperature and pressure (see Fig. 4). A reasonable qualitative explanation for the dependence upon η is that the greater number of chromium atoms which are present at higher values of η result in larger number densities of free electrons once a given fraction of Cr has become ionized. The ionization process is evidently

of an autocatalytic character, that is, the electrons liberated from Cr tend to accelerate the rate of ionization.

2. Relaxation behavior of Cr I radiation

Since the populations of Cr I excited states which were 2.90 and 5.65 ev above the ground state show qualitatively the same relaxation behavior, it is reasonable to attempt to explain this behavior in terms of a simple model which involves only a single excited state. Consider the mechanism represented by

$$\mathrm{Cr} \underset{\tau'_{1,r}}{\overset{\tau'_1}{\rightleftharpoons}} \mathrm{Cr}' \xrightarrow{\tau'_2} \mathrm{Cr}^+ \qquad \tau^{rad}_{Cr'}$$

where Cr represents the ground state and Cr' a "lumped" excited state of a chromium atom, and Cr^+ represents a chromium ion. The τ's denote mean lifetimes for the transitions indicated. Electron-ion recombination is neglected. The lifetimes τ_1', $\tau'_{1,r}$ and τ_2' depend upon the electron density, and therefore upon the degree of ionization, α, while the radiative lifetime, $\tau^{rad}_{Cr'}$, remains constant. If the heavy-particle and electron temperatures, T_a and T_e, remain fairly constant during the relaxation period, the variation of τ_1 and τ_2 with α will be given approximately by

$$\begin{aligned} (\tau_1')^{-1} &= \tau_1^{-1}(\varepsilon_1 + \alpha) \\ (\tau_2')^{-1} &= \tau_2^{-1}(\varepsilon_2 + \alpha), \end{aligned} \tag{5}$$

where τ_1, τ_2, ε_1, and ε_2 are constants. Such a relationship implies a linear dependence of the reaction rate upon α, with ε_1 and ε_2 accounting for the slow initial reaction rates for $\alpha = 0$. The values of τ_1' and $\tau_{1,r}'$ must be related to each other by an idealized form of the principle of detailed balancing,

$$\frac{\tau_{1,r}'}{\tau_1'} = \left(\frac{n_{Cr'}}{n_{Cr}}\right)_{eq.} \equiv \mu \qquad (\mu << 1) \tag{6}$$

$$(\tau_{1,r}')^{-1} = \mu^{-1}(\varepsilon_1 + \alpha)\,\tau_1^{-1} \tag{7}$$

The population $n_{Cr'}$ of the excited state obeys the differential equation

$$\frac{d}{dt} n_{Cr'} = \tau_1^{-1}(\varepsilon_1 + \alpha)\, n_{Cr} - \mu^{-1}\tau_1^{-1}(\varepsilon_1 + \alpha)\, n_{Cr'}$$

$$-n_{Cr'}(\tau_{Cr'}^{rad})^{-1} - \tau_2^{-1}(\varepsilon_2 + \alpha) n_{Cr'} \tag{8}$$

where α is a function of time. If the excitation processes were dominated by atom-atom collisions, one could neglect α in comparison to ε_1 and ε_2 in Eq. (8), thus obtaining a linear differential equation with constant coefficients. After passage of the reflected shock, $n_{Cr'}/n_{Cr}$ would reach a quasi-steady value which may be calculated by setting the derivative in Eq. (8) equal to zero,

$$\frac{n_{Cr'}}{n_{Cr}} = \frac{\mu\varepsilon_1/\tau_1}{(\tau_{Cr'}^{rad})^{-1} + \varepsilon_1/\tau_1 + \varepsilon_2/\tau_2}, \quad \varepsilon_1, \varepsilon_2 >> \alpha\ . \tag{9}$$

The time required for this ratio of $n_{Cr'}/n_{Cr}$ to become established would be of the same order as the mean lifetime for the most rapid

process which depopulates the upper state, i.e., less than 10^{-7} sec. The maximum value of n_{Cr}, would be obtained within an unobservably short time after reflected shock passage, and thereafter $n_{Cr'}$ would diminish as the supply of neutral Cr becomes depleted.

The time which elapsed between passage of the reflected shock wave and the attainment of maximum Cr I excited state populations was, however, found to be between 5 and 20 μ sec, rather than the 10^{-7} sec which would be expected if only Cr-Ar inelastic collisions had been important. A logical explanation of why the times were this long involves a scheme whereby inelastic collisions with electrons are responsible for populating the excited level, while radiative transitions are chiefly responsible for depopulating it. In this case we may assume $\varepsilon_1, \varepsilon_2 = 0$ and, once again, neglect the contribution of the derivative term in Eq. (8). The equation for $n_{Cr'}/n_{Cr}$ then becomes

$$\frac{n_{Cr'}}{n_{Cr}} = \frac{\mu \frac{a}{\tau_1}}{\tau_{Cr'}^{rad} + \frac{a}{\tau_1} + \frac{a}{\tau_2}} \qquad a \gg \varepsilon_1, \varepsilon_2 \qquad (10)$$

For small values of a, $n_{Cr'}/n_{Cr}$ increases gradually as Cr becomes ionized and the freed electrons accelerate the rate of excitation to the upper level. The "overshoot" behavior results from the tendency of $n_{Cr'}/n_{Cr}$ to increase with time while n_{Cr} is decreasing due to depletion of the neutral species by ionization.

3. Electron temperature

Since it has been determined that the ionization and excitation of chromium was mainly due to inelastic collisions with electrons, it must be inferred that the electron temperature, T_e, rather than the heavy-particle temperature, T_a, is the appropriate quantity to use in order to obtain activation energy and cross section data from the observed relaxation rates. The temperature which one computes from the incident shock speed using one-dimensional shock wave theory is T_a. The relationship between T_e and T_a during the relaxation period can be established by solving Eq. (3) if the energy transfer rates Q_{in} and $Q_{e\ell}$ are known. Since the energy transfer rates exceed the rate of change of electron thermal energy, the derivative in Eq. (3) may be neglected, yielding the relation

$$Q_{in} = Q_{e\ell}. \tag{11}$$

The quantity $Q_{e\ell}$, the rate of transfer of energy to electrons by elastic collisions with argon, is given approximately by[1]

$$Q_{e\ell} \approx \frac{m_e}{m_{Ar}} 3kT_a \left(1 - \frac{T_e}{T_a}\right) n_{Ar} n_e \overline{\sigma(c_e)c_e} \tag{12}$$

$$= \frac{m_e}{m_{Ar}} \times \frac{3kT_a}{\tau_{e\text{-}Ar}^{e\ell}} \left(1 - \frac{T_e}{T_a}\right) n_e$$

$$\approx 10^8 \left(1 - \frac{T_e}{T_a}\right) \text{erg cm}^{-3} \text{ sec}^{-1},$$

where we have used the value of $\tau_{e\text{-}Ar}^{e\ell}$ from p. 134 and $n_e = 10^{14}$ cm^{-3}. A reasonable estimate for the maximum rate of electron energy loss

due to inelastic collisions is

$$Q_{in} \approx n^{o}_{Cr} \frac{I_{Cr\ I}}{2\tau_i} \approx 3 \times 10^{7} \text{ erg cm}^{-3} \text{ sec}^{-1}$$

where $n^{o}_{Cr} \approx 10^{14}$ cm^{-3} is the number density of Cr atoms before ionization, $I_{Cr\ I}$ the ionization potential, and $2\tau_i$ the approximate time required for ionization. Setting $Q_{in} = Q_{e\ell}$, one obtains $T_e \approx 0.7 T_a$. It is apparently possible that T_e may have been appreciably less than T_a during the relaxation period. However, since the estimates of $Q_{e\ell}$ and Q_{in} are only believed to be correct to within a factor of about three, we cannot state with any certainty whether or not the reaction rates were significantly affected by the lowering of T_e below T_a.

4. Relaxation of Cr II population

The reason for basing the definition of τ_i upon the maximum rate of increase of Cr II radiation (see Fig. 2) rather than some other measured time such as the total relaxation time or the time required for Cr I radiation to reach a maximum, is that the Cr II radiation intensity is believed to have been directly proportional to the fraction of chromium ionized, a. Since Cr II excited states, unlike those of Cr I, were not depleted by further ionization and are not expected to have had radiative lifetimes shorter than collisional de-excitation lifetimes (cf. p. 122), the relative populations of Cr II excited states and the ground state during the relaxation period should have been given very nearly by the value corresponding to local thermodynamic

equilibrium. If it is assumed that the final Cr II intensity level behind the reflected shock corresponds to the equilibrium degree of ionization $\alpha^{(e)}$, then according to the definition of τ_i,

$$\left(\frac{d\alpha}{dt}\right)_{max} = \frac{\alpha^{(e)}}{\tau_i} \quad , \tag{13}$$

which is very nearly equal to $(\tau_i)^{-1}$, since $\alpha^{(e)}$ was at least 92% for all runs. The maximum rate of ionization, it is believed, should be capable of being more directly related to the experimental variables than the "total relaxation time", which is also critically dependent upon the unknown electron density ahead of the reflected shock wave. The maximum rate of ionization was always observed to occur for $\alpha = 0.5 \pm 0.1$.

It is of interest to consider whether most of the chromium becomes ionized by means of (1) direct transitions from the ground state of Cr I to the ionization continuum, or (2) raising of neutral Cr to an excited state, from which ionization takes place although de-excitation is more likely, or (3) raising of neutral Cr to an excited state, from which ionization is more likely than de-excitation. These three possible mechanisms are represented by the following simplified reactions:

$$(1) \quad Cr \xrightarrow{\tau_3 \approx \tau_i} Cr^+$$

$$(2) \quad Cr \underset{\tau_{1,r} < \tau_2}{\overset{\tau_1}{\rightleftharpoons}} Cr' \xrightarrow{\tau_2} Cr^+$$

$$(3)\quad Cr \underset{\tau_{1,r} > \tau_2}{\overset{\tau_1 \approx \tau_i}{\rightleftharpoons}} Cr' \xrightarrow{\tau_2} Cr^+$$

The temperature dependence of the ionization rate may be expected to be dominated by an Arrenhius factor $\exp(-E_a/kT_e)$, where E_a is an effective activation energy for ionization. The characteristic lifetimes τ_1, τ_2 and τ_3 should have approximately the following dependence upon T_e:

$$\tau_3 \sim \exp(I_{Cr\ I}/kT_e)$$

$$\tau_1 \sim \exp(E_{Cr'}/kT_e)$$

$$\tau_2 \sim \exp\left[(I_{Cr\ I} - E_{Cr'})/kT_e\right]$$

where $I_{Cr\ I}$ denotes the ionization potential of Cr I, and $E_{Cr'}$ the energy difference between level Cr' and the Cr I ground state.

In the first of these cases the activation energy for the ionization process would be expected to be the ionization potential of Cr I, 6.74 ev. For the second case, one obtains

$$\frac{dn_{Cr^+}}{dt} \approx \frac{n_{Cr'}}{\tau_2} \qquad \frac{n_{Cr}}{\tau_1} \approx \frac{n_{Cr'}}{\tau_{1,r}}$$

and

$$\frac{dn_{Cr^+}}{dt} \approx \frac{n_{Cr}}{\tau_2}\,\frac{\tau_{1,r}}{\tau_1} \approx \frac{n_{Cr}}{\tau_2}\exp(-E_{Cr'}/kT_e).$$

A mechanism such as this would also involve an activation energy equal to the ionization potential.

The third reaction mechanism would have a lower activation energy than the others, since for this case

$$\frac{n_{Cr}}{\tau_1} \approx \frac{n_{Cr'}}{\tau_2}$$

and

$$\frac{dn_{Cr^+}}{dt} \approx \frac{n_{Cr'}}{\tau_2} \approx \frac{n_{Cr}}{\tau_1}$$

In this instance the first step is rate-controlling, and the overall activation energy is just the energy difference between the ground state and the excited state, Cr'.

In Fig. 4 the parameter $\log_e \left[\tau_i n_5 (\eta/10^{-5})^{\gamma}\right]$ is plotted as a function of $1/T_a$ for two assumed values of γ. The quantity n_5 represents the total number density behind the reflected shock wave. It is apparent from the figure that a relation of the form

$$\tau_i^{-1} \sim n_5 \eta^{0.6} e^{-E_a/kT_a}$$

fits the observed experimental points reasonably well. Because of the limited amount of data, the possibility that T_c was significantly less than T_a, and the fact that the assumed linear dependence upon n_5 was not verified by varying n_5 and T_a independently, it is admittedly somewhat presumptuous to interpret E_a as an activation energy. The slope of the straight line in Fig. 4 corresponds to E_a=3.1 ev. Straight lines for which E_a=2.8 or 3.4 ev fit the experimental points nearly as well.

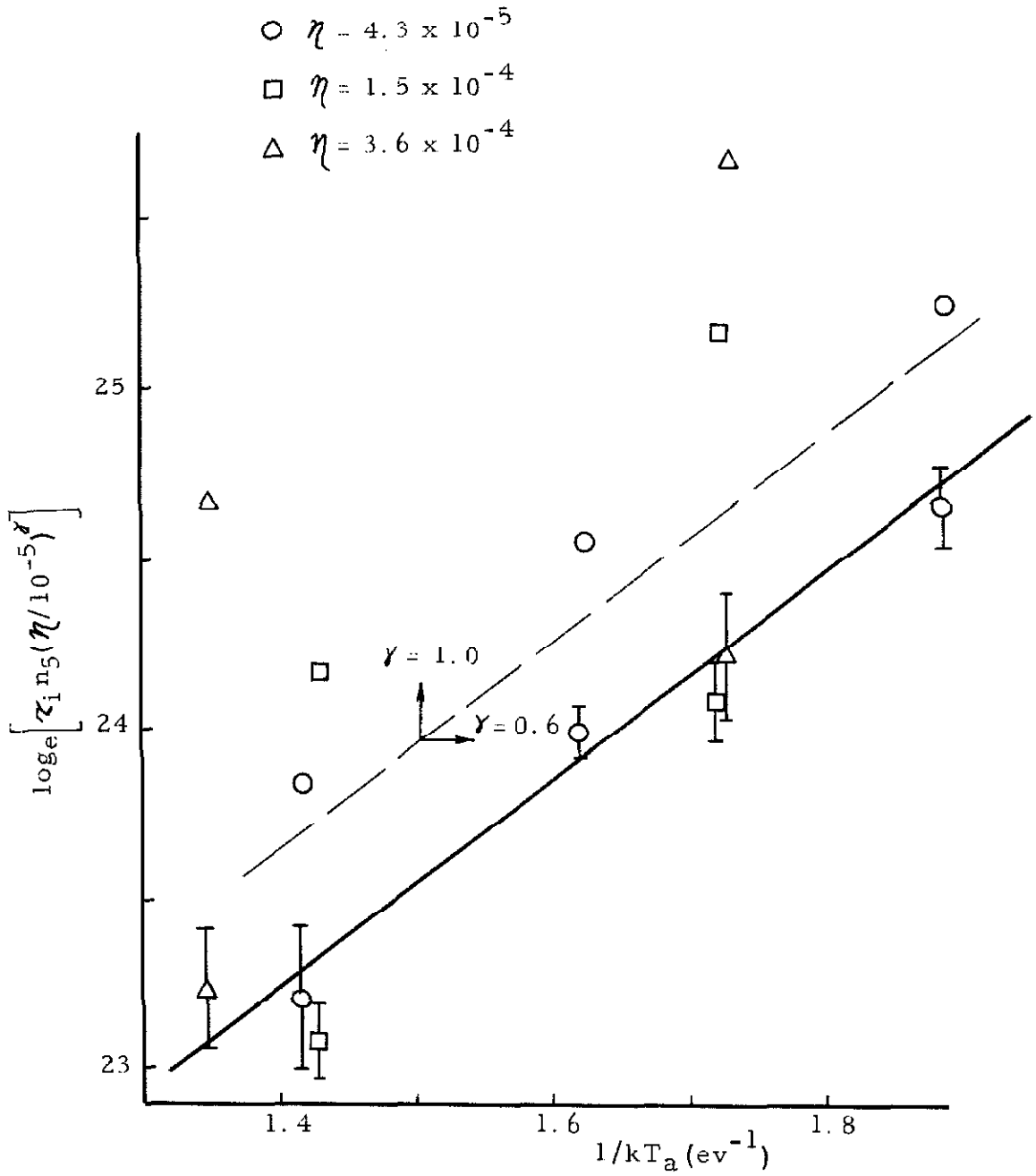

Fig. 4. Effect of temperature, T_a, upon the relaxation time τ_i. In drawing the straight line through the points, it is assumed that $\tau_i^{-1} \sim n_5 \eta^{\gamma} \exp(-E_a/kT_a)$, where n_5 is the total number density, η the Cr concentration, E_a an activation energy, and γ an empirically determined exponent. Experimental points are plotted for two assumed values of γ : $\gamma = 0.6$ (below dashed line, showing error limits), and $\gamma = 1.0$ (above dashed line).

If we assume that T_e and T_a did not differ appreciably during the relaxation period, the interpretation of E_a as the activation energy for the ionization process is plausible. A value of 3.1 ± 0.3 ev for the activation energy would indicate that the dominant mechanism for ionization is that which involves excitation of Cr I to levels approximately 3.1 ev above the ground state, from which subsequent ionization was more probable than de-excitation or radiative transition to lower states.

Assuming the reaction mechanism is of this type, the observed relaxation times may be used to estimate a mean cross section for the rate-controlling process,

$$\mathrm{Cr}\ (E=0) + e^- \xrightarrow{\gamma_i} \mathrm{Cr}\ (E=3.1\ \mathrm{ev}) + e^-$$

The cross section for excitation of a given level is a sensitive function of the kinetic energy of the incident electron, being zero for energies less than the threshold value (which is assumed to be 3.1 ev in this case), and varying in some unknown way for electron energies greater than the threshold value. In order to obtain an effective mean value of the cross section for collisions in which the incident-electron energy, E, is greater than 3.1 ev, we shall make the following simplifying assumption:

$$\sigma(E) = \begin{cases} 0 & , \ E < E_a = 3.1\ \mathrm{ev} \\ \sigma^{\mathrm{inel}}_{\mathrm{Cr-e}} & , \ E \geq E_a = 3.1\ \mathrm{ev} \end{cases}$$

where σ^{inel}_{Cr-e} is the effective mean cross section for the reaction being considered. For a Maxwell-Boltzmann distribution of electron velocities corresponding to a temperature T_e, the rate of the excitation reaction, ν_e (cm^{-3} sec^{-1}), is given by[23]

$$\nu_e = n_e n_{Cr,E=0}\left(\frac{2kT_e}{\pi m_e}\right)^{1/2} \sigma^{inel}_{Cr-e}\left(\frac{E_a}{kT_e}+1\right) e^{-E_a/kT_e}, \qquad (14)$$

and since we are assuming that this excitation reaction was the rate-controlling step of the ionization process, the rate of the excitation reaction should be equal to the observed ionization rate, i.e.,

$$\nu_e \approx \nu_i = \frac{dn_{Cr^+}}{dt} \approx \frac{n_{Cr,E=0}}{\tau_i} \qquad (15)$$

If we now assume $T_e = T_a$ and take the following values of T_a, n_e and τ_i corresponding to run no. 4 (Table I),

$n_e = 10^{14}$ cm^{-3} (corresponding to 50% ionization of Cr)

$\tau_a \cong T_e = 8140^{\circ}K$

$\tau_i = 15 \times 10^{-5}$ sec,

the value of σ^{inel}_{Cr-e} obtained by solving Eqs. (12) and (13) is

$$\sigma^{inel}_{Cr-e} \approx 4 \times 10^{-16} \text{ cm}^2,$$

a value which is not inconsistent with experimental and theoretical values of cross sections for excitation of resonance lines of HgI and NaI.[24] If the activation energy for ionization were equal to the

ionization potential of Cr I (6. 74 ev) rather than the 3.1 ± 0. 3 ev value which we obtained, the cross sections would have to be a factor of about 10^3 larger (i. e., $\sigma^{inel}_{Cr-e} \approx 4 \times 10^{-13}$ cm^2) in order to be consistent with the observed relaxation rates. No evidence has ever been found for electron-atom inelastic cross sections of this order.

V. CONCLUSIONS

The magnitude of the experimental relaxation times, the dependence of these times upon temperature and Cr concentration, and the existence of a population overshoot for Cr I radiation, can be explained by making the following assumptions: 1. Most of the Cr becomes ionized after first being excited to levels approximately 3.1 ev above the ground state. 2. The rate-controlling step for ionization involves excitation of these intermediate levels by inelastic collisions between electrons and ground-state chromium atoms. In order for this first step to be rate-controlling, the probability of ionization from excited levels approximately 3.1 ev above the ground state must exceed the probability of collisional de-excitation or spontaneous radiative transitions to lower levels. Such a mechanism is similar to that proposed by Harwell[7] to explain the observation that the activation energy for thermal ionization of inert gases by atom-atom collisions is equal, within experimental error, to the energy difference between the ground state and the lowest excited state of the neutral species.

Further studies of the relaxation of Cr I and Cr II excited-state populations behind shock waves in $Cr(CO)_6$-inert gas mixtures should lead to useful information concerning electron-atom and atom-atom inelastic cross sections. The interpretation of the excitation and ionization kinetics would be facilitated if, together with population measurements, simultaneous measurements of the electron density and electron temperature were made.

REFERENCES FOR PART II

1. H. E. Petschek and S. Byron, Annals of Physics 1, 270 (1957).

2. H. E. Petschek, P. H. Rose, H. S. Glick, A. Kane, and A. Kantrowitz, J. Appl. Phys. 26, 83 (1955).

3. E. B. Turner, U. of Mich. Eng. Research Institute AFOSR TN-56-150, ASTIA Document No. AD 86309 (1956).

4. S. C. Lin, E. L. Resler, and A. Kantrowitz, J. Appl. Phys. 26, 95 (1955).

5. R. A. Alpher and D. R. White, Phys. Fluids 2, 162 (1961).

6. S. C. Lin, R. A. Neal, and W. I. Fyfe, Phys. Fluids 5, 1633 (1962).

7. K. E. Harwell, Ph. D. Thesis, Calif. Inst. of Technology (1963); K. E. Harwell and R. G. Jahn, Phys. Fluids 7, 214 (1964).

8. H. D. Weymann, University of Maryland Institute for Fluid Dynamics and Applied Mathematics TN BN-144 (1958).

9. P. Gloersen, Phys. Fluids 3, 857 (1960).

10. D. S. Hacker and H. Bloomberg, J. Chem. Phys. 39, 3263 (1963).

11. T. Wilkerson, U. of Mich., O. R. A. Report No. 02822-3T, AFOSR 1151 (1961); Ph. D. Thesis (1961).

12. A. F. Haught, Phys. Fluids 5, 1337 (1962).

13. E. Hinnov and J. G. Hirschberg, Phys. Rev. 125, 795 (1962).

14. H. S. W. Massey and E. H. S. Burhop, Electronic and Ionic Impact Phenomena, Oxford (1952), p. 532.

15. ibid., p. 422.

16. C. W. Allen, Astrophysical Quantities, Athlone Press, London (1955).

17. C. H. Corliss and W. R. Bozman, Experimental Transition Probabilities for Spectral Lines of Seventy Elements, National Bur. Stand., Washington, Monograph 53 (1962).

18. G. Charatis, Ph. D. Thesis, U. of Mich. (1962).

19. S. Byron, R. D. Stabler, and P. I. Bortz, Phys. Rev. Letters 8, 376 (1962).

20. H. Mirels, Phys. Fluids 6, 1201 (1963).

21. H. S. W. Massey and E. H. S. Burhop, op. cit., p. 116.

22. J. J. Thomson, Phil. Mag. 47, 337 (1924).

23. S. Chapman and T. G. Cowling, The Mathematical Theory of Non-Uniform Gases, Cambridge (1960).

24. M. Gryzinski, Phys. Rev. 115, 308 (1959).

J. Quant. Spectrosc. Radiat. Transfer. Vol. 2, pp. 263–271. Pergamon Press Ltd. Printed in Great Britain

APPROXIMATE SPECTRAL ABSORPTION COEFFICIENT CALCULATIONS FOR ELECTRONIC BAND SYSTEMS BELONGING TO DIATOMIC MOLECULES*

R. W. PATCH† W. L. SHACKLEFORD† and S. S. PENNER

Division of Engineering
California Institute of Technology
Pasadena, California

(*Received* 22 *November* 1961)

Abstract—The spectral absorption coefficients in electronic band systems of diatomic emitters have been computed in the past by models that may be described as 'the just overlapping line model' and a model 'utilizing a smeared out rotational structure'. Although the basic relations are obtained by utilizing somewhat different physical arguments, the resulting equations are, in fact, identical.

Spectral absorption coefficients have been calculated for the NO γ-bands at 2000°K by using the approximate theoretical relations. The calculated results are in good agreement with estimates derived by numerical calculations in which, however, the absorption coefficient data were averaged over intervals of 2000 cm^{-1}.

NOMENCLATURE

B_e rotational constant, (cm^{-1})
ΔB difference in rotational constants, (cm^{-1})
c velocity of light, (cm sec^{-1})
C band factor, (cm^{-1}-atm^{-1})
D exponential coefficient, (cm)
e charge of electron, (e.s.u.)
E energy of level, (ergs)
f electronic absorption oscillator strength, dimensionless
h Planck's constant, (erg-sec)
j rotational quantum number, dimensionless
k Boltzmann constant, (erg-°K^{-1})
m mass of electron, (g)
n number of lines per j'' level for $v''v'$-band, dimensionless
N particle density, (cm^{-3})
P_ω average spectral absorption coefficient, (cm^{-1}-atm^{-1})
p pressure, (atm)
q Franck–Condon factor, dimensionless.
Q partition function, dimensionless
r internuclear distance, (cm)

*Supported by the Air Force Office of Scientific Research under Contract AF 49 (638)-984.
†NSF Predoctoral Fellow.

S integrated absorption coefficient for line, (cm^{-2}-atm^{-1})
T temperature, (°K)
v vibrational quantum number, dimensionless
$\delta\omega$ average line spacing, (cm^{-1})
α integrated absorption coefficient for band, (cm^{-2}-atm^{-1})
ϕ band smearing factor, dimensionless
ψ normalized time-independent vibrational eigenfunction, ($cm^{-1/2}$)
ω term value or wave number, (cm^{-1})

Superscripts

$'$ upper electronic state
$''$ lower electronic state

Subscripts

h band head
j rotational quantum number
v vibrational quantum number
00 0-0 rotationless transition
0 vibrational quantum number 0

I. DERIVATION OF THE THEORETICAL EQUATIONS

THE origin of the theoretical equations obtained for the 'just-overlapping line model' is documented in the literature.[1] Since full appreciation of the results requires considerable familiarity with quantitative spectroscopy, a somewhat simpler derivation is presented in the following section IA. The results derived by using a procedure for smearing the rotational fine structure in electronic band systems have been published and used by KECK *et al.*[2]. Since no derivation of the basic equations is given in Ref. 2, we rederive the desired expressions in section IB.

A. *The 'just-overlapping line model'*

Consider the simplified energy level diagram for a diatomic molecule shown in Fig. 1. Two electronic states are indicated. The vibrational and rotational term values (or energy levels) of the upper electronic state are identified by the subscripts v' and j', respectively; the corresponding term values of the lower electronic state bear the subscripts v'' and j'', respectively. Radiative transitions may take place between vibrational levels of the two electronic states, subject to the rotational selection rules

$$j'-j'' = \pm 1 \text{ or } j'-j'' = 0. \tag{1}$$

The rotational term values for the large values of j'' and j' which make the dominant contributions to the spectral absorption coefficients are given by the expressions

$$\omega_{j''} = j''(j''+1)B_e'' \tag{2}$$

and

$$\omega_{j'} = j'(j'+1)B_e' \simeq j''(j''+1)B_e'. \tag{3}$$

The fraction of the v'' molecules in the j'' state is given by the relation

$$\frac{N_{v''j''}}{N_{v''}} = \frac{(2j''+1)\exp\left[-j''(j''+1)B_e''hc/kT\right]}{\sum_{j=0}^{\infty}(2j''+1)\exp\left[-j''(j''+1)B_e''hc/kT\right]}. \tag{4}$$

It is well known that we may use the approximation

$$\sum_{j''=0}^{\infty}(2j''+1)\exp\left[-j''(j''+1)B_e''hc/kT\right] \simeq \int_0^{\infty} 2j''[\exp(-j''^2 B_e''hc/kT)]\mathrm{d}j'' = \frac{kT}{B_e''hc} \tag{5}$$

at moderate and high temperatures. Hence it follows that

$$\frac{N_{v''j''}}{N_{v''}} \simeq \frac{2j''B_e''hc\exp-[j''(j''+1)B_e''hc/kT]}{kT}. \tag{6}$$

In a given vibration–rotation band involving transitions between v' and v'', each j''-level is found to participate in the formation of $n = 2$ or more rotational lines when proper allowance is made for the selection rules and for spin splitting. We shall simplify the following analysis by assuming that all of these lines have equal integrated absorption coefficients, $S_{v''v';j''}$, viz.,

$$S_{v''v';j''} \equiv \int_0^{\infty} P_{\omega;v''v';j''}\,\mathrm{d}\omega. \tag{7}$$

The sum of $S_{v''v';j''}$ for all of the lines belonging to a specified j''-level is proportional to the population of that level. Letting $\alpha_{v''v'}$ be the integrated absorption coefficient for all lines of all rotational levels for the $v''v'$-band, we find that, approximately,

$$S_{v''v';j''} = \frac{\alpha_{v''v'}}{n}\frac{N_{v''j''}}{N_{v''}} \tag{8}$$

if n represents the number of rotational lines per j''-level. Combining equations (6) and (8), we now obtain

$$S_{v''v';j''} = \frac{2\alpha_{v''v'}j''B_e''hc}{nkT}\exp\left[-j''(j''+1)B_e''hc/kT\right]. \tag{9}$$

Equation (9) is identical with equation (14–31) of Ref. 1 if we use the approximation $j''(j''+1)\simeq j''^2$.

The approximate wave number ω at which a line occurs is given by the difference between the final and initial term values (compare Fig. 1), i.e.,

$$\omega = \omega_{v'} - \omega_{v''} + \omega_{j'} - \omega_{j''}. \tag{10}$$

Combining equations (2), (3), and (10), we obtain

$$\omega = \omega_{v'} - \omega_{v''} - j''(j''+1)(B_e'' - B_e'). \tag{11}$$

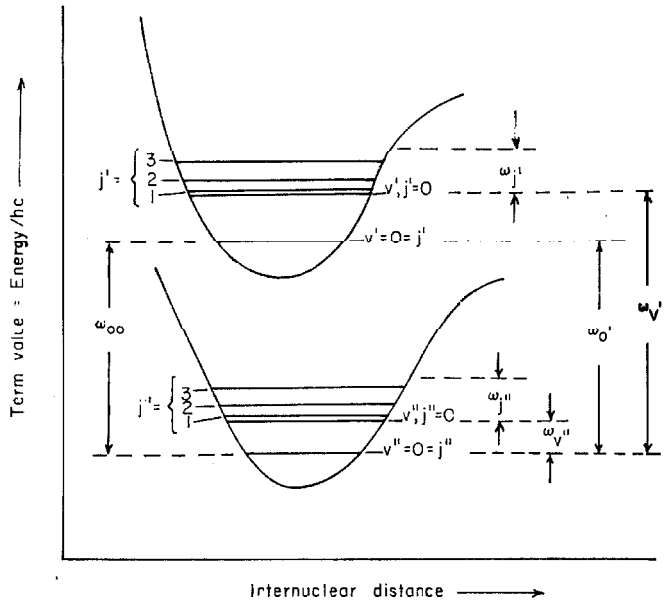

FIG. 1. Simplified energy level diagram for diatomic molecules. The spacing of the rotational levels is exaggerated for the sake of clarity.

For a given vibrational transition, $\omega_{v'}$ and $\omega_{v''}$ are constant whence it follows that the average line spacing $\delta\omega_{j''}$ in a band where each j''-level is associated with n lines is*

$$\delta\omega_{j''} = \frac{2j''|B_e'' - B_e'|}{n} = \frac{2j''\Delta B}{n} \tag{12}$$

where

$$\Delta B \equiv |B_e'' - B_e'|. \tag{13}$$

Combining equations (9) and (12), and setting $P_{\omega;v''v'}$ equal to the local value of $S_{v''v';j''}$ divided by the local line spacing (i.e. using a 'just-overlapping' line model), we find for the $v''v'$-band that

$$P_{\omega;v''v'} = \frac{S_{v''v';j''}}{\delta\omega_{j''}} = \frac{\alpha_{v''v'}B_e''hc}{kT\Delta B}\exp-[j''(j''+1)B_e''hc/kT]. \tag{14}$$

We may replace $j''(j''+1)$ in equation (14) by writing equation (11) in the form

$$j''(j''+1) = \frac{\omega - \omega_{v'} + \omega_{v''}}{B_e' - B_e''} \tag{15}$$

provided that the right-hand side of equation (15) is positive. If it is negative, ω lies in a wave number region where no rotational transitions occur and, therefore, $P_{\omega;v''v'}$ is to be set equal to zero.

*Equations (12) and (14) are equivalent to equations (14–33) and 14–34) of Ref. 1, if we note that the line spacing in Ref. 1 is computed for each *branch* of a band. The present method appears simpler conceptually since we do not require a final summation over band branches.

The integrated absorption coefficient, $\alpha_{v''v'}$, is related to the electronic absorption oscillator strength, f, and the Franck–Condon factor, $q_{v''v'}$ by the expression

$$\alpha_{v''v'} = \frac{\pi e^2 N f q_{v''v'}}{mc^2 p Q_{v''}} \exp(-hc\omega_{v''}/kT) \tag{16}$$

if induced emission terms are negligibly small, which will normally be justified except at high temperatures. The Franck–Condon factor is defined, as usual, by the square of the vibrational overlap integral

$$q_{v''v'} = |\int \psi_{v'} \psi_{v''} \, dr|^2. \tag{17}$$

Equation (16) follows directly from equation (2–21) of Ref. 1 and from the definition of the electronic f-number (compare p. 150 of Ref. 1). The vibrational partition function is

$$Q_{v''} = \sum_{v''} \exp -(hc\omega_{v''}/kT) \tag{18}$$

and should be summed from zero over all integral values of v'' to the value corresponding to the dissociation limit.

Combining equations (14) and (16) leads to the relation

$$P_{\omega;v''v'} = \frac{\pi e^2 N f q_{v''v'} h B_e''}{mcp Q_{v''} kT \Delta B} \left\{ \exp -[j''(j''+1)B_e'' + \omega_{v''}] \frac{hc}{kT} \right\}. \tag{19}$$

The actual value of the spectral absorption coefficient is the sum of the contributions made by individual bands in the band system; thus

$$P_\omega = \sum_{v''} \sum_{v'} P_{\omega;v''v'}. \tag{20}$$

Combining equations (11), (19), and (20) we obtain the form of the results given by KECK *et al.*[2] viz.,

$$P_\omega = \frac{\pi e^2 N f h}{mcpkT} \left\{ \exp[-(\omega_{00} - \omega)hc/kT] \right\} \phi \tag{21}$$

where

$$\phi = \frac{B_e''}{Q_{v''} \Delta B} \sum_{v''} \sum_{v'} q_{v''v'} \exp \left\{ -[j''(j''+1)B_e' + \omega_{v'} - \omega_{00}]hc/kT \right\}. \tag{22}$$

It is interesting to observe that the final expression for P_ω is independent of the number of band branches, i.e. it is independent of the value of n.

B. *The 'smeared rotational line model'*

Although KECK *et al.*[2] do not present a detailed derivation of their results, they suggest that equations (21) and (22) may be obtained by refining the procedure described

in an earlier paper by KIVEL, MAYER and BETHE[3], which has recently been adapted to the calculation of spectral absorption coefficients in infrared vibration–rotation bands.[1] The results given in Ref. 4 may also be derived by using a procedure analogous to that described in the preceding section IA.

We start with the equation*

$$\frac{1}{f_{v'v''}}\frac{\mathrm{d}f_{v'v''}}{\mathrm{d}\omega} \propto \frac{\mathrm{d}}{\mathrm{d}\omega}\left[\exp(-E_{j''}/kT)\right], \tag{23}$$

and we find therefore that

$$\frac{\mathrm{d}f_{v'v''}}{\mathrm{d}\omega} \simeq f_{v'v''}\frac{hcB_e''}{|B_e' - B_e''|kT}\exp(-E_{j''}/kT) \tag{24}$$

since

$$E_{j''} \simeq j''(j''+1)hcB_e'' \simeq \frac{hcB_e''}{B_e' - B_e''}(\omega - \omega_{v'v''}). \tag{25}$$

Equation (24) holds for $B_e' \neq B_e''$ if $|B_e' - B_e''|$ represents the absolute value of the difference between the rotational constants. For a band system, we must again sum over v'' and v' in order to obtain all contributions at a given wave number. Thus

$$\sum_{v'}\sum_{v''}\frac{N_{v''}}{p}\frac{\mathrm{d}f_{v'v''}}{\mathrm{d}\omega} \simeq \sum_{v'}\sum_{v''}\frac{N_{v''}}{p}f_{v'v''}\frac{hcB_e''}{|B_e' - B_e''|kT}\exp(-E_{j''}/kT) \tag{26}$$

where $N_{v''}$ is the total number of molecules per unit volume in the lower electronic state with vibrational quantum number v'' and p denotes the pressure.

In terms of the Franck–Condon factors $q_{v'v''}$, we may write

$$f_{v'v''} = fq_{v'v''} \tag{27}$$

where f is the electronic f-number. Setting N equal to the total concentration of absorbing species, and noting the equilibrium relation

$$\frac{N_{v''}}{N} = \frac{\exp(-E_{v''}/kT)}{Q_{v''}}, \tag{28}$$

we find that

$$\frac{N_{v''}}{p}\frac{\mathrm{d}f_{v'v''}}{\mathrm{d}\omega} \simeq \frac{hcB_e''f}{|B_e' - B_e''|kT}\frac{N}{p}\frac{1}{Q_{v''}}q_{v'v''}\left[\exp-(E_{v''}+E_{j''})/kT\right]. \tag{29}$$

The spectral absorption coefficient at the wave number ω associated with the $v''v'$-band, $P_{\omega;v''v'}$, may now be obtained from the relation

$$P_{\omega;v''v'} = \frac{\pi e^2}{mc^2}\frac{N_{v''}}{p}\frac{\mathrm{d}f_{v'v''}}{\mathrm{d}\omega} \tag{30}$$

whence it follows, in view of equation (29), that equation (19) is obtained. Proceeding as before, we may again derive equations (21) and (22).

*Compare equation (14–6) of Ref. 1 and the basic equation used in Ref. 4.

II. CALCULATIONS OF SPECTRAL ABSORPTION COEFFICIENTS FOR THE NO γ-BANDS AT 2000°K

From equations (15), (21), and (22) we obtain the relation

$$P_\omega = \frac{\pi e^2 N f h B_e''}{mcpkTQ_{v''}\Delta B}\sum_{v''}\sum_{v'} q_{v''v'}\exp\left\{-\left[\frac{\omega-\omega_{v'}+\omega_{v''}}{B_e'-B_e''}B_e'+\omega_{v'}-\omega\right](hc/kT)\right\} \quad (31)$$

or

$$P_\omega = \sum_{v''}\sum_{v'}\frac{\pi e^2 N f h B_e'' q_{v''v'}}{mcpkTQ_{v''}\Delta B}\left[\exp-\left(\frac{\omega_{v''}B_e'-\omega_{v'}B_e''}{B_e'-B_e''}\right)\frac{hc}{kT}\right]\left[\exp-\left(\frac{B_e''}{B_e'-B_e''}\right)\frac{hc\omega}{kT}\right]. \quad (32)$$

Let

$$C_{v''v'} = \frac{\pi e^2 N f h B_e'' q_{v''v'}}{mcpkTQ_{v''}\Delta B}\left[\exp-\left(\frac{\omega_{v''}B_e'-\omega_{v'}B_e''}{B_e'-B_e''}\right)\frac{hc}{kT}\right] \quad (33)$$

and

$$D \equiv \frac{B_e'' hc}{(B_e'-B_e'')kT}. \quad (34)$$

Then

$$P_{\omega;v''v'} = C_{v''v'}\exp(-D\omega) \quad (35)$$

or

$$\ln P_{\omega;v''v'} = -D\omega + \ln C_{v''v'}. \quad (36)$$

Reference to equation (36) shows that $\ln P_{\omega;v''v'}$ varies linearly with ω and that the slopes of these plots are independent of ω. To the order of approximation to which the present theory has been worked out, it is apparent that the band head coincides with the band origin (compare equation (11)).* Consequently, it is only necessary to compute $P_{\omega;v''v'}$ at $\omega = \omega_{v'}-\omega_{v''}$ and then to draw appropriate straight lines. The value of $P_{\omega;v''v'}$ at the band head is

$$P_{\omega;v''v';h} = \frac{\pi e^2 N f h B_e'' q_{v''v'}}{mcpkTQ_{v''}\Delta B}\exp(-hc\omega_{v''}/kT). \quad (37)$$

Once $P_{\omega;v''v'}$ is known, we may obtain P_ω according to equation (20) by performing a numerical or graphical addition.

The NO γ-bands corresponding to the transitions $A^2\Sigma^+ \rightarrow X^2\Pi$ are important in radiant heat transfer from heated air. An electronic f-number of about 0·0025 has been obtained by WEBER and PENNER[5] and by BETHKE[6] experimentally for this band system. Franck–Condon factors have been calculated by KIVEL, MAYER and BETHE[3]. Assuming an f number of 0·0025, MEYEROTT, SOKOLOFF and NICHOLLS[7] obtained curves of spectral absorption coefficients as a function of wave number for the NO γ-band contribution to the absorption coefficient of air. In order to compare our results directly with

*For the NO γ-system, the band head is actually close to the band origin (cf. p. 405 of Ref. 1).

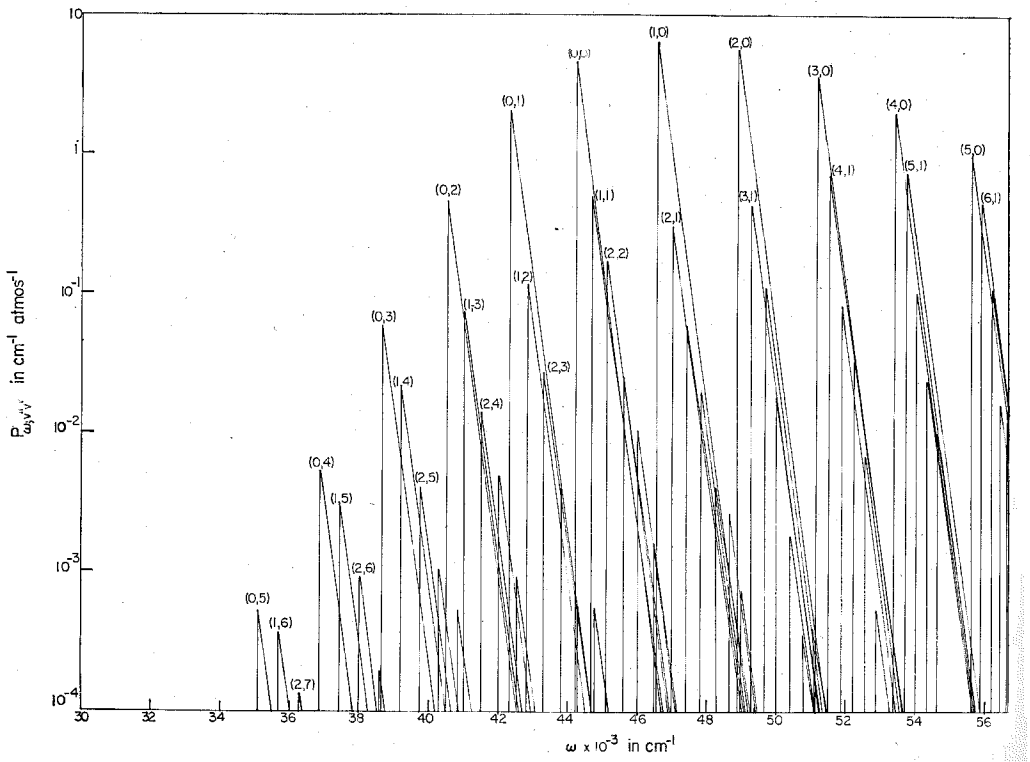

FIG. 2. Approximate values for the spectral absorption coefficients of various NO γ-bands at 2000°K; the numbers in parentheses correspond to (v', v''). The solid curves were computed from equations (34), (35) and (37).

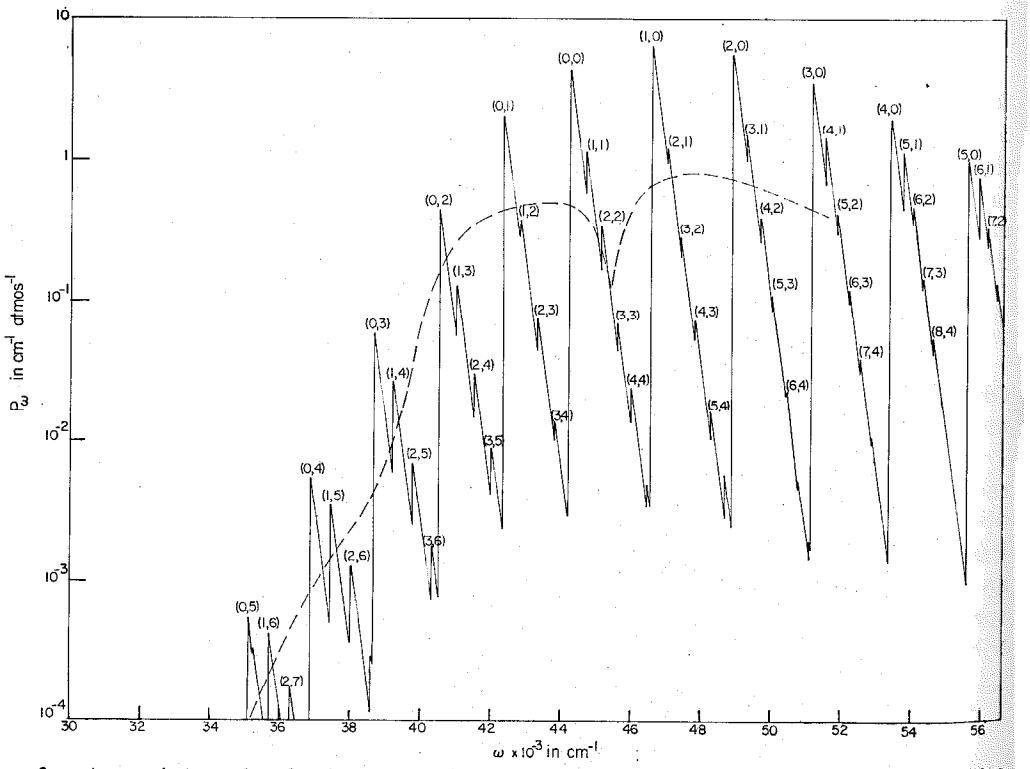

FIG. 3. Approximate values for the spectral absorption coefficients of the NO γ-band system at 2000°K. The solid curves were obtained from the data given in Fig. 2; the dotted curves are taken from Ref. 7. Band heads (v', v'') are indicated on the absorption coefficient curves.

those of MEYEROTT *et al.*, we have also used $f = 0{\cdot}0025$.* Spectroscopic constants were obtained from HERZBERG[8].

Results computed from equations (36) and (37) for $P_{\omega;v''v'}$ at 2000°K are shown in Fig. 2; the final values of P_ω are plotted in Fig. 3, together with the values given in Ref. 7. The method that was used by MEYEROTT *et al.* is not specified in detail, but it is noted that averages were employed over frequency intervals of 2000 cm^{-1}. Consequently, the results shown in Fig. 3 must be considered to be in good agreement.

REFERENCES

1. S. S. PENNER, *Quantitative Molecular Spectroscopy and Gas Emissivities*. Sections 11–8, 11–20 and 14–6. Addison–Wesley, Reading, Mass. (1959).
2. J. C. KECK, J. CAMM, B. KIVEL and T. WENTINK, Jr., *Ann. Phys.* **7**, 1 (1959).
3. B. KIVEL, H. MAYER and H. BETHE, *Ann. Phys.* **2**, 57 (1957).
4. S. S. PENNER, K. P. G. SULZMANN and C. B. LUDWIG, *J.Q.S.R.T.* **1**, 96 (1961).
5. D. WEBER and S. S. PENNER, *J. Chem. Phys.* **26**, 860 (1957).
6. G. W. BETHKE, *J. Chem. Phys.* **31**, 662 (1959).
7. R. E. MEYEROTT, J. SOKOLOFF and R. W. NICHOLLS, *Absorption Coefficients of Air*, Lockheed Aircraft Corporation, Missiles and Space Division, Report LMSD-288052 (1959).
8. G. HERZBERG, *Molecular Spectra and Molecular Structure, Volume I, Spectra of Diatomic Molecules*, Van Nostrand, Princeton, N.J. (1950).

*KECK *et al.* have obtained the value $f = 0{\cdot}001 \pm 0{\cdot}0005$ from high-temperature emission measurements.